Biophysical and Economic Constraints on China's Natural Climate Solutions

Nan Lu[1,2], Hanqin Tian[3, 4], Bojie Fu[1,2,5*], Huiqian Yu[1,2], Shilong Piao[6,7], Shiyin Chen[5], Ya Li[1,2], Xiaoyong Li[1,2], Mengyu Wang[1,2], Zidong Li[5], Lu Zhang[1,2], Philippe Ciais[8], Pete Smith[9]

[1]State Key Laboratory of Urban and Regional Ecology, Research Center for Eco-Environmental Sciences, Chinese Academy of Sciences; Beijing 100085, China.

[2] University of Chinese Academy of Sciences; Beijing 100049, China

[3] Schiller Institute for Integrated Science and Society, and Department of Earth and Environmental Sciences, Boston College, Chestnut Hill, MA 02467, USA

[4]International Center for Climate and Global Change Research, College of Forestry, Wildlife and Environment, Auburn University; Alabama 36849, USA

[5] Faculty of Geographical Science, Beijing Normal University; Beijing 100875, China

[6] Sino-French Institute for Earth System Science, College of Urban and Environmental Sciences, Peking University; Beijing 100871, China

[7] Institute of Tibetan Plateau Research, Chinese Academy of Sciences; Beijing 100085, China

[8] Laboratoire des Sciences du Climat et de l'Environnement, CEA CNRS UVSQ; Gif-sur-Yvette, France

[9] Institute of Biological and Environmental Sciences, University of Aberdeen; Aberdeen, AB24 3UU, Scotland, UK

*Corresponding author: Bojie Fu, bfu@rcees.ac.cn

Main Text:

Text: 3678 words (excluding references, tables, figure captions, figure/table place holders, and box)

Figures: 3 (presented following the Methods section in this file)

References: 1-37

Methods:

Methods: 2387 words

References: 38-52

Extended Data:

Figures: 7

Supplementary information:

Figures: 12

Tables: 38

References: 1-375

Abstract:

Natural Climate Solutions (NCS) are strategies for climate mitigation in the land sector, that increase carbon storage or avoid greenhouse gases (GHG) emissions. Here, we estimate China's historic NCS mitigation at 0.6 (0.5-0.7) Pg CO_2e yr^{-1} (95% CI) during 2000-2020 (8% of fossil CO_2 emission in the contemporary period). Through new NCS activities, the future maximum potential for NCS is projected at 0.6 (0.3-1.0) Pg CO_2e yr^{-1} (6% of fossil CO_2 emission) during 2020-2030 and 1.0 (0.6-1.4) Pg CO_2e yr^{-1} during 2020-2060. 26-31%, 62-65%, and 90-91% of the future NCS potentials can be achieved at mitigation costs of 10, 50 and 100 USD Mg CO_2e^{-1}, respectively. Thus, NCS can contribute substantially to China's National Determined Contributions (NDCs) over the next 10 to 40 years, but require a national strategy to reach climate goals and ensure co-benefits for people and nature.

Main

Natural climate solutions (NCS), a suite of land management options including protecting, restoring and sustainably managing ecosystems [1], provide readily implementable approaches to sequester carbon in terrestrial pools and/or reduce GHG emissions [2]. NCS are a complement to, not a substitute for, emission reductions related to decreased use of fossil fuels and decarbonization of energy and transportation sectors. They are expected to slow down the rate of global warming in the next 10-40 years, in parallel with the development of mitigation technologies and energy transformation [3].

Following the first submission in 2015, China submitted its updated Nationally Determined Contribution (NDCs) in 2021. This included a "net-zero" commitment with a peak in CO_2 emission before 2030 and net carbon neutrality being achieved by 2060 [4]. Over the past decades (especially since 1999), China has strengthened its efforts in ecological restoration and protection [5]. While not all the projects were originally designed for carbon sequestration and climate change mitigation, collectively they made a substantial contribution to China's terrestrial ecosystem carbon sink [6-8]. Some adaptive action strategies such as *China's Achievements, New Goals and New Measures for Nationally Determined Contributions* [9] and *Master plan of Major Projects of National Important Ecosystem Protection and Restoration (2021-2035)* [5] have been released, proposing a series of strategies for ecosystem management in the next decades to support implementation of the NDCs. So far, the contributions to emission reductions from recent projects equivalent to NCS activities have not been fully quantified. More importantly, the mitigation potential of future NCS activities and their contribution to

China's climate goals is largely unknown [2].

Here, we quantified 16 distinct pathways (see definitions and descriptions in Supplementary Table S1&2) to provide an integrated evaluation of the climate mitigation capacity of previous projects during 2000-2020, and the future NCS potentials during 2020-2030 and 2020-2060 by conserving, restoring, and improving management of forests, croplands, grasslands, and wetlands in China. The evaluation of the mitigation capacity of previous projects for 2000-2020 is a foundation to understand the historical contribution and also a baseline for setting feasible boundaries for future additional NCS pathway projections (Supplementary Table S1&2). We first provide estimates of the historical mitigation capacity of projects during 2000-2020, as well as the future "maximum additional mitigation potential" (MAMP) of NCS by additional stewardship options under biophysical constraints in the next 10 (by 2030) and 40 years (by 2060), measured in CO_2 equivalents per year (CO_2e yr^{-1}). We then constrain NCS levels by mitigation cost thresholds. We note that the essence of NCS is to seek new opportunities and approaches with additionality over the baseline (i.e., 2000-2020 in this study).

Overall NCS potential

During 2000-2020, the total mitigation capacity of the 9 pathways related to previous projects was 0.6 (0.5-0.7) Pg CO_2e yr^{-1} (95% confidence interval, CI) (Fig.1a), counterbalancing 8% of the mean annual fossil CO_2 emission in the same period (7.4 Pg CO_2e yr^{-1}), in which the increased carbon sequestration from ecosystems (0.5 Pg

CO_2 yr^{-1}, excluding CH_4 and N_2O) is about 54% (28-80%) of the overall land *carbon* sink in China (0.18-0.51 Pg C yr^{-1}) [10]. During 2020-2030, the maximum potential of NCS (i.e., MAMP) of the 16 pathways is projected at 0.6 (0.3-1.0) Pg CO_2e yr^{-1} (Fig.1b), which is 6% of the mean annual CO_2 emission during the same period (assuming the industrial CO_2 emission at year 2030 to be around 10 to 12 Pg CO_2 yr^{-1}) [11]. The MAMP is projected at 1.0 (0.6-1.4) Pg CO_2e yr^{-1} during 2020-2060 (Fig.1c).

[Figure 1 here]

The realization and importance of diverse NCS pathways comprehensively reflects a nation or region's stewardship of certain ecosystems, land cover history, the status of the ecosystems, land ownership, human intervention, technological progress, and governance [12]. In the context of China, the land area that can be used for restoration (e.g., reforestation, grassland and wetland restoration) (Extended Data Fig. 1&2), the technology and land practices that can be applied (e.g., water and nutrient management in croplands and grazing in rangelands), as well as the land transfer risk control (e.g., avoiding loss of natural land cover to cropland or built-up) are the direct determinants of ecosystem restoration, management, and protection, respectively [1,13].

NCS potential by pathway

Historical and future fluxes of individual pathways have contributed to the overall estimates presented above (Fig. 1a-c, Supplementary Table S1-3).

Forest ecosystems.

Forest pathways are most important for the historical mitigation capacity and future potential in China (Fig. 1a-c, Supplementary Table S3). During 2000-2020, the carbon sink in managed forests (including reforestation, natural forest management, and fire management) was estimated to be 446 Tg CO_2 yr^{-1}, contributing 73% of the total flux of the 9 NCS pathways (Fig. 1a). Of this total, more than 55% was contributed by reforestation (247 Tg CO_2 yr^{-1} on an area of 44.7 Mha) and 42% by natural forest management (i.e., restricted timber logging) (189 Tg CO_2 yr^{-1} on an area of 41.3 Mha). Fire management made a small contribution of 3% (10 Tg CO_2 yr^{-1}), in which 9 Tg CO_2 yr^{-1} was contributed by fire prevention and 1 Tg CO_2 yr^{-1} by prescribed fire.

In the future, the total MAMP from the five forest pathways (including two new pathways) would be 436 Tg CO_2 yr^{-1} by 2030 and 627 Tg CO_2 yr^{-1} by 2060, representing 64-68% of the total NCS of the 16 pathways (Fig. 1b-c, scenario setting in Supplementary Table S2). Considering the constraints of water stress, the *Farmland Red Line* (the minimum acceptable arable land area in China), urbanization, as well as the 26% forest coverage goal by 2035 (similar to the historical value in 1700) [14,15], the maximum additional area for future reforestation after 2020 will be limited to be 31.8 Mha (Extended Data Fig. 2&3), similar to the estimate in ref [16] , and the MAMP would be 77 Tg CO_2 yr^{-1} and 235 Tg CO_2 yr^{-1} by 2030 and 2060, respectively (assuming that 21.7 Mha be reforested by 2030 and 31.8 Mha by 2060). The lower NCS potential of reforestation during 2020-2030 compared to the historical capacity in 2000-2020 is due to the lower carbon flux rate in the 10-yr forest and also the smaller reforested area. The magnitude of CO_2 sequestration during 2020-2060 is comparable to the historical value, with the forests getting older (Fig. 1a-c, Supplementary Table S2&3). The

MAMP of natural forest management would be almost double (336 Tg CO_2 yr^{-1}) within the next 40 years because a larger area of natural forests (79.1 Mha) will be restricted from logging (clearcutting of natural forests for fuelwood and timber is prohibited by law in China since 2020), although the carbon sequestration rate of these unlogged forests would slightly decrease as they would shift from younger (mean age 43 years in 2010) to older age classes with a lower uptake rate (mean age 63-93 years in 2030-2060) (Extended Data Fig. 4) [17]. Natural forest management would account for 77% of the total NCS of forest pathways by 2030 and 54% by 2060, when reforestation will have a higher NCS potential (37%) compared to the historical period. Only 5-9% of the total CO_2 flux resides in improved plantations, avoided forest conversion, and fire management. Improved plantations by reducing harvest and improving wood residue treatments could contribute a net sink of 17 and 49 Tg CO_2 yr^{-1} by 2030 and 2060, respectively (Fig. 1b-c). The risk of forest conversion to other land uses would be relatively small (0.01 Mha yr^{-1}). Reducing conversion from forest to cultivated or developed land will contribute 6 and 7 Tg CO_2 yr^{-1} of emission reduction by 2030 and 2060, respectively. The mean annual burnt area due to wildfire was greatly reduced (from 0.89 Mha yr^{-1} during 1949-1999 to 0.12 Mha yr^{-1} during 2000-2017) (Extended Data Fig. 5) since the implementation of fire prevention policy in 1987 [18], and future wildfire may also be maintained at a low level (<1 Tg CO_2 yr^{-1}).

Forest volume is estimated to increase by 8.26 billion m^3 (equivalent to 7.34 Pg CO_2 of carbon sequestration) by 2030 over the 2000 level due to reforestation and natural forest management based on our projections, indicating that achieving the goal specified in China's NDCs (6.0 billion m^3 over the 2005 level) [4] is achievable.

Cropland ecosystems

Cropland NCS showed promising opportunities for climate mitigation *via* improved cropland management. During 2000-2020, the total mitigation from the three cropland pathways was 84 Tg CO_2e yr^{-1} (Fig. 1a), 14% of the overall historical flux of the 9 NCS pathways. Cropland nutrient management decreased N_2O emissions by 79 Tg CO_2e yr^{-1} from reduced nitrogenous fertilizer use and improved fertilizer production technology (Supplementary Table S3, Extended Data Fig. 6). Cover crops (on 4.5 Mha of winter fallow) contributed 5 Tg CO_2 yr^{-1} through soil carbon sequestration. The mitigation capacity of biochar was minimal (0.5 Tg CO_2 yr^{-1}) as the amount of crop residues used for biochar production is small (0.11% of the total of 708 million tons per year).

In the future, the MAMP of the cropland pathways (including a new pathway of improved rice cultivation) could reach 104 Tg CO_2e yr^{-1} by 2030 and 223 Tg CO_2e yr^{-1} by 2060 (scenario setting in Supplementary Table S2) (Fig. 1b-c). These values are 1.2 and 2.6 times as large as the historical value, respectively, contributing 16% and 23% to the overall NCS potential of the 16 pathways. Specifically, the potential additional N_2O emission reduction through improved N management could be 46 Tg CO_2e yr^{-1} by 2030 and 153 Tg CO_2e yr^{-1} by 2060, assuming that our reduction scenario of N fertilizers by 13-49% would not affect crop yield [19]. The contribution from cover crops could increase to be 25 Tg CO_2 yr^{-1} if the maximum area of 15.1 Mha of winter fallow is applied with cover crops. Biochar would remain as a less important NCS pathway (0.1 Tg CO_2 yr^{-1}). In comparison, rice cultivation is extensive in China (30.5 Mha) and improved rice cultivation as a new NCS pathway could contribute 33-44 Tg CO_2e yr^{-1} in CH_4 emission reductions in the next 40 years through improved soil management and drainage processing [20].

Grassland ecosystems

Grazing optimization and grassland restoration was estimated to be a net sink of 80 Tg CO_2 yr^{-1} during the period 2000-2020, contributing 13% to the overall mitigation capacity of the 9 pathways (Fig. 1a), of which 59 Tg CO_2 yr^{-1} was from grazing optimization (fencing or sowing on an area of 99.6 Mha [21]) and 21 Tg CO_2 yr^{-1} from grassland restoration (on 5.8 Mha cropland) (Fig. 1a, Supplementary Table S2&3). In the future, the total additional MAMP from grassland ecosystems is estimated at 68-82 Tg CO_2 yr^{-1} during 2020-2060 (8-11% of the overall NCS potential) (Fig. 1b-c, scenario setting in Supplementary Table S2). Grassland grazing optimization could be applied on a smaller area in the future (15.6 Mha by 2030 and 62.4 Mha by 2060) and consequently would contribute a smaller NCS potential of 8 Tg CO_2 yr^{-1} and 29 Tg CO_2 yr^{-1}, respectively. For grassland restoration in cropland over steep slopes, the additional area available in the future would be only 0.54 Mha (Extended Data Fig. 1&2). Thus, the MAMP of grassland restoration would remain constant at 3 Tg CO_2 yr^{-1} during 2020-2060. Cropland expansion is the major cause of grassland conversion in China at rate of 0.53 Mha yr^{-1}. Avoided grassland conversion to cropland will provide a new mitigation opportunity, reducing an additional 50-57 Tg CO_2 yr^{-1} (Fig. 1b-c).

Wetland ecosystems

The mitigation capacity from actual wetland projects during 2000-2020 was negligible (<1 Tg CO_2e yr^{-1}) compared to the other pathways (Fig. 1a), but shows great potential as a NCS in the next decades (35 and 52 Tg CO_2e yr^{-1} by 2030 and 2060, respectively (Fig. 1b-c), contributing 4-5% to the overall NCS potential of the 16 pathways), especially for peatland (Supplementary Table S3). Avoided peatland loss could potentially reduce CO_2 emissions 24 Tg CO_2 yr^{-1} over the next 40 years (on 0.09-0.38 Mha of area). Peatland restoration by soil re-wetting could contribute an additional 4 and 14 Tg CO_2e yr^{-1} mitigation potential (the net effect of decreasing CO_2 emission and increasing carbon accumulation but increasing CH_4 emission) by 2030 and 2060 (0.05 and 0.19 Mha), respectively (Fig. 1b-c). Coastal wetland restoration could sequestrate 2 and 4 Tg CO_2 yr^{-1} (0.11 and 0.38 Mha). Avoided coastal wetland impacts (including salt marshes and seagrass beds) could reduce CO_2 emissions 6 and 10 Tg CO_2 yr^{-1} by 2030 and 2060 (0.10 and 0.41 Mha), respectively. Although the loss rate of coastal ecosystems and wetlands is small (<0.01 Mha yr^{-1}), they need extra attention because the carbon flux per unit area released from wetland loss is substantial (Fig. 1b-c, Supplementary Table S2&3).

Spatial distribution of the NCS

The climate mitigation from the 16 NCS pathways show large spatial differences across the country. Inner Mongolia (IM), Heilongjiang (HLJ), Sichuan (SC) and Yunnan (YN) are the top four provinces with the highest levels of historical achieved capacity and future potential (Fig. 2). Except for some provinces in Northwest and East China, natural forest management and/or reforestation contributes the most to the overall NCS.

For Xinjiang and Qinghai, grazing optimization had the biggest contribution to the historical flux, and grassland and peatland management will be important NCS opportunities in the future. In some provinces in Central and East China (including Henan, Hubei, Hunan, Shandong, Anhui, Jiangxi and Jiangsu), cropland nutrient management and improved rice cultivation are also important options for future NCS. Improved plantations are non-negligible in Guangxi province.

At the national level, the dominant type of the NCS was restoration and improved management before 2020, but it would shift towards improved management in future decades, with protection becoming more important (Fig. 3a-c, the type of NCS defined in Methods). At the provincial level, ten NCS types were further identified as the predominant options, including six single types and four mixed or combined types (Fig. 3e-f), indicating the need for diverse NCS activities.

[Figure 2 here]

[Figure 3 here]

Cost-effectiveness

By using marginal abatement cost (MAC) curves, the cost of the climate mitigation of each NCS pathway was estimated. During 2000-2020, only 125 Tg CO_2e yr^{-1} (20% of the total) was achieved at a mitigation cost below 10 USD Mg CO_2e^{-1} (Fig. 1a-c). In the future, 165 Tg CO_2e yr^{-1} (26%) and 298 Tg CO_2e yr^{-1} (30%) out of the total NCS will be achievable by 2030 and 2060, respectively, at 10 USD Mg CO_2e^{-1}. At a mitigation cost of 50 USD Mg CO_2e^{-1}, 354 Tg CO_2e yr^{-1} (58%), 390 Tg CO_2e yr^{-1} (62%) and 641 Tg CO_2e yr^{-1} (65%) of the total NCS are available during 2000-2020, 2020-2030, and 2020-2060, respectively. 406 Tg CO_2e yr^{-1} (66%), 573 Tg CO_2e yr^{-1} (90%) and 898 Tg CO_2e yr^{-1} (91%) are achievable for mitigation costs up to 100 USD Mg CO_2e^{-1}. Natural forest management is the most cost-effective option at all of the three mitigation costs and will achieve the highest MAMP (336 Tg CO_2 yr^{-1}) at 100 USD Mg CO_2e^{-1} during 2020-2060 (Fig. 1a-c). The portion of achievable NCS at the three cost thresholds is similar to that of the US but higher than that of Canada. The US's total NCS is 1.2 Pg CO_2e yr^{-1} during 2015-2035 (19% of industrial CO_2 emission of the 1990-2018 level), 25, 76 and 91% of which would be achieved at 10, 50 and, 100 USD Mg CO_2e^{-1}, respectively [22]. For Canada, the total NCS is 78 Tg CO_2e yr^{-1} during 2021-2030 (100% of all heavy industry emissions of the 2018 level); 12, 34 and 51% of which would be available at 10, 50 and, 100 CAD Mg CO_2e^{-1}, respectively [23].

Besides climate mitigation, the NCS measures bring co-benefits including improving biodiversity, air purification, soil enrichment, and water retention [24] (Fig. 1) [25]. The value of these co-benefits is not accounted for in our estimation of cost-effectiveness of the NCS, but they will save economic costs and improve human well-[26].

[Box 1 here]

Calibration upon the global assessment for China

A relative comparison between our estimates and those in Griscom et al. [1] can be made in terms of implementation extent and GHG flux rate (per unit area) within a given time period (Extended Data Fig. 7). Griscom et al.'s estimate of reforestation for China is as high as 1257 Tg CO_2e yr^{-1} (2010-2030), five times more than our estimate (247 Tg CO_2 yr^{-1}, 2000-2020), mainly because they used a much higher value for carbon sequestration rates (4.14 Mg C ha^{-1} yr^{-1}). They also assumed that 25-30% of total NCS by reforestation can be achieved at 100 USD (referencing to a study on commercial plantations in the United States), i.e., 319 Tg CO_2 yr^{-1} [27,28]. We estimated that 55% (136 Tg CO_2 yr^{-1}) of the total NCS (247 Tg CO_2 yr^{-1}) can be realized at 100 USD during 2000-2020 based on our MAC curves using actual data from regions that implemented reforestation in China (Extended Data Fig.7). The CO_2 sink of natural forest management in 2000-2020 is 189 Tg CO_2 yr^{-1} in this study, against only 35 Tg CO_2 yr^{-1} in Griscom's [1]. This large difference is because we separated natural forests into different age classes with different sequestration rates (40-90 years) to obtain a weighted mean carbon sequestration rate (0.71-1.25 Mg C ha^{-1} yr^{-1}), whereas Griscom et al. set sequestration rates to a mean value (0.14-0.39 Mg C ha^{-1} yr^{-1}) uniform across all forests. Much higher NCS estimates of biochar are reported by the Natural Conservancy [27] (65 Tg CO_2e yr^{-1} at the price of 100 USD) and Yang [29] (86 Tg CO_2e yr^{-1}) who assumed that 73% or 90% China's crop residues can be used to produce biochar in the future, but this fraction is actually less than 1% and it will be a gradual process to transform crop residues utility from others to produce a large amount of biochar. Based on this, biochar NCS is very small (< 1 Tg CO_2e yr^{-1}) in both historical and future estimates in our study (Extended Data Fig. 7). The differences between our study and the global studies indicate that baseline setting as well as the use of regional data can greatly impact NCS assessment. Thus, well-calibrated national assessments are necessary to improve upon rough global estimates. For further comparative analysis please see corresponding sections in each of individual pathways in the Supplementary Information.

The implications

To achieve the maximum potential of NCS and enhanced the co-benefits of multiple ecosystem services, it is critical that integrated land planning and management optimization is applied at different jurisdictional levels and spatial scales, especially since the NCS pathways will be implemented on such a large land area nationwide (Extended Data Fig. 1&2). Specifically, overall land use planning should focus on systematic layout (i.e., total area control) of land restoration [30] and replacement [31] at the national level based on accurate land surveys, emphasizing coordination between restoration/protection and management at the provincial or regional level, and highlighting livelihood and realization of social justice at the local level by implementing ecological compensation [26]. The case of the Loess Plateau of China — the pioneer area of the Grain for Green Project — has proven that food security can be maintained through improved management practices such as improving nutrient use efficiency, water-saving irrigation, and construction of terraces and check dams [32], while at the same time capturing carbon in vegetation and soil, and reducing soil sediment in the Yellow River [33,34]. We also suggest that the government should set a percentage target of NCS based on the resource status of each region/province, continuing to strictly implement ecosystem protection policies, as the damage of ecosystems will outweigh the benefits to manage and restore without protection [35]. Alongside protection, improving management of ecosystems and promoting ecological restoration should be implemented for maintaining the long-term benefits of NCS. Our spatial maps clearly show different opportunity options in each province throughout the country. At the national or provincial level, since natural resource abundance and economic capital are limited, it is important for policy makers to transform their thinking from ‘expanding the extent of ecosystems’ to ‘improving the benefits per unit land area’, maintaining the overall strength of investment, fair and effective fund distribution (e.g., *via* improving ecosystem services payment system) [36], and management and technological creativity (e.g., improving fertilizer production process or developing digital fencing).

Challenges and next steps

Climate change and ecosystem spatial shifts may bring great uncertainties to the carbon sequestration rates estimated based on the existing spatial locations of the samples. The feedback between climate change and ecosystem change (such as forest albedo, particularly for the temperate zone and the boreal forest on the northeast) may also reduce the mitigation potential of the NCS [37]. These aspects, related to long-term ecosystem change and climate feedback, should be further explored for better estimating future NCS potential. In addition, due to limited data availability, biomass and soil carbon or other GHG were not fully considered. Other pathway options including actions to avoid carbon loss due to natural disturbances (such as pests, diseases and climate extremes), or NCS potential from managing the urban green infrastructure, livestock and aquaculture sectors, need be quantified. Lastly, the inclusion of co-benefits brought by NCS will also greatly change the assessment of cost-effectiveness. Finally, the implementation of an NCS plan will also be affected by national economic development level, population change, policies and investment, pandemic events (such as COVID-19) and other socio-economic factors.

In this work, we showed that China's NCS could counterbalance 6% (11-12% if including legacy effect) of industrial carbon emissions between now and 2030. This modest proportion highlights that energy transformation and the rapid application of low-carbon technologies are an urgent priority for climate mitigation. Nevertheless, NCS pathways can still make an important contribution through additional carbon sequestration or avoided GHG emissions, buying time for the development and implementation of new technologies. Multilevel governance strategies that consider the spatial heterogeneity of the NCS pathways are needed to increase the synergies among multiple NCS pathways for realizing climate mitigation and co-benefits of ecosystem services.

Acknowledgments: B. Fu and N. Lu acknowledge financial support from the National Natural Science Foundation of China (41991230) and the National Key R&D Program of China (2017YFA0604700); H. Tian acknowledges funding support from the National Science Foundation of the United States (Grant No. 1903722) and Andrew Carnegie fellowship Program (Grant No. G-F-19-56910).

Author contributions: B. Fu, H. Tian and N. Lu co-designed and coordinated this research with substantial inputs from all authors; N. Lu, H. Yu, S. Chen, Y. Li, X. Li, M. Wang, Z. Li, and L. Zhang performed data collections, calculations and analysis; S. Piao, P. Ciais, and P. Smith contributed interpretation of the results and editing of the manuscript. All authors discussed and commented on the manuscript.

Competing interests: The authors declare no competing interests.

Figure legends

Fig. 1. Historical mitigation capacity and future NCS potential in China. Historical capacity during 2000-2020 (**a**), and future potential during 2020-2030 (**b**) and 2020-2060 (**c**). Light to dark colors of the bars indicate cost-effective mitigation levels at the mitigation costs of 10, 50 and 100 USD Mg CO_2e^{-1}, respectively. Black lines represent the 95% confidence interval (CI). Ecosystem service benefits (air, biodiversity, soil, and water) linked with each NCS pathway are indicated by colored short bars. Pathway names: *Reforestation (RF), Avoided Forest Conversion (AVFC), Improved Plantation (IMP), Natural Forest Management (NFM), Fire Management (FM), Biochar (BIOC), Cover Crops (CVCR), Cropland Nutrient Management (CRNM), Improved Rice Cultivation (IMRC), Avoided Grassland Conversion. (AVGC), Grazing Optimization (GROP), Grassland Restoration (GRR), Avoided Coastal Wetland Impacts (AVCI), Avoided Peatland Impacts (AVPI), Coastal Wetland Restoration (CWR), Peatland Restoration (PTR)*. See Supplementary Table S1&2 for pathway definition and extent of application. Note only nine pathways (in gray) have mitigation capacities during 2000-2020, and the other seven pathways do not have the historical capacities as no activities have been taken before 2020.

Fig. 2. Historical mitigation capacity and future NCS potential by each NCS pathway across the provinces of China. The numbers above each of the three bars for each province represent the total flux (Tg CO_2e yr^{-1}) in the time periods of 2000-2020, 2020-2030 and 2020-2060, respectively.

Fig. 3. NCS pathway types at the provincial level for the three time periods. Proportional distribution of NCS types during 2000-2020 (**a**), 2020-2030 (**b**), and 2020-2060 (**c**). Four types of pathways are classified: ‘Restoration’ (>50% restoration), ‘Protection’ (>50% protection), ‘Management’ (>50% management), and ‘Mixed’ (no pathway type contributes the majority). The red star represents the national barycentre of NCS types. The provinces are further classified into ten groups based on the ecosystem type of pathways contributing the most mitigation potential (**d, e, f**). Mixed types are not specified ecosystem types as they contain many combinations.

Box 1. Baseline setting and NCS estimation

Existing NCS estimates for China, including the national assessment by the Nature Conservancy (TNC) [27] and the China Country Report by Nature4Climate (N4C) [28], mainly refer to the global assessment by Griscom et al.[1], in which the baseline is 2000s-2010s and scenarios include 2010s-2030. Setting 2000-2020 as a baseline in this study partly makes the estimate of the future NCS potential smaller than their studies for the same target year 2030, because for the specific time point in 2030, the NCS implementation extent counted in the assessments is different. Particularly, reforestation was implemented on a large land area of 44.7 Mha during 2000-2020 (sequestering 247 Tg CO_2 yr^{-1} by 2020), and will continue to sequester carbon after 2020 (which we refer to as the legacy effect). The post 2020 legacy carbon sink from previous reforestation is projected to be 484 Tg CO_2 yr^{-1} by 2030 and 494 Tg CO_2 yr^{-1} by 2060, which will be counted in China's future land carbon budget, but is excluded from our estimates of the future NCS potential, as the essense of NCS is to seek new opportunities. Counting the legacy effect and the future potential will counterbalance a higher percentage of contemporary CO_2 emissions (11-12%) during 2020-2030. Therefore, baseline setting is critical for defining and projecting future activities in NCS assessments and making comparisons among studies. In this research, setting 2000-2020 as the baseline is to evaluate the contribution of the 20-yr efforts of previous ecological projects to climate mitigation and establish how much additional NCS potential we could get in a shorter (10 years) and longer term (40 years) if we take actions from now (corresponding to the release of the updated NDCs in *2021*, and the goals of peak in CO_2 emission before *2030* and net carbon neutrality by *2060*).

References

1. Griscom, B. W. et al. Natural climate solutions. *Proc. Natl. Acad. Sci. U.S.A*. **114**, 11645-11650 (2017).
2. Duan, H. et al. Assessing China's efforts to pursue the 1.5 degrees C warming limit. *Science*. **372**, 378-385 (2021).
3. Field, C. B. & Mach, K. J. Rightsizing carbon dioxide removal. *Science*. **356**, 706-707 (2017).
4. China Updated NDC. Available at Climate Action Tracker. (Submitted to UNFCCC in 2021) https://climateactiontracker.org/climate-target-update-tracker/china/.
5. National Development and Reform Commission & Ministry of Natural Resources of China, "The Master plan of Major Projects of National Important Ecosystem Protection and Restoration (2021-2035)". (2020; www.ndrc.gov.cn/xxgk/zcfb/tz/202006/P020200611354032680531.pdf).
6. Bryan, B. A. et al. China's response to a national land-system sustainability emergency. *Nature*. **559**, 193-204 (2018).
7. Qin, Z. C. et al. Natural Climate Solutions for China: The Last Mile to Carbon Neutrality. *Adv. Atmos. Sci.* **38**, 889-895 (2021).
8. Lu, F. et al. Effects of national ecological restoration projects on carbon sequestration in China from 2001 to 2010. *Proc. Natl. Acad. Sci. U.S.A.* **115**, 4039-4044 (2018).
9. China’s achievements, new goals and new measures for Nationally Determined Contributions (2021). The translatead version can be downloaded from " |"
10. Wang, Y., Wang, X., Wang, K. et al. The size of the land carbon sink in China. *Nature*. **603**, E7-E9. https://doi.org/10.1038/s41586-021-04255-y (2022).
11. Sun, Z., Liu, Y. & Yu, Y. China's carbon emission peak pre-2030: Exploring multi-scenario optimal low-carbon behaviors for China's regions. *J. Clean. Prod.* **231**, 963-979 (2019).
12. Griscom, B.W. et al. 2020 National mitigation potential from natural climate solutions in the tropics. *Phil. Trans. R. Soc.* B **375**: 20190126. http://dx.doi.org/10.1098/rstb.2019.0126.
13. Anderson, C. M. et al. Natural climate solutions are not enough. *Science*. **363**, 933-

934 (2019).

14. Ge, Q., Dai, J., He, F., Pan, Y. & Wang, M. Land use changes and their relations with carbon cycles over the past 300 a in China. *Sci. China Ser. D-Earth Sci.* **51**, 871-884 (2008).

15. Liu, M. & Tian, H. China's land cover and land use change from 1700 to 2005: Estimations from high-resolution satellite data and historical archives. *Glob. Biogeochem. Cycle.* **24** (2010).

16. Bastin, J. F. et al. The global tree restoration potential. *Science*. **365**, 76-79 (2019).

17. Zhang, Y., Yao, Y., Wang, X., Liu, Y. & Piao, S. Mapping spatial distribution of forest age in China. *Earth. Space. Sci*. **4**, 108-116 (2017).

18. Lü, A., Tian, H., Liu, M., Liu, J. & Melillo, J. M. Spatial and temporal patterns of carbon emissions from forest fires in China from 1950 to 2000. *J. Geophys. Res*. **111** (2006).

19. Tian, H. et al. Food benefit and climate warming potential of nitrogen fertilizer uses in China. *Environ. Res. Lett*. **7**, 044020 (2012).

20. U.S. Environmental Protection Agency (EPA). "Global Non-CO2 Greenhouse Gas Emission Projections & Mitigation Potential: 2015-2050," (EPA, 2019; www.epa.gov/global-mitigation-non-CO2-greenhouse-gases).

21. Ministry of Agriculture of the People Republic of China. "National Grassland Protection and Utilization the 13th Five-year Plan," (2017; www.moa.gov.cn/nybgb/2017/dyiq/201712/t20171227_6129885.htm).

22. Fargione, J. E. et al., Natural climate solutions for the United States. *Sci. Adv*. **4**, eaat1869 (2018).

23. Drever, C. R. et al. Natural climate solutions for Canada. *Sci. Adv*. **7**, eabd6034 (2021).

24. Seddon, N. et al. Getting the message right on nature-based solutions to climate change. *Glob. Chang Biol*. **27**, 1518-1546 (2021).

25. Gosnell, H., Charnley, S. & Stanley, P. Climate change mitigation as a co-benefit of regenerative ranching: insights from Australia and the United States. *Interface Focus*. **10**, 20200027 (2020).

26. Pihl, E. et al. Ten new insights in climate science 2020 – a horizon scan. *Global Sustain*. **4**, e5 (2021).

27. Leavitt, S.M. et al. Natural Climate Solutions Handbook: A Technical Guide for Assessing Nature-Based Mitigation Opportunities in Countries. The Nature Conservancy, Arlington, VA, USA. (2021).

28. Nature Climate Solutions, China Country Report. Nature4climate.org. http://nature4climate.s3.amazonaws.com/ctry-factsheets/China_factsheet.pdf (2020).

29. Yang, Q. et al. Country-level potential of carbon sequestration and environmental benefits by utilizing crop residues for biochar implementation. *Appl. Energy*, **282**, 116275 (2021).

30. Liu, H. It is difficult for China's greening through large-scale afforestation to cross the Hu Line. *Sci. China-Earth Sci.* **62**, 1662-1664 (2019).

31. Kuang, W. et al. Cropland redistribution to marginal lands undermines environmental sustainability. *Natl. Sci. Rev*. **9**, nwab091 (2022).

32. Shi, P. et al. Has "Grain for Green" threaten food security on the Loess Plateau of China? *Ecosyst. Health Sustain.* **6**, 1709560 (2020).

33. Wang, S. et al. Reduced sediment transport in the Yellow River due to anthropogenic changes. *Nat. Geosci.* **9**, 38 (2016).

34. Lu, Y., Lu, D., Feng, X. & Fu, B. Multi-scale analyses on the ecosystem services in the Chinese Loess Plateau and implications for dryland. *Curr. Opin. Environ. Sustain*. **48**, 1-9 (2021).

35. Cook-Patton, S.C., Drever, C.R., Griscom, B.W. et al. Protect, manage and then restore lands for climate mitigation. *Nat. Clim. Chang.* **11**, 1027-1034 (2021). doi.org/10.1038/s41558-021-01198-0.

36. Pan, X., Xu, L., Yang, Z. & Yu, B. Payments for ecosystem services in China: Policy, practice, and progress. *J. Clean. Prod.* **158**, 200-208 (2017).

37. Naudts, K., et al. Europe’s forest management did not mitigate climate warming. *Science* **351**, 597-600 (2016).

Methods

This study presents a comprehensive quantification of carbon sequestration as well as CO_2/CH_4/N_2O emission reductions from terrestrial ecosystems based on multiple sources of data from literature, inventories, public databases and documents. The pathways considered ecosystem restoration and protection from being converted into cropland or built-up areas, reforestation, management with improved nitrogen use in cropland, restricted deforestation, grassland recovery, reducing risk from forest wildfire, and others. Here, we describe the cross-cutting methods that apply across all 16 NCS pathways. The definitions, detailed methods and data sources for evaluating individual pathways can be found in the Supplementary Information.

Cross-cutting methods

Baseline setting. We set 2000 as the base year because the large-scale national ecological projects, such as the Grain for Green Project were started since then. We firstly evaluate the historical mitigation capacity during 2000-2020, which is the first twenty-year of implementing the projects. From this procedure we can determine how much mitigation capacity has been realized through the previous projects in the past two decades, and to what extent additional actions can be made after 2020. Relative to the baseline 2000-2020, we then evaluate the maximum potentials of the NCS mitigation in the future 10 (2020-2030) and 40 years (2020-2060), corresponding to the timetable of China's NDCs, i.e., carbon peak before 2030 and carbon neutrality by 2060.

The settings of baseline in this study are different from the existing assessments (2000s-2010s as a baseline and 2010-2025/2030/2050 as a scenario) [1,22,23,27,28]. Baseline sets the temporal and spatial reference for NCS pathway scenarios, which may have a great impact on the NCS estimates. Notably, NCS actions during 2000-2020 will have a great impact in the future time periods, which we refer to as the "legacy effect". The legacy effect, mainly reforestation, itself is independent of being assessed, but it is conceptually attributed to natural flux and excluded from future NCS potential estimates.

Maximum potential. The MAMP refers to the additional CO_2 sequestration or avoided GHG emission measured in CO_2 equivalents (CO_2e) at given flux rates in a period on the maximum extent to which the stewardship options are applied (numbers are expressed as Tg CO_2e yr^{-1} for individual pathways and Pg CO_2e yr^{-1} for national total) (Extended Data Fig. 1, Supplementary Table S2). And "additional" means mitigation outcomes due to human actions taken beyond business-as-usual land use activities (i.e., since 2020), and excluding existing land fluxes not attributed to direct human activities [1]. The MAMP of CH_4 and N_2O are accounted by three cropland and wetland pathways (i.e., cropland nutrient management, improved rice cultivation, and peatland restoration). We adopt 100-year Global Warming Potential (GWP_{100}) to calculate the warming equivalent for CH_4 (25) and N_2O (298), respectively [38,39] because these values are used in National Greenhouse Gas Inventories, although some researchers have argued that using the fixed GWP_{100} to calculate the warming equivalents may be problematic because they cannot differentiate the contrasting impacts of the long- and short-lived climate pollutants [39]. Because the flux rate of the GHG by ecosystems may vary with the time of recovery or growth, the MAMP may also change for different periods even given the same extent.

The "maximum" is constrained by varied factors across the NCS pathways. We constrain forest and grassland restoration by the rate of implementation, *farmland red line* and tree surviving rate (Extended Data Fig. 2). Surviving rate here is the ratio of the area with increased vegetation cover due to reforestation to the total reforestation area. The *farmland red line* refers to "the minimum area of cultivated land" given by the Ministry of Land and Resources of China. It defines the lowest limit and the current red line is ~120 Mha. It is a rigid constraint below which the total amount of cultivated land cannot be reduced. From this total amount, there is provincial farmland red line. This red line sets a constraint on the implementation of the NCS pathways associated with land use change. We set the future scenario of farmland area that can be used for grassland or forest restoration based on the provincial farmland red line. Basic farmland is closely related to national food security. By 2050, China's population is predicted to decrease slightly, but with economic development, the *per capita* demand for food may increase [40]. We assume that the food production in the future can meet the food demand *via* increasing agricultural investment and technological advancement. The N fertilizer reduction scenario is set to be below the level 60%, under which crop yield is not significantly affected [19], in the fact that N fertilizer is surplus in many Chinese croplands.

For timber production, we assume that the demand for timber can be met if the production level is maintained at the level of 2010-2020 (83.31 million m^{-3} yr^{-1}). As deforestation of natural forests is 100% forbidden since 2020, before that harvest is on the verge of depletion, the future timber will mainly come from tree plantations. For grazing optimization, we assume that livestock production is not affected by grassland fencing due to refined livestock management such as improving feed nutrient and fine-seed breeding [41].

The areas of historical NCS implementation during 2000-2020 were estimated using statistical data, published literature and public documents, with a supplement from remote sensing data. The flux rates were obtained by either directly using the values from multiple literature or from estimates using the empirical formulae. For the estimates of future NCS potential, the flux rate and extent of the pathway were determined based on the baseline (i.e., 2000-2020). The extent is assumed to be achieved by using the same rate but limited by the multiple constraints stated above, unless the implementation scopes have been reported in national planning documents. We estimate the legacy effect by multiplying the implementation area in the past by the flux rates in the future two periods for NCS estimation.

Saturation. The future mitigation potential that we estimate for 2030 and 2060 will not persist indefinitely because the finite potential for natural ecosystems to store additional carbon will saturate. For each NCS pathway, we estimate the expected duration of the potential for sequestration at the maximum rate (Supplementary Table S3). Forests can continue to sequester carbon for >70-100 years. Restored grasslands and fenced grasslands can continue to sequestrate carbon for >50 years. Forest fire management and cover crops can continue to sequestrate carbon for over 40-50 years. Seagrasses and peatlands can continue to sequestrate carbon for millennia. Avoided pathways do not saturate as long as the business as usual (BAU) cases indicate that there are potential area for avoided losses of ecosystems. In this case, seagrass and salt marsh would disappear entirely after 64 years, but >100-300 years for forest, grassland and peatland.

Estimation of uncertainties. The extent (i.e., area or biomass amount) and flux (i.e., sequestration or reduced emission per area or biomass amount in unit time) are considered to estimate uncertainty of the historical mitigation capacity or future potential for each NCS pathway. We use the IPCC approaches to combine uncertainty [42]. Where mean and standard deviation (SD) are possible to be estimated from collected literature, 95% confidence intervals (CI) are presented based on multiple published estimates. Where a sample of estimates is not available but only having the range of a factor, we report uncertainty as a range and use Monte Carlo simulations (with normal distribution and 100,000 iterations) to combine the uncertainties of extent and flux (IPCC Approach 2). The overall uncertainty of the 16 NCS pathways were combined using IPCC Approach 1 [42]. If the extent estimate is based on a policy determination, rather than an empirical estimated of biophysical potential, we do not consider it as a source of uncertainty.

Marginal Abatement Costs. The economic/cost constraints refer to the amount of NCS that can be achieved at a given social cost. The marginal abatement cost (MAC) curve is fitted according to the total publicly funded investment and total mitigation capacity or potential during a time period. The MAC curves are drawn to estimate the MAMP at the cost thresholds of 10, 50 and 100 USD Mg CO_2e^{-1}, respectively. The trading price in China's current carbon market is ~10 USD (as the minimum cost [43]) and the cost-effective price point [44,45] to achieve the Paris Agreement goal of limiting global warming to below 2°C above pre-industrial levels is 100 USD (as the maximum cost). A carbon price 50 USD is regarded as a medium value [1,46]. For the pathways of reforestation, natural forest management, avoided grassland conversion, grazing optimization, and grassland restoration, we collected the statistical data of investments in China from 2000 to 2020, and estimated the affordable MAMP below the three mitigation costs. Due to data limitations, the points used for fitting the MAC curve are values for cost (i.e. invested funds) and benefit (i.e. mitigation capacity) in each of the provinces. We rank the ratio of benefit to cost in a descending order to obtain the maximum marginal benefit for MAC, by assuming that NCS measures are firstly implemented in the region with the highest cost-benefit rate. We refer to the investment standard before 2020 as the benchmark and estimate the cost of each pathway for the future time periods with discount rates of 3% and 5%, respectively. The social discount rate 4-6% is usually used as a benchmark discount value in carbon price studies in China compared with lower scenarios (e.g., 3.6%) [46,47]. In a global study for estimating country-level social cost of carbon, 3% and 5% are used for scenario analysis [48]. Note that the mean value from the two discount rates was used in presenting the results. For the other pathways where investment data cannot be obtained, we refer to relevant references to estimate MAC. All the cost estimates are expressed in 2015 dollars, transformed based on CNY and USD exchange rate of the same year. The year 2015 represents a relatively stable condition of economic increase over the past decade (i.e., 2011-2020) in China (i.e., the increase rate of GDP 2015 is similar to the ten-year mean). In the cases when the MAC curves exceed the estimated maximum potentials in the time period, we identify the historical capacity or the MAMP as limited by the biophysical estimates.

Additional mitigation required to meet Paris Agreement NDCs. On October 28, 2021, China officially submitted "China's Achievements, New Goals and New Measures for Nationally Determined Contributions" (called 'New Measures 2021' hereafter) and "China's Mid-Century Long-Term Low Greenhouse Gas Emission Development Strategy" to the Secretariat of the United Nations Framework Convention on Climate Change (UNFCCC), as an enhanced strategy to the updated China's NDCs (first submission in 2015). The goal of China's updated NDCs is to strive to peak CO_2 emission before 2030 and achieve carbon neutralization by 2060. It specified the goals to include: before 2030, China's carbon dioxide emission per unit of GDP are expected be more than 65% lower than that in 2005; and the forest stock volume is expected to be increased by around 6.0 (previously 4.5) billion cubic meters on the 2005 level. In the 'New Measures 2021' [9] and *Master plan of Major Projects of National Important Ecosystem Protection and Restoration (2021-2035)*[5], many NCS-related opportunities are proposed to consolidate the carbon sequestration of ecosystems and increase the future NCS potential, including protecting the existing ecosystems, implementing engineering to precisely improve forest quality, continuously increasing forest area and stock volume, strengthening grassland protection and recovery and wetland protection, and improving the quality of cultivated land and the agricultural carbon sinks.

Industrial CO_2 emission. The historical CO_2 emission data from 2000-2017 [49,50] is used as the benchmark of industrial CO_2 emission during 2000-2020. For future projections, we use the peak value of the A1B2C2 scenario (in the range of 10000 to 12000 Mt) in 2030 from Sun et al. [11].

Characterizing co-benefits. NCS activities proposed in the future measures or plans may enhance co-benefits. Four generalized types of ecosystem services are identified, including improving biodiversity, water-, soil-, and air-related ecosystem services (Fig. 1). Biodiversity benefits refer to the increase in different levels of diversity (alpha, beta, and/or gamma diversity) [51]. Water, soil, and air benefits refer to flood regulation and water purification, improved fertility and erosion prevention, and improvements in air quality, respectively, as defined in the Millennium Ecosystem Assessment [52]. The evidence that each pathway produces co-benefits from one or more-peer reviewed publications was collected through reviewing the literature (see the details for co-benefits of each pathway in Supplementary Information).

Mapping province-level mitigation. The data for extent of implementing forest pathways is obtained from the statistical yearbook that are reported at the province level. To be consistent with the forest pathways, the other pathways were also aggregated to the provincial-level estimate from the spatial data. If the flux data was available in different climate regions, the provinces are firstly assigned into climate regions. When a province spans multiple climate zones, the weight value is set according to the proportion of area, and finally an estimated value of rate was calculated (for fire management, some grassland and wetland pathways). For the forest pathways, we firstly collected the flux rate data from reviewing literature, and then averaged these flux rates to the province level by each age group. The flux rates for reforestation (including artificial forests) and natural forest management were calculated separately by province and age group. Similarly, specified flux rates are applied for different time after ecosystem restoration or conversion for other pathways.

Classification of NCS types: protection, management, and restoration. Three types of NCS pathways were classified, i.e., protection (of intact natural ecosystems), improved management (on managed lands), and restoration (of native cover)[41]. In our study, **4** (AVFC, AVGC, AVCI, AVPI), **8** (IMP, NFM, FM, BIOC, CVCR, CRNM, IMRC, GROP) and **4** (RF, GRR, CWR, PTR) NCS pathways were identified as protection, management and restoration types, respectively (Supplementary Information Table S1). These pathways can be further divided into groups of ‘Single’ type or ‘Mixed’ type according to their contribution to individual pathways. Specifically, in a certain area, when the mitigation capacity of a certain pathway accounts for more than 50% of the total, it is regarded as a single or dominant NCS type; if no single pathway accounts for more than 50%, it is a mixed type, named by the top pathways whose NCS sum exceeds 50% of the total mitigation capacity.

Data availability: All data generated or analysed during this study are provided with data sources in the Supplementary Information file.

Code availability statement: We acknowledge the ArcMap Software: Version 10.6 (https://www.esri.com/en-us/arcgis/products/arcgis-desktop/resources); R Software Foundation: Version R x64 4.0.3 (https://mirrors.tuna.tsinghua.edu.cn/CRAN/); and Python Software Foundation: Python Language Reference, Version 3.7.7; (http://www.python.org).

References

38. Tian, H. et al. The terrestrial biosphere as a net source of greenhouse gases to the atmosphere. *Nature*. **531**, 225-228 (2016)

39. Lynch J., Cain, M., Pierrehumbert, R., Allen, M. Demonstrating GWP*: a means of reporting warming-equivalent emissions that captures the contrasting impacts of short- and long-lived climate pollutants. *Environ. Res. Lett.* **15**, 044023 (2020)

40. Gu, B., Ju, X., Chang, J., Ge, Y. & Vitousek, P. M. Integrated reactive nitrogen budgets and future trends in China. *Proc. Natl. Acad. Sci. U.S.A.* **112**(28), 8792-

8797 (2015).

41. Yang, M. et al. Trade-offs in ecological, productivity and livelihood dimensions inform sustainable grassland management: Case study from the Qinghai-Tibetan Plateau. *Agric. Ecosyst. Environ.* **313**, 207377 (2021).

42. Frey, C. et al. Chapter 3: Uncertainties, in 2006 IPCC Guidelines for National Greenhouse Gas Inventories (Intergovernmental Panel on Climate Change, 2006), p. 3.1–3.66. (2006). www.ipcc-nggip.iges.or.jp/public/2006gl/pdf/1_Volume1/V1_3_Ch3_Uncertainties. pdf.

43. Research report on the formation mechanism of carbon price in China. EDF (Environmental Defense Fund). https://ricn.sjtu.edu.cn/Web/Show/5 (in Chinese) (2021).

44. Dietz, S. & Stern, N. Endogenous Growth, Convexity of Damage and Climate Risk: How Nordhaus' Framework Supports Deep Cuts in Carbon Emissions. *Econ. J (Oxf)*. **125**, 574-620 (2015).

45. Glanemann, N., Willner, S.N., Levermann. A. Paris Climate Agreement passes the cost-benefit test. *Nature Comm.* **11**(1):110. DOI: 10.1038/s41467-019-13961-1. (2020).

46. Tian, L., Ye, Q., Zhen, Z. A new assessment model of social cost of carbon and its situation analysis in China. *J. Clean. Prod.* **211**, 1434-1443, https://doi.org/10.1016/j.jclepro.2018.11.117 (2019).

47. Wang, K., Mao, Y., et al., 2018. The optimal research and development portfolio of low-carbon energy technologies: a study of China. *J. Clean. Prod.* **176**, 1065e1077.

48. Ricke, K., Drouet, L., Caldeira, K. et al. Country-level social cost of carbon. *Nature Clim. Change* **8**, 895-900. https://doi.org/10.1038/s41558-018-0282-y (2018).

49. Shan, Y., Huang, Q., Guan, D. & Hubacek, K. China CO_2 emission accounts 2016-2017. *Sci. Data* **7** (1) (2020).

50. Shan, Y., Guan, D., Zheng, H., Ou, J. & Qiang, Z. China CO_2 emission accounts

1997-2015. *Sci. Data* **5**, 170201 (2018).

51. United Nations, Convention on Biological Diversity (United Nations, 1992); www.cbd.int/doc/legal/cbd-en.pdf.

52. Millennium Ecosystem Assessment, Ecosystems and Human Well-being: Synthesis (Island Press). www.millenniumassessment.org/en/Synthesis.html (2005).

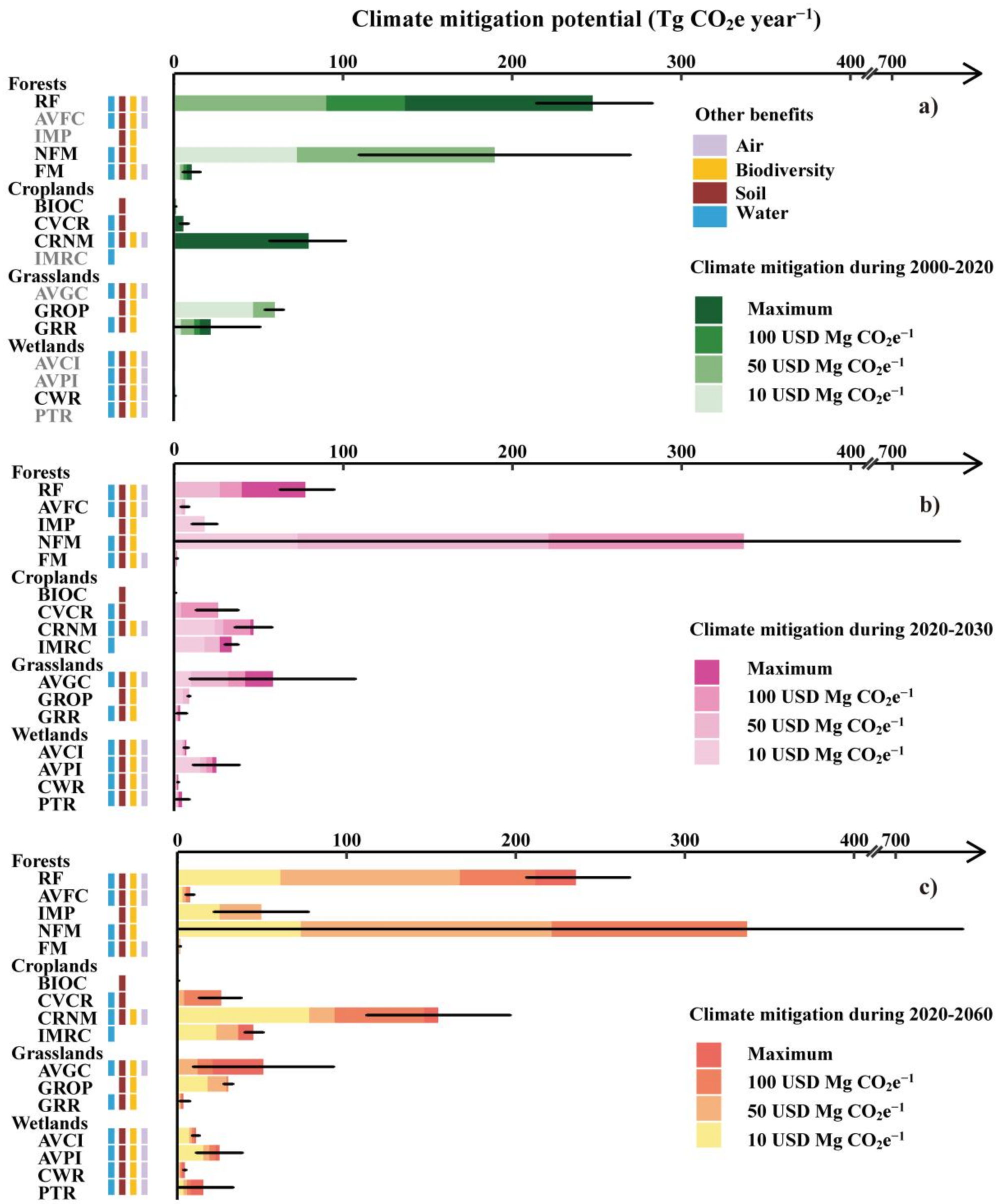

Climate mitigation potential (Tg CO_2e year^{-1})
0
100
200
300
400
700
a)
b)
c)
Forests
RF
AVFC
IMP
NFM
FM
Croplands
BIOC
CVCR
CRNM
IMRC
Grasslands
AVGC
GROP
GRR
Wetlands
AVCI
AVPI
CWR
PTR
Other benefits
Air
Biodiversity
Soil
Water
Climate mitigation during 2000-2020
Climate mitigation during 2020-2030
Climate mitigation during 2020-2060
Maximum
100 USD Mg CO_2e^{-1}
50 USD Mg CO_2e^{-1}
10 USD Mg CO_2e^{-1}

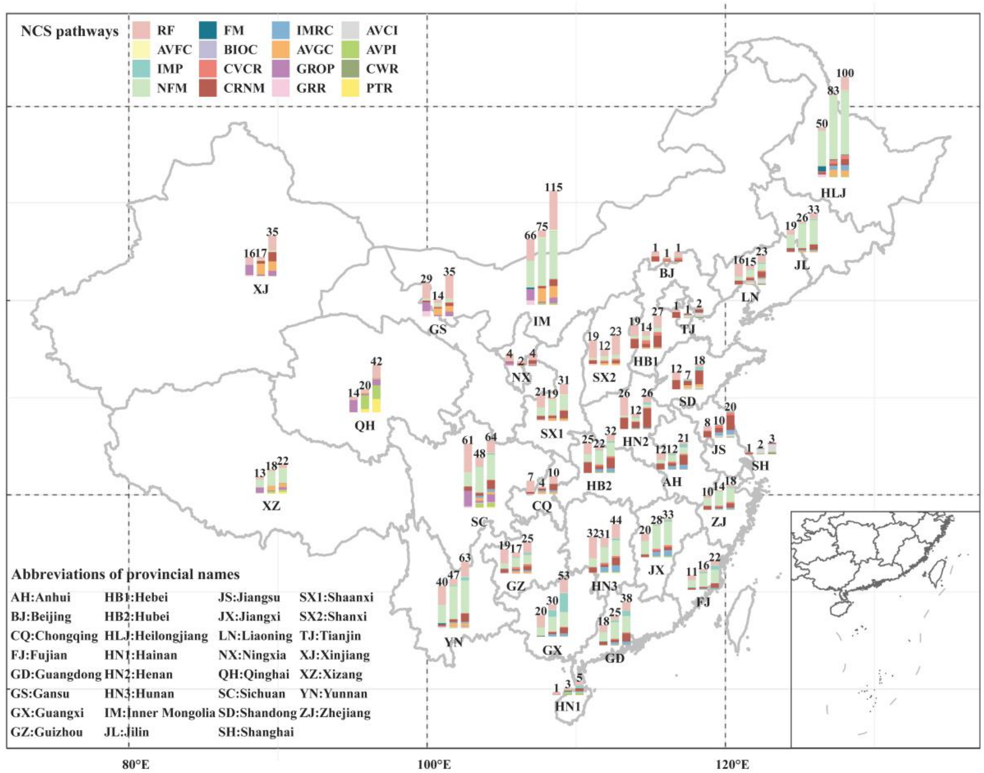

NCS pathways
RF
AVFC
IMP
NFM
FM
BIOC
CVCR
CRNM
IMRC
AVGC
GROP
GRR
AVCI
AVPI
CWR
PTR
50°N
40°N
30°N
20°N
80°E
100°E
120°E
Abbreviations of provincial names
AH:Anhui
BJ:Beijing
CQ:Chongqing
FJ:Fujian
GD:Guangdong
GS:Gansu
GX:Guangxi
GZ:Guizhou
HB1:Hebei
HB2:Hubei
HLJ:Heilongjiang
HN1:Hainan
HN2:Henan
HN3:Hunan
IM:Inner Mongolia
JL:Jilin
JS:Jiangsu
JX:Jiangxi
LN:Liaoning
NX:Ningxia
QH:Qinghai
SC:Sichuan
SD:Shandong
SH:Shanghai
SX1:Shaanxi
SX2:Shanxi
TJ:Tianjin
XJ:Xinjiang
XZ:Xizang
YN:Yunnan
ZJ:Zhejiang

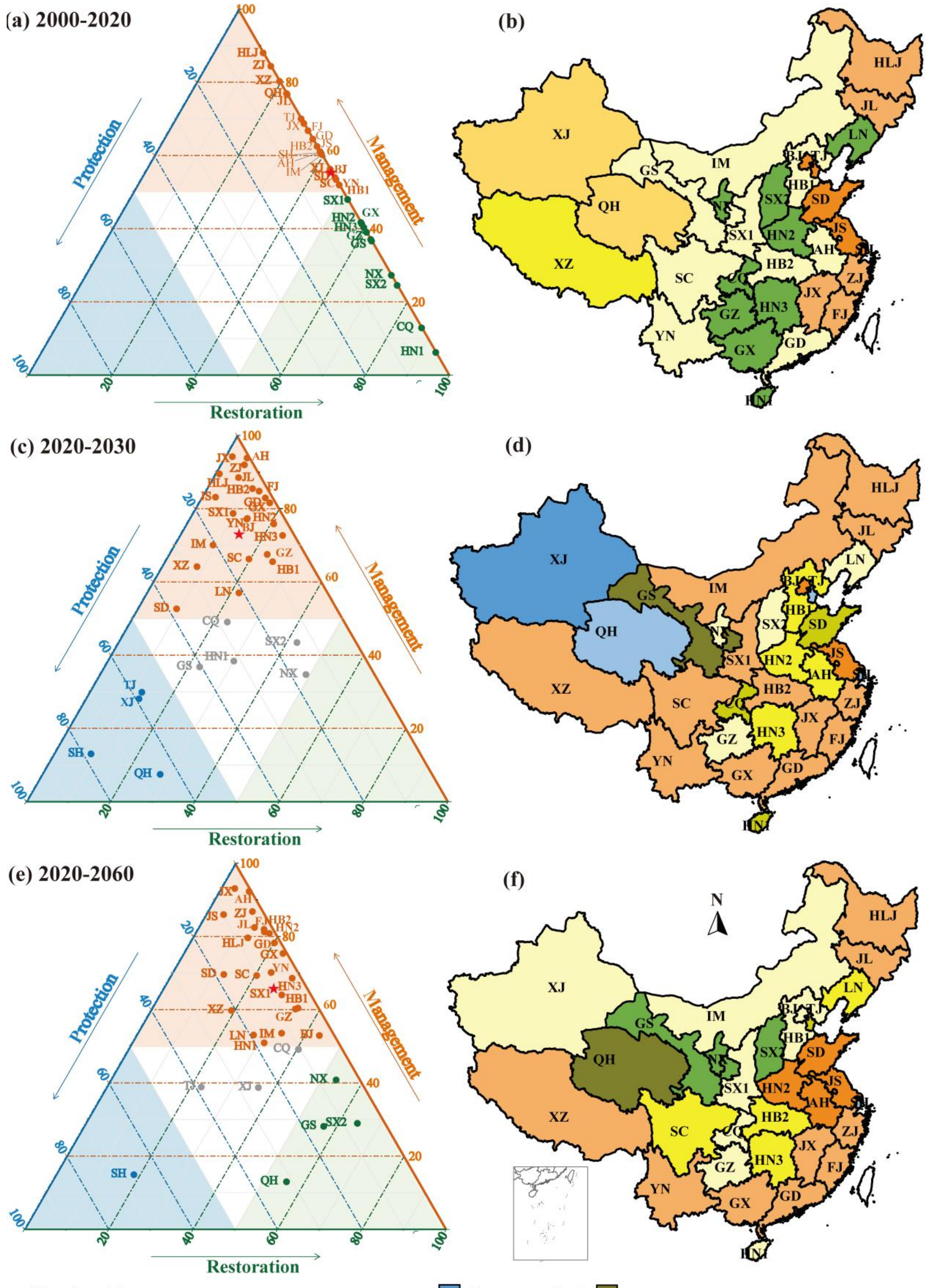
(a) 2000-2020
(b)
(c) 2020-2030
(d)
(e) 2020-2060
(f)
Protection
Management
Restoration
N
Dominant type
Restoration
Management
Protection
Mixed
National
Provincial
Protect grassland
Protect wetland
Manage cropland
Manage forest
Manage grassland
Restore forest
Mixed type of Protection and Restoration
Mixed type of Management and Protection
Mixed type of Management
Mixed type of Management and Restoration

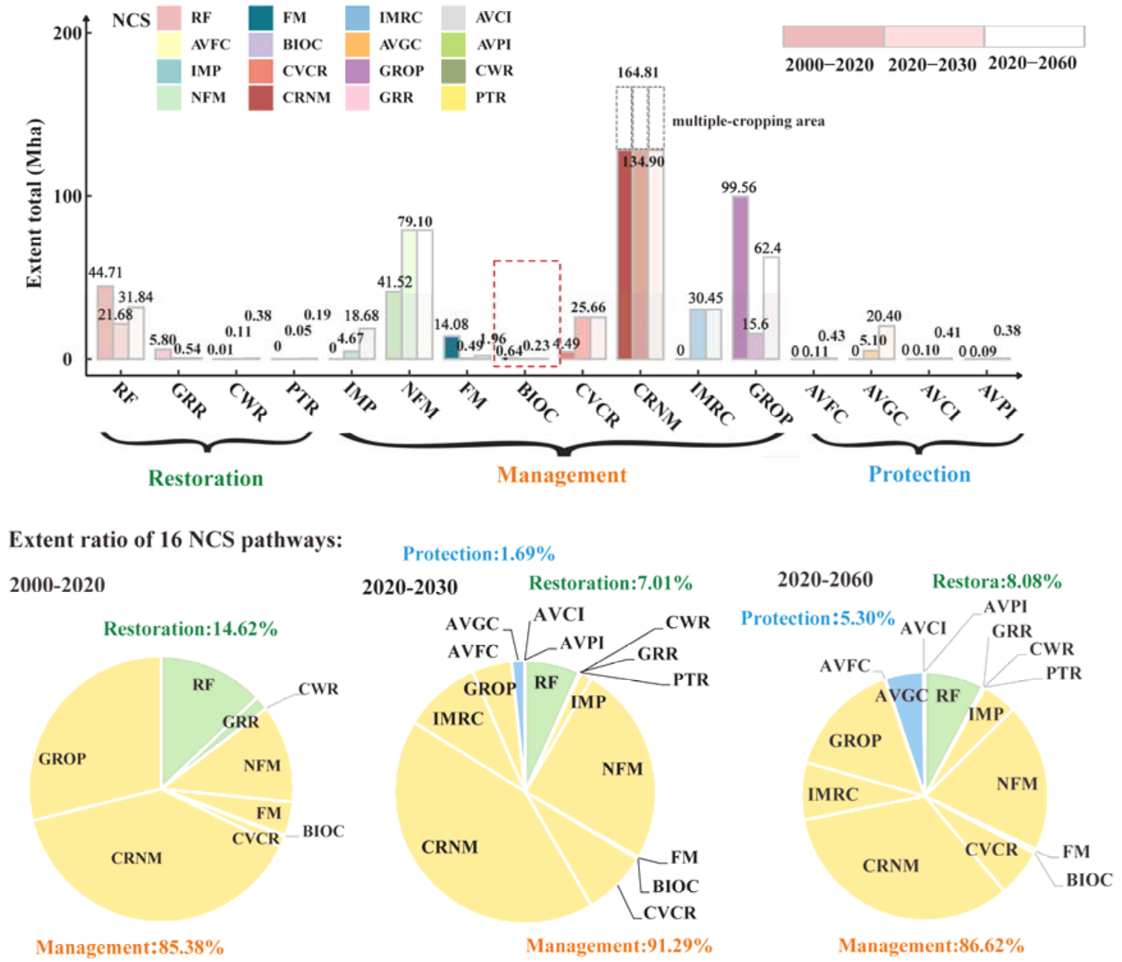

Extended Data Fig. 1. The extents of land area that adopt the different NCS pathways. The numbers in the bar chart represent the applicable extents (except for BIOC) of the different pathways during each of the three periods. Note: the areas that implement CVCR and IMRC are some proportions of the total area in CNM. The area for CNM is the cumulative area of sowing, including rotation (i.e., the dotted line bars for CNM), and therefore is greater than the total cropland area. The numbers for BIOC is not an area but the mass of crop residue (Tg dry mass). Pathway name abbreviations please see Fig. 1.

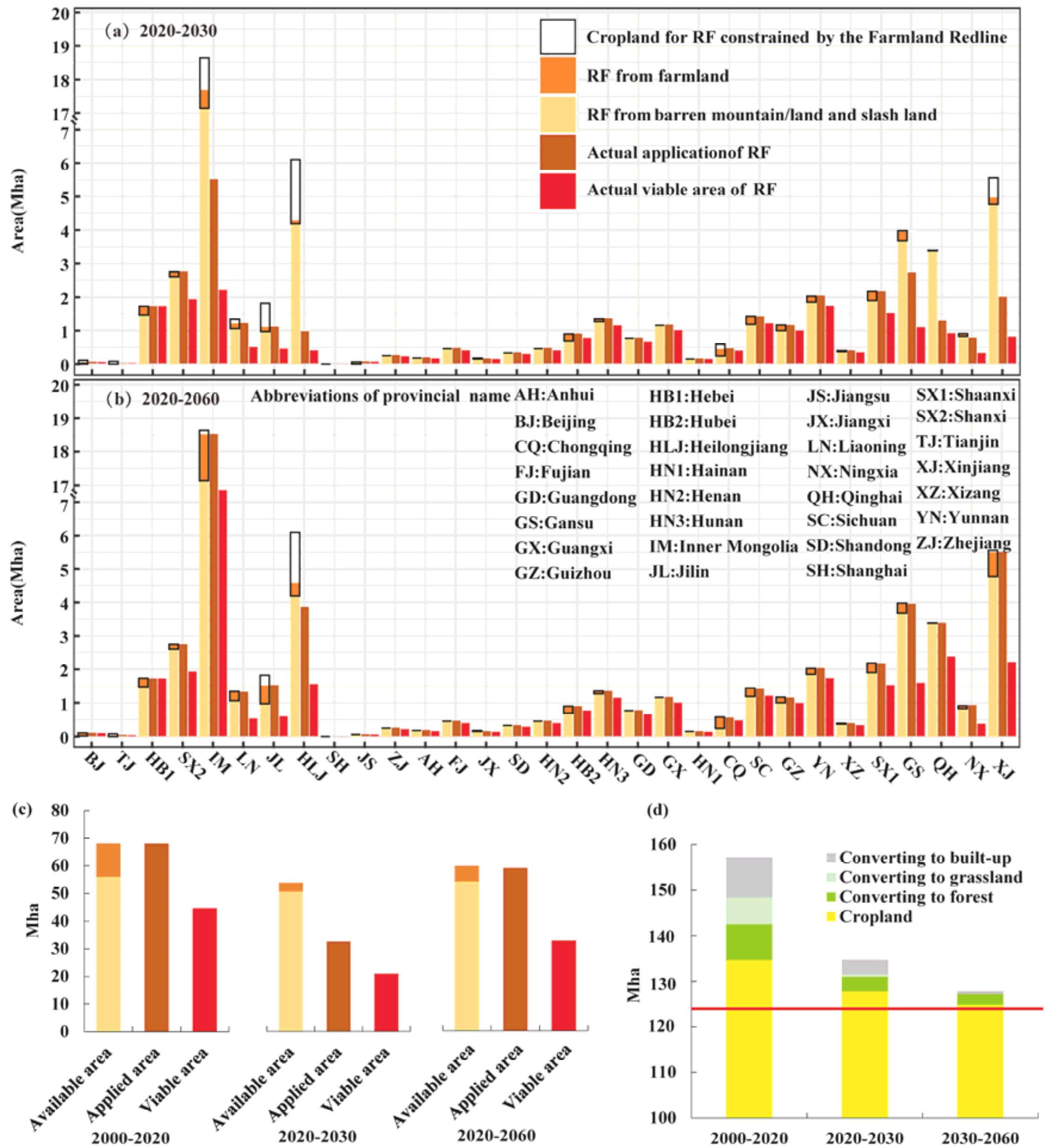

pExtended Data Fig. 2. Areas available for forest and grassland restoration. Area available for reforestation constrained by the farmland red line, water stress, and urbanization at the provincial level during (a) 2020-2030, (b) 2020-2060, and (c) the national level. Farmland area available for grassland restoration constrained by the *Farmland Red Line* and urbanization (d). The remaining cropland area (yellow bar) is approaching the *Farmland Red Line* (123.44 Mha, the red line in the Figure). Here cropland gain converting from other land cover types is not considered as these gains usually come from low-quality lands, which should be avoided in the future[31].

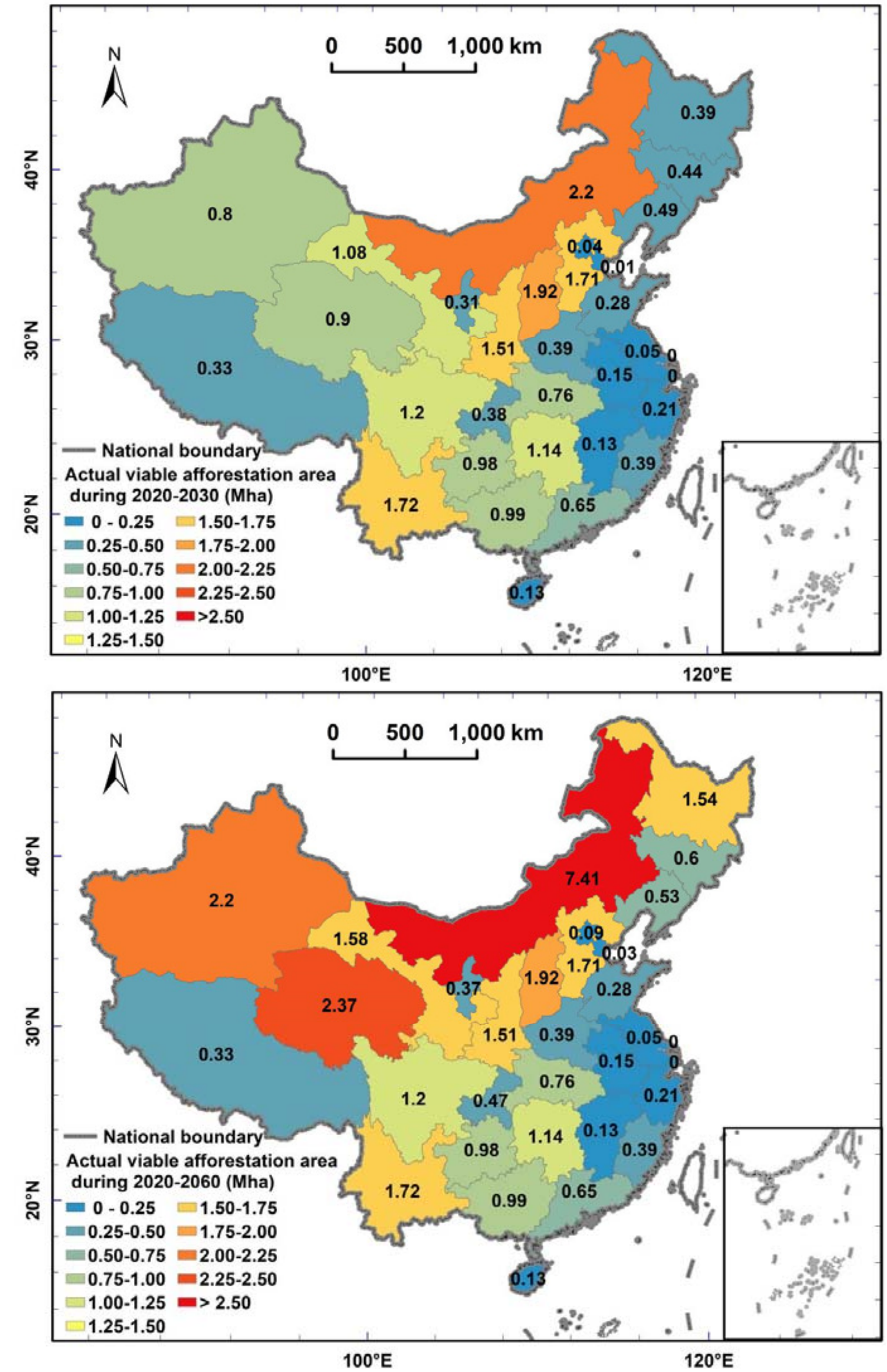

Extended Data Fig. 3. Spatial distribution of projected actual surviving area of reforestation during 2020-2030 and 2020-2060. The number represents the area for each province.

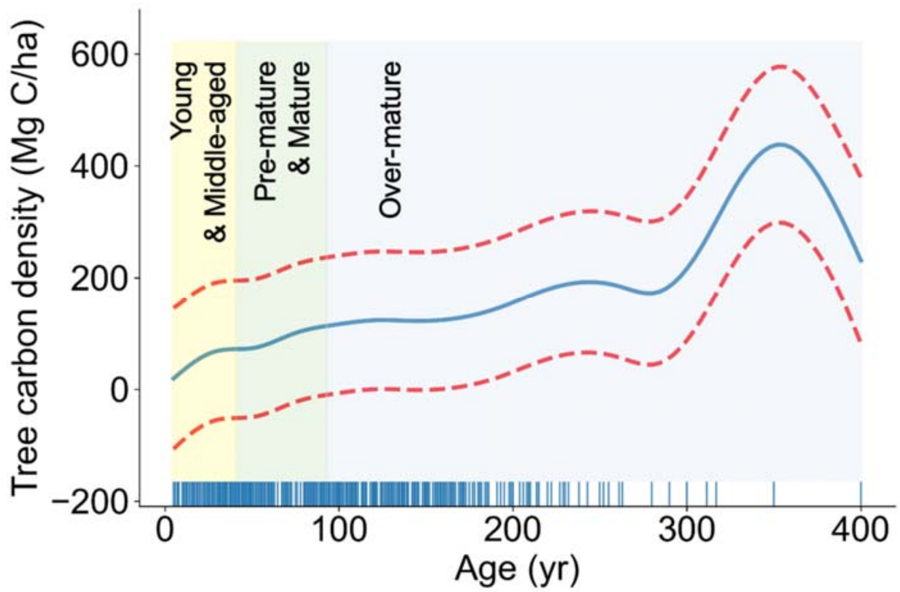

Extended Data Fig. 4. Data distribution of carbon density of tree layer with stand age (not including shrub, herb and floor layers). The data points are collected from the literature, including 762 sites and 2363 plots. The blue bars represent the age distribution of sites. The fitting curve is based on linear generative additive model (r^2 = 0.30, p<0.001).

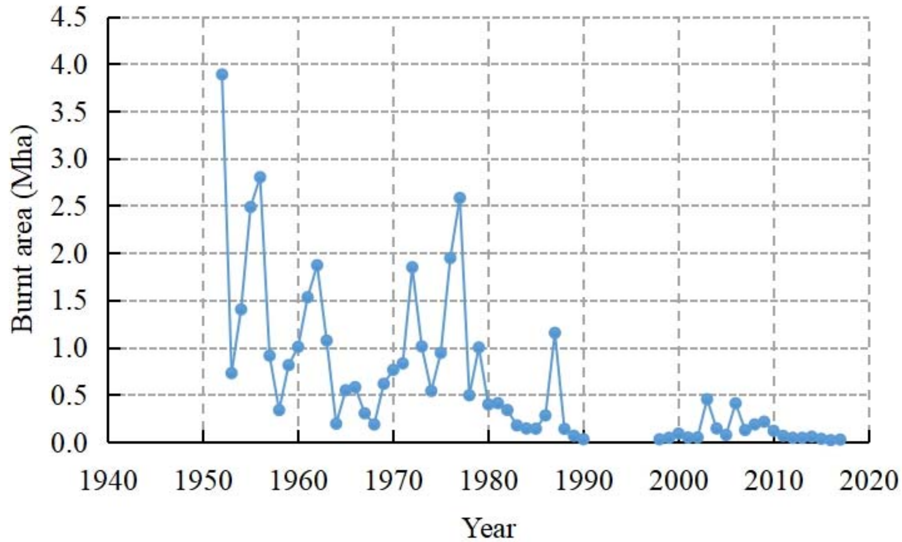

Extended Data Fig. 5. The burnt area by forest fire from 1949 to 2017. Data is obtained from http://forest.ckcest.cn/zh/lytjsjfx.html. Data is unavailable from 1991 to 1997.

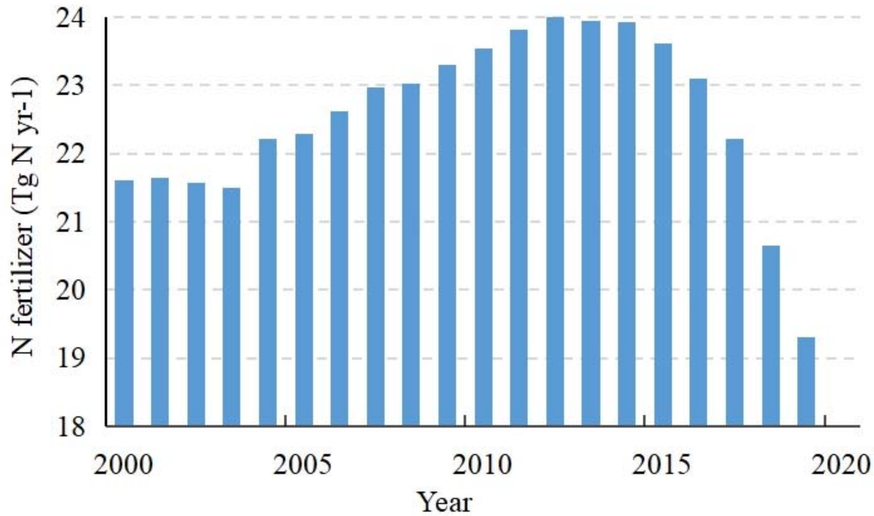

Extended Data Fig. 6. N fertilizer use changes during 2000-2019. Data is obtained from http://www.stats.gov.cn/tjsj/ndsj/.

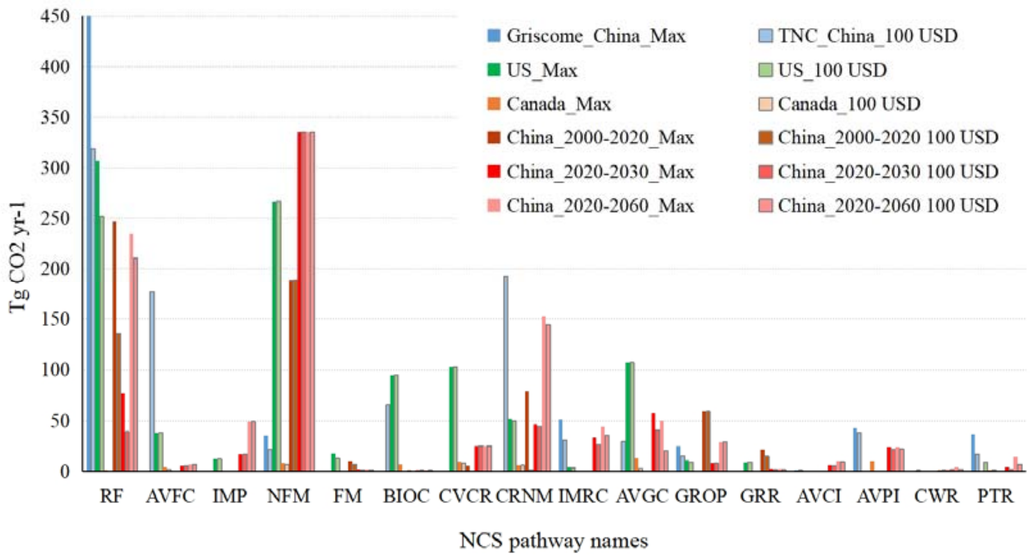

Extended Data Fig. 7. Comparison of mitigation capacity between this study and previous studies (Griscome[1], TNC[27], US[22], and Canada[23]). Note that the estimates are maximum mitigation capacity (_Max) or the amount of mitigation that can be achieved under 100 USD of mitigation price (_100 USD). The estimates of climate mitigation is at a 2030 reference year for global and Canada, and 2025 for the US. Pathway name abbreviations please see Fig. 1.

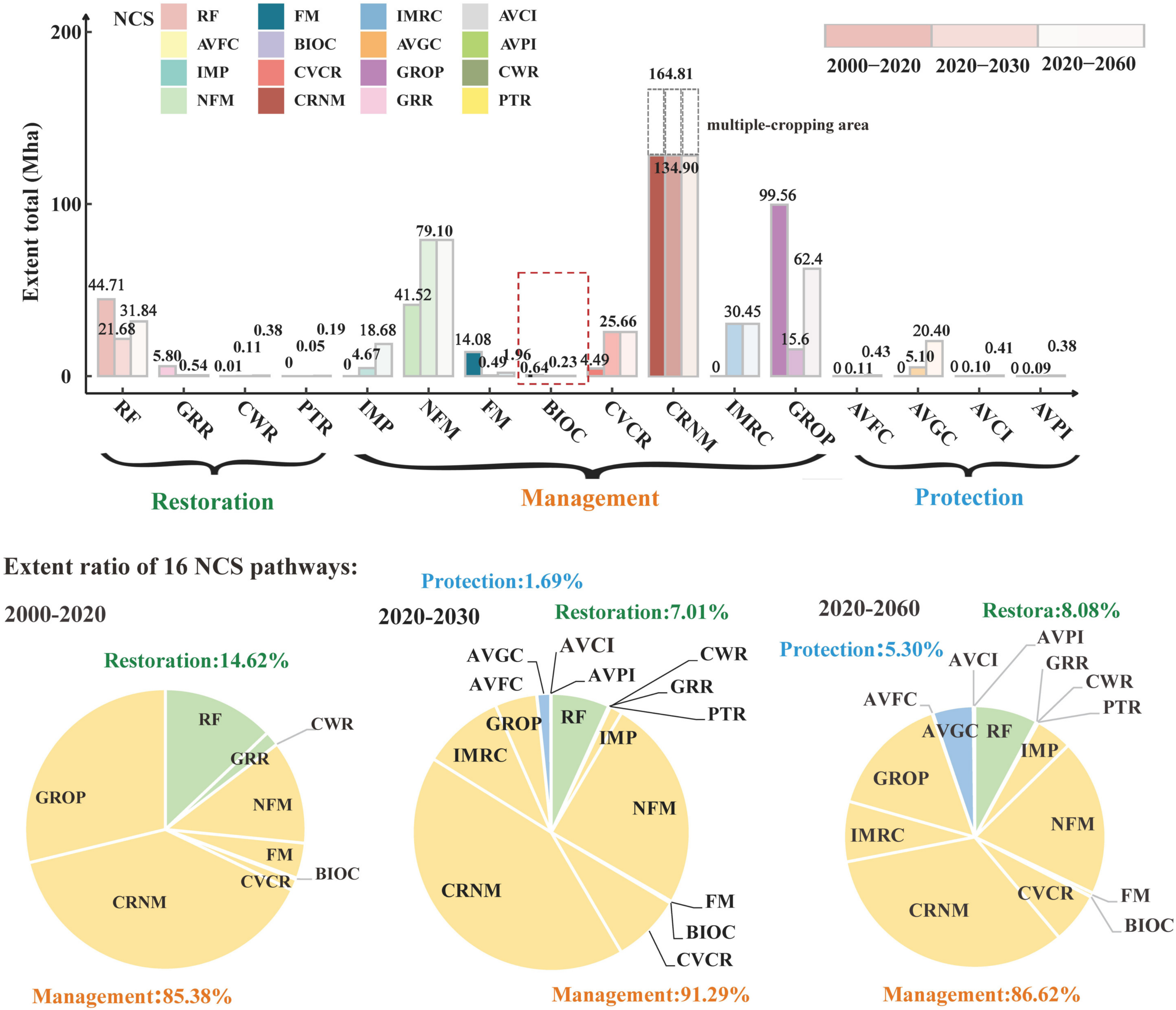

NCS
RF
AVFC
IMP
NFM
FM
BIOC
CVCR
CRNM
IMRC
AVGC
GROP
GRR
AVCI
AVPI
CWR
PTR
2000−2020
2020−2030
2020−2060
Extent total (Mha)
200
100
0
164.81
multiple-cropping area
134.90
99.56
62.4
79.10
41.52
44.71
31.84
21.68
5.80
0.54
0.01
0.11
0.38
0
0.05
0.19
0
4.67
18.68
14.08
0.49
1.96
0.64
0.23
4.49
25.66
0
30.45
15.6
0 0.11
0.43
0
5.10
20.40
0 0.10
0.41
0 0.09
0.38
RF
GRR
CWR
PTR
IMP
NFM
FM
BIOC
CVCR
CRNM
IMRC
GROP
AVFC
AVGC
AVCI
AVPI
Restoration
Management
Protection
Extent ratio of 16 NCS pathways:
2000-2020
Restoration:14.62%
RF
CWR
GRR
GROP
NFM
FM
BIOC
CVCR
CRNM
Management:85.38%
2020-2030
Protection:1.69%
Restoration:7.01%
AVGC
AVCI
AVPI
CWR
GRR
PTR
AVFC
GROP
RF
IMP
IMRC
NFM
CRNM
FM
BIOC
CVCR
Management:91.29%
2020-2060
Restora:8.08%
Protection:5.30%
AVPI
AVCI
GRR
CWR
AVFC
PTR
AVGC
RF
IMP
GROP
IMRC
NFM
CRNM
CVCR
FM
BIOC
Management:86.62%

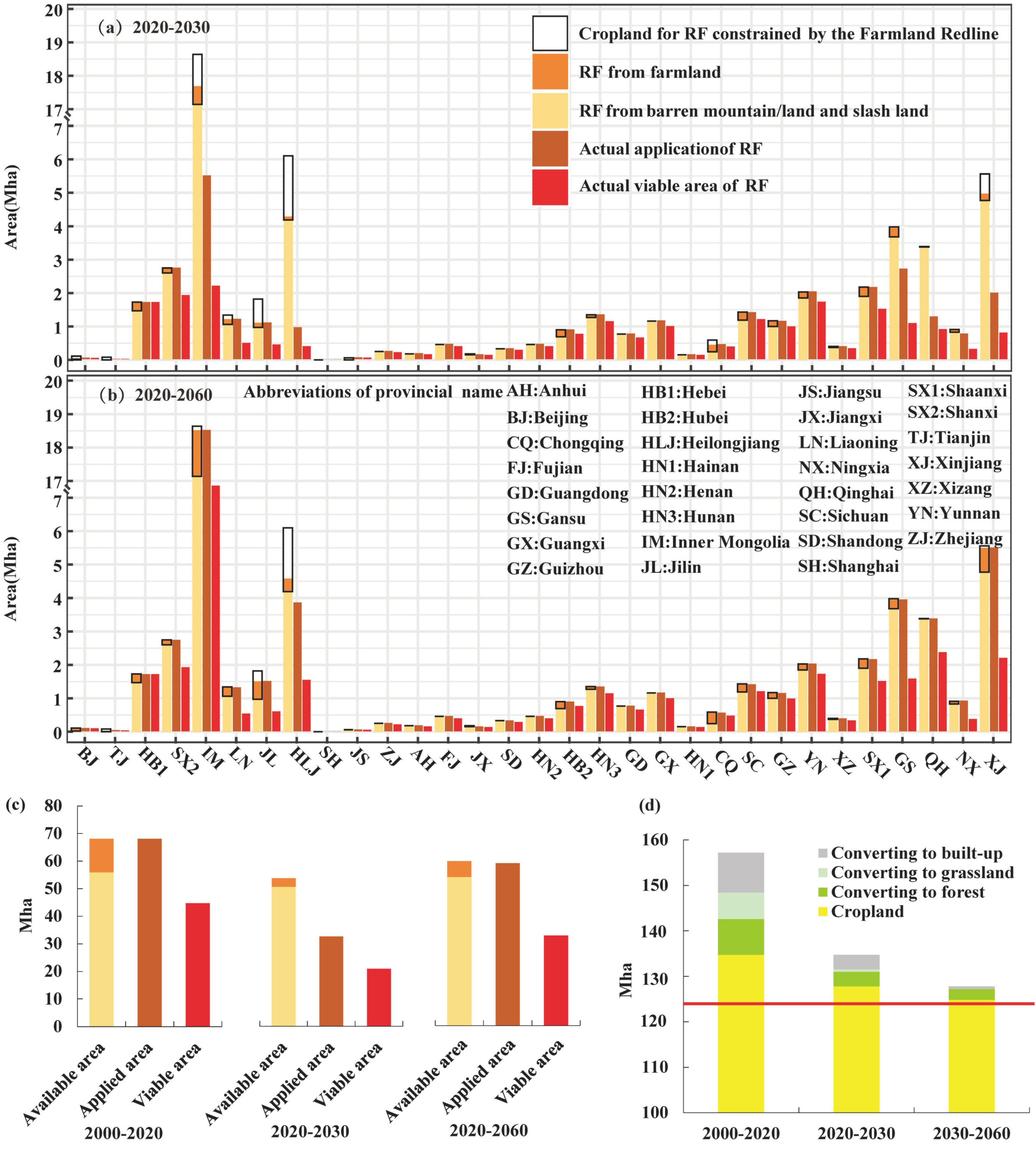
(a) 2020-2030
Cropland for RF constrained by the Farmland Redline
RF from farmland
RF from barren mountain/land and slash land
Actual applicationof RF
Actual viable area of RF
Area(Mha)
(b) 2020-2060
Abbreviations of provincial name
AH:Anhui
BJ:Beijing
CQ:Chongqing
FJ:Fujian
GD:Guangdong
GS:Gansu
GX:Guangxi
GZ:Guizhou
HB1:Hebei
HB2:Hubei
HLJ:Heilongjiang
HN1:Hainan
HN2:Henan
HN3:Hunan
IM:Inner Mongolia
JL:Jilin
JS:Jiangsu
JX:Jiangxi
LN:Liaoning
NX:Ningxia
QH:Qinghai
SC:Sichuan
SD:Shandong
SH:Shanghai
SX1:Shaanxi
SX2:Shanxi
TJ:Tianjin
XJ:Xinjiang
XZ:Xizang
YN:Yunnan
ZJ:Zhejiang
Area(Mha)
BJ TJ HB1 SX2 IM LN JL HLJ SH JS ZJ AH FJ JX SD HN2 HB2 HN3 GD GX HN1 CQ SC GZ YN XZ SX1 GS QH NX XJ
(c)
Mha
Available area
Applied area
Viable area
2000-2020
2020-2030
2020-2060
(d)
Converting to built-up
Converting to grassland
Converting to forest
Cropland
Mha
2000-2020
2020-2030
2030-2060

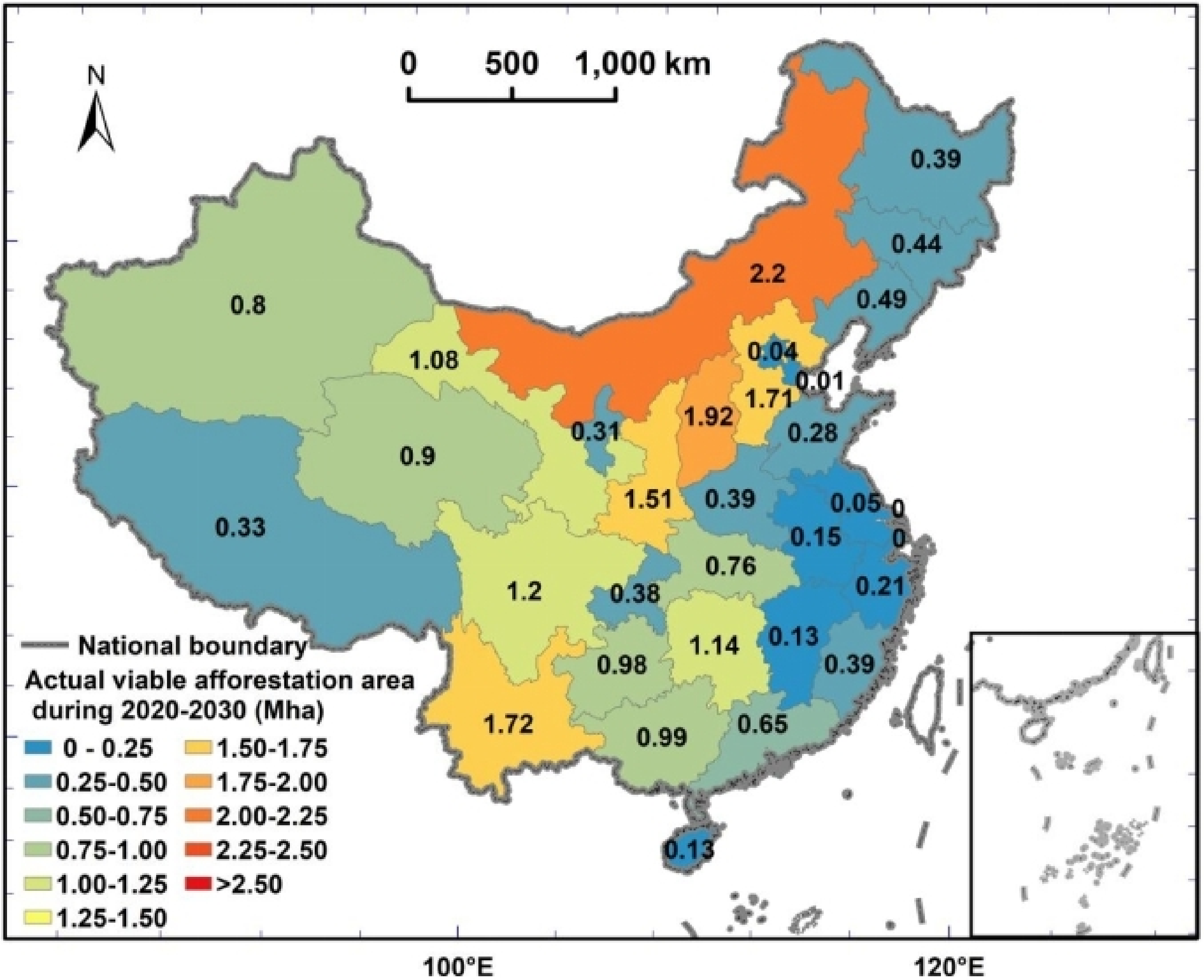

0 500 1,000 km
N
National boundary
Actual viable afforestation area during 2020-2030 (Mha)
0 - 0.25
0.25-0.50
0.50-0.75
0.75-1.00
1.00-1.25
1.25-1.50
1.50-1.75
1.75-2.00
2.00-2.25
2.25-2.50
>2.50
0.39
0.44
0.49
2.2
0.8
1.08
0.04
0.01
1.71
1.92
0.31
0.28
0.9
0.33
1.51
0.39
0.05
0
0.15
0
0.76
1.2
0.38
0.21
1.14
0.13
0.98
0.39
1.72
0.99
0.65
0.13
40°N
30°N
20°N
100°E
120°E

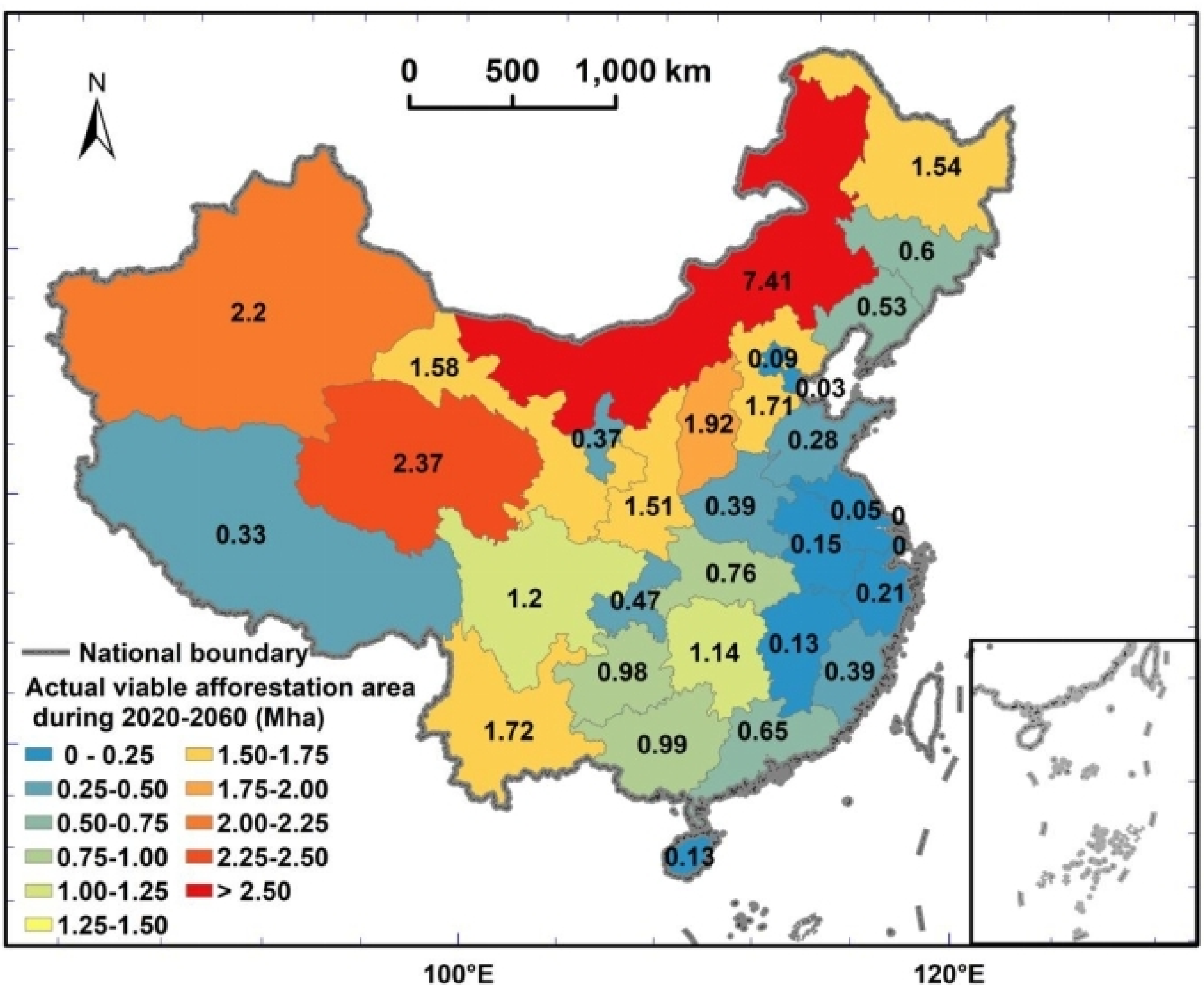

0 500 1,000 km
N
National boundary
Actual viable afforestation area during 2020-2060 (Mha)
0 - 0.25
0.25-0.50
0.50-0.75
0.75-1.00
1.00-1.25
1.25-1.50
1.50-1.75
1.75-2.00
2.00-2.25
2.25-2.50
> 2.50
1.54
0.6
7.41
0.53
2.2
1.58
0.09
0.03
1.71
1.92
0.37
0.28
2.37
0.33
1.51
0.39
0.05
0
0.15
0
0.76
1.2
0.47
0.21
1.14
0.13
0.98
0.39
1.72
0.99
0.65
0.13
40°N
30°N
20°N
100°E
120°E

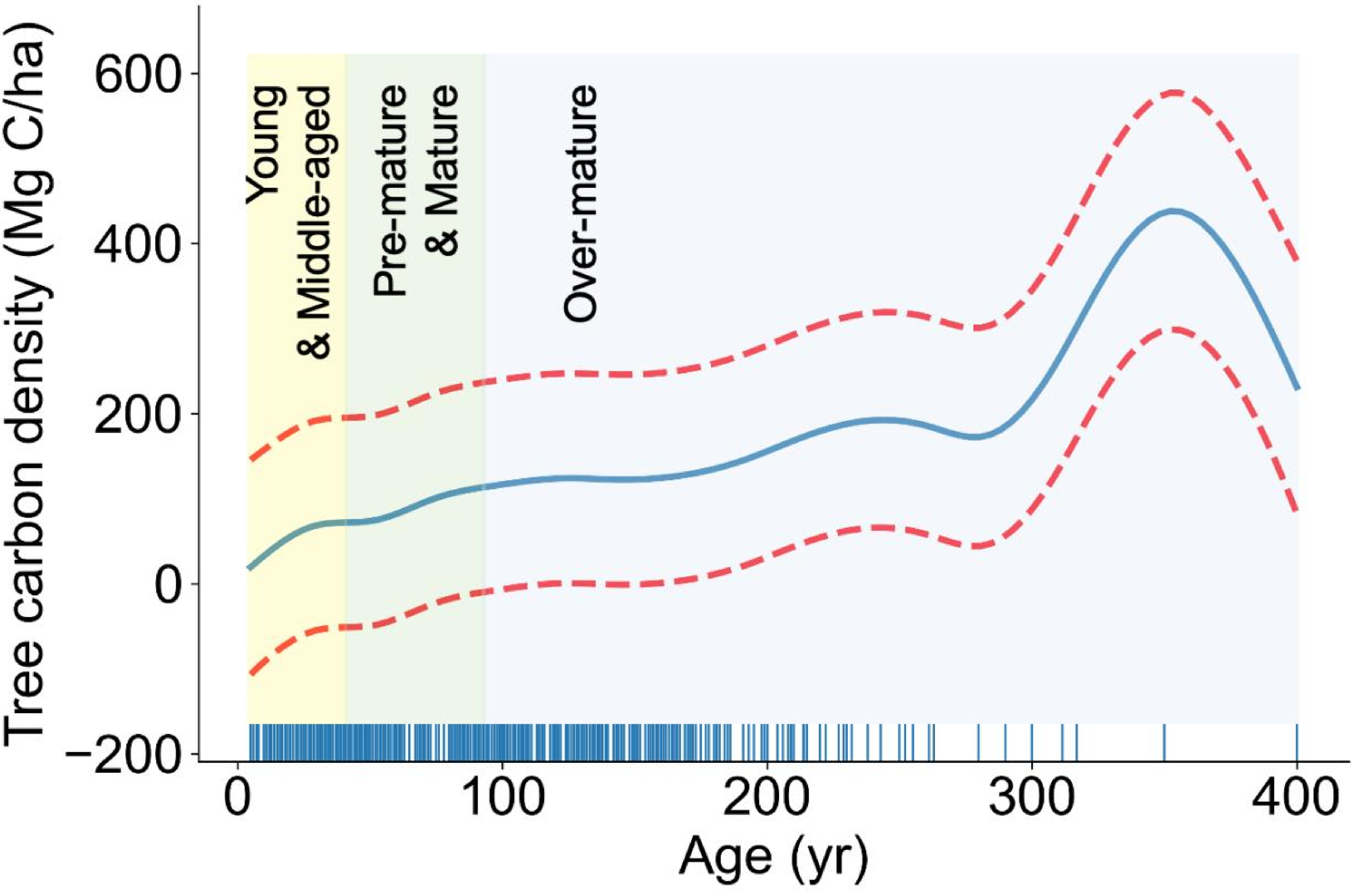

Tree carbon density (Mg C/ha)
600
400
200
0
−200
0
100
200
300
400
Age (yr)
Young
& Middle-aged
Pre-mature
& Mature
Over-mature

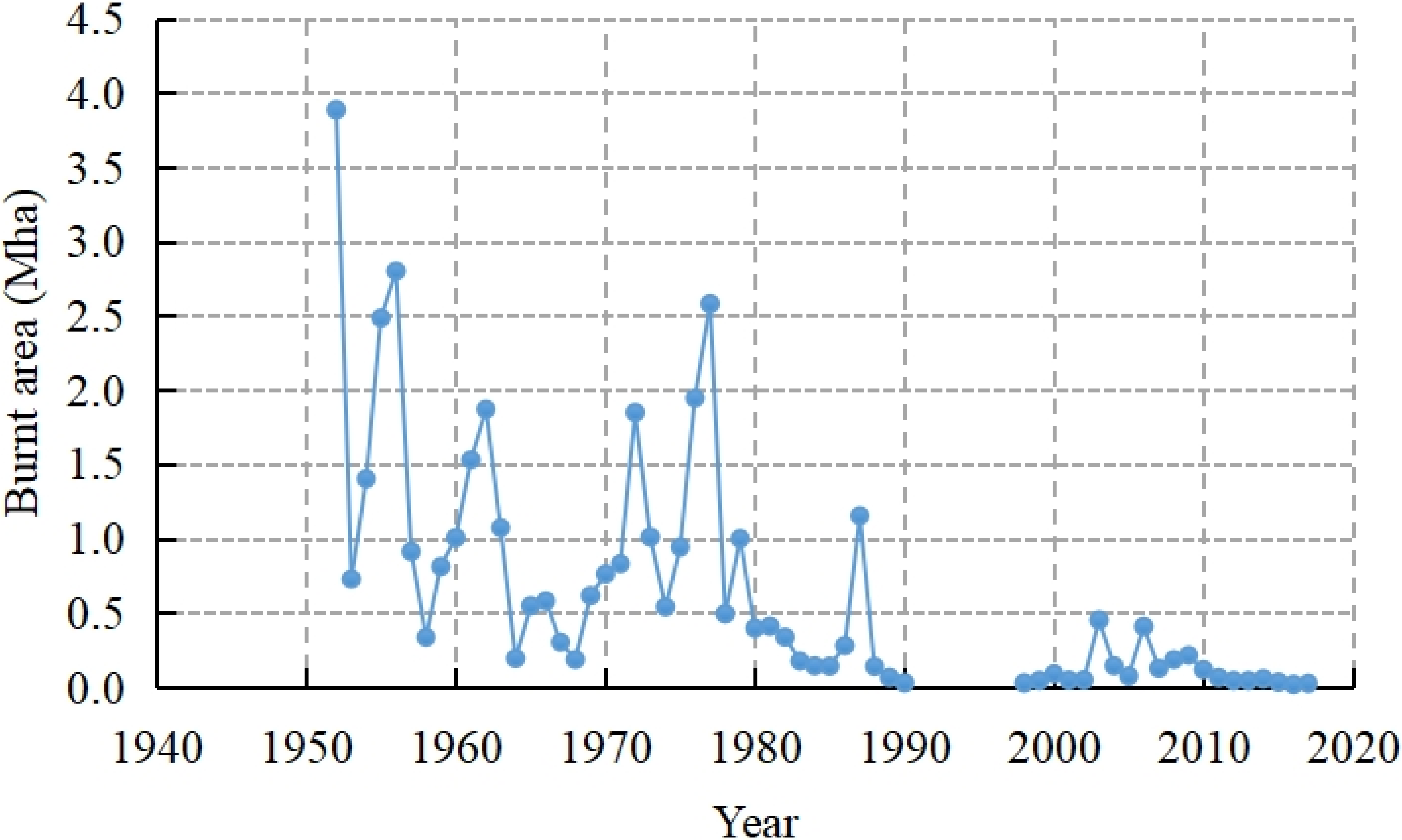

Burnt area (Mha)
4.5
4.0
3.5
3.0
2.5
2.0
1.5
1.0
0.5
0.0
1940
1950
1960
1970
1980
1990
2000
2010
2020
Year

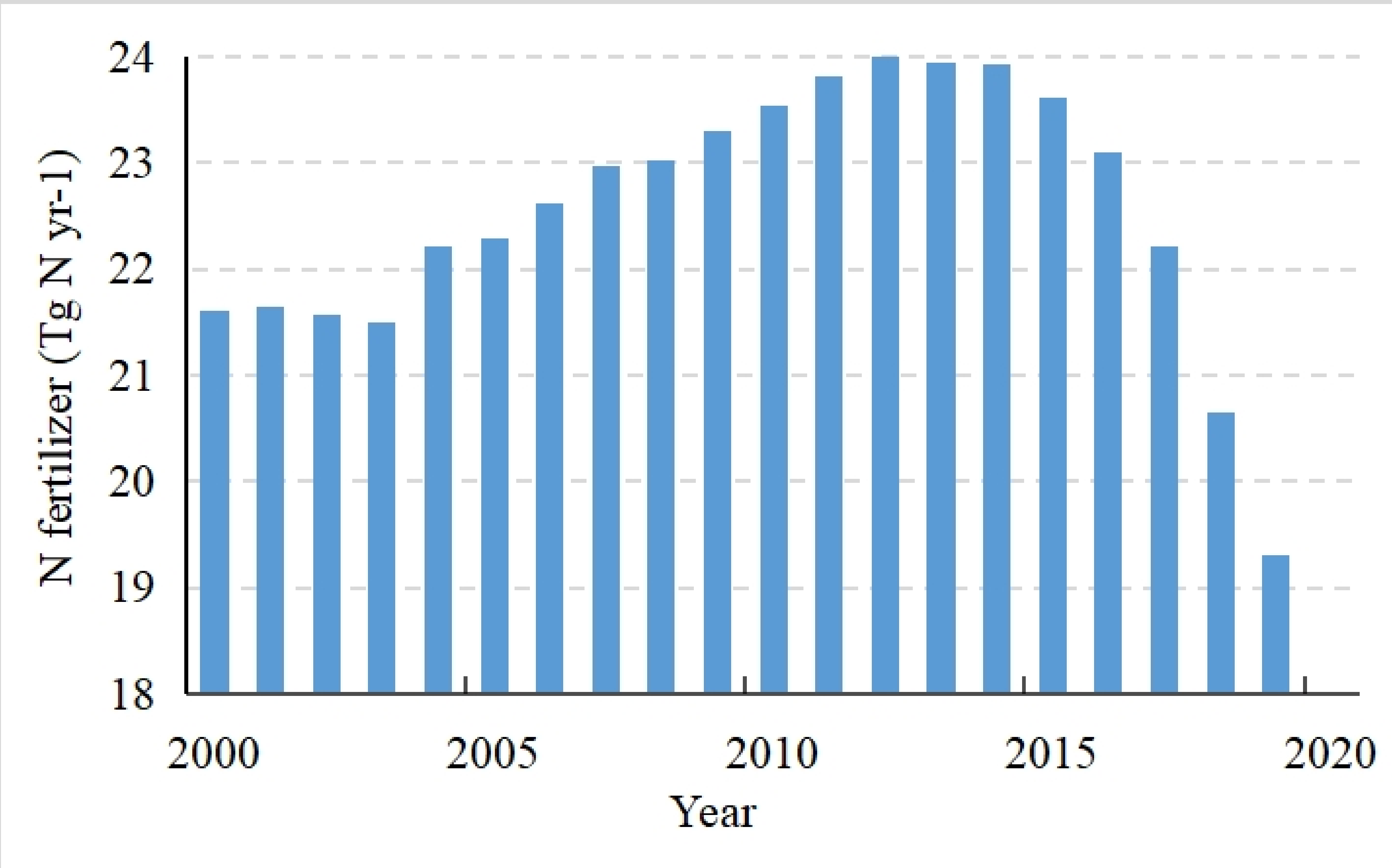

24
23
22
21
20
19
18
N fertilizer (Tg N yr-1)
2000
2005
2010
2015
2020
Year

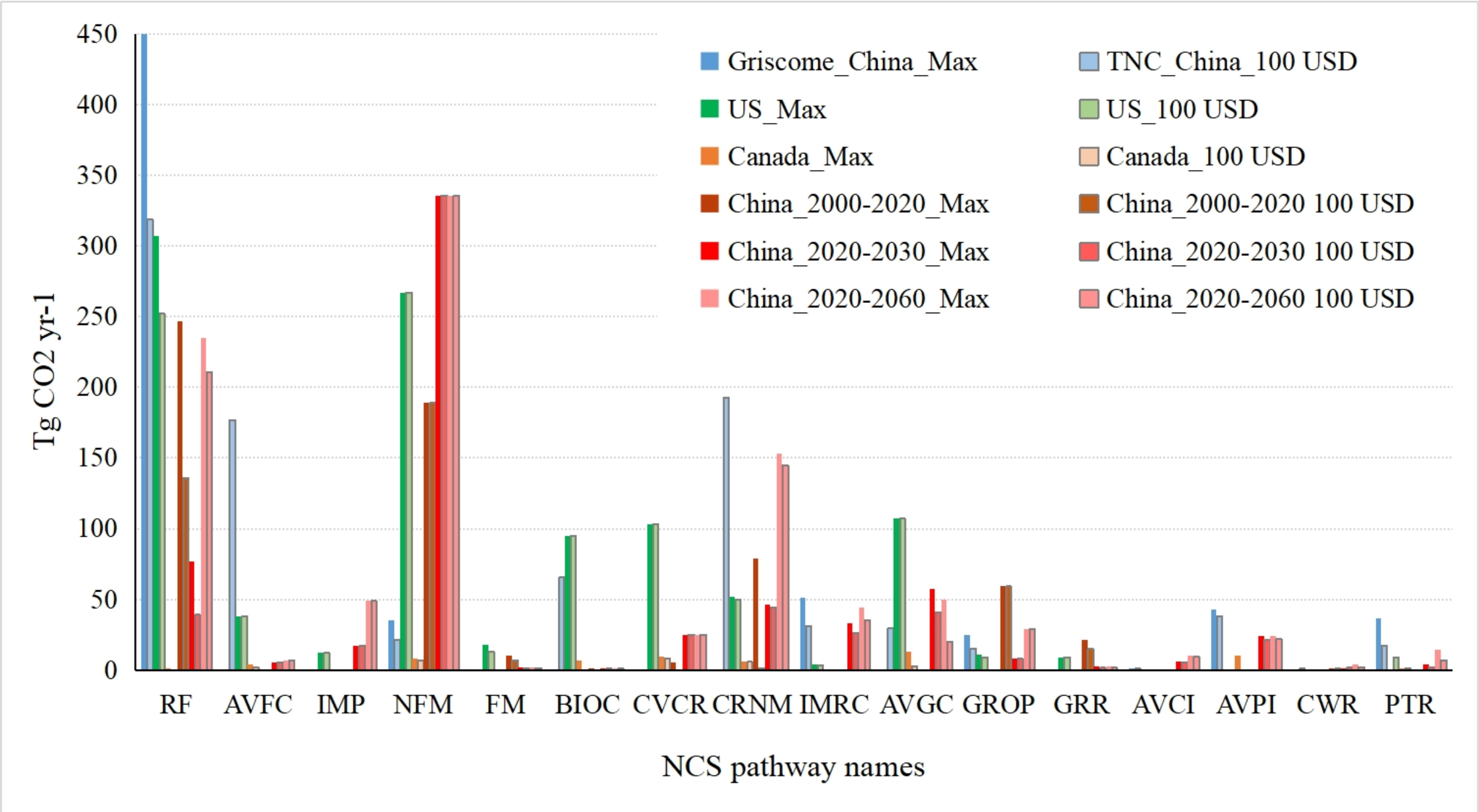
Griscome_China_Max
TNC_China_100 USD
US_Max
US_100 USD
Canada_Max
Canada_100 USD
China_2000-2020_Max
China_2000-2020 100 USD
China_2020-2030_Max
China_2020-2030 100 USD
China_2020-2060_Max
China_2020-2060 100 USD
Tg CO2 yr-1
450
400
350
300
250
200
150
100
50
0
RF
AVFC
IMP
NFM
FM
BIOC
CVCR
CRNM
IMRC
AVGC
GROP
GRR
AVCI
AVPI
CWR
PTR
NCS pathway names

Supplementary Materials for

Biophysical and Economic Constraints on China's Natural climate solutions

Nan Lu, Hanqin Tian, Bojie Fu*, Huiqian Yu, Shilong Piao, Shiyin Chen, Ya Li, Xiaoyong Li, Mengyu Wang, Zidong Li, Lu Zhang, Philippe Ciais, Pete Smith

*Correspondence to: Bojie Fu, bfu@rcees.ac.cn

This PDF file includes:

Supplementary Materials and Methods for Pathway 1 to 16

Fig. S1 to S12

Tables S1 to S38

Materials and Methods

Here, we provide detailed descriptions of the methods used for each individual pathway. The definitions, extents of implementation, and estimates of climate mitigation of all pathways are summarized in Table S1-S3 and Extended Data Fig. 1.

Pathway 1: Reforestation (RF)

Area

We define forestation as the maximum potential for conversion from non-forest cover to forest cover. Since the 1970s, China has carried out several inventories of the national forest resources, which involves a regular and accurate survey of the quantity, quality and dynamics of forests at the national and provincial levels, as well as a comprehensive evaluation of forest resources and ecological conditions. The inventories are an important basis for formulating and adjusting forestry policies and plans, and to monitor regional changes in forest resources. At present, nine consecutive inventories of national forest resources have been completed (Table S4) [1, 2].

According to the definition of slash and suitable land for forestry in the *Regulations of National Inventory of Forest Resources* released in 2014, slash land mainly includes logged, burnt, and other types of land. Logged land or burnt land refers to lands where the tree vigor of the arbor forest cannot reach the standard of sparse forest land and have not been renewed within 3 years after logging or fire. The other refers to shrubby forests that are reduced to less than 30% of coverage after cutting or fire. As for suitable land for forestry, it means the land area that the local government plans to use for developing forestry, including the lands with unsuccessful forestation or planning for forestation. The total area for reforestation during 2000-2020 was 44.71 Mha, according to the National Inventory of Forest Resources (http://www.forestry.gov.cn). In order to avoid duplicate categorization, the area suitable for mangrove restoration is removed from this pathway.

To estimate the future area for reforestation, we consider the area of slash and suitable land for forestry, at the provincial level is estimated based on the latest results of the 9th National Inventory of Forest Resources (http://www.forestry.gov.cn/gjslzyqc.html; Table S5). Besides, the sloping and degraded farmlands also have an opportunity to be restored to forest as required by the Grain for Green project. In the white Paper *Returning Farmland to Forest and Grassland in Twenty Years*, issued by the Forestry Administration [3], the proportion of cropland that is to be converted to forest and grassland was calculated. Specifically, a total of 4.52 Mha of cultivated land was returned to forest and grassland from 2014 to 2019 in China, of which 4.17 Mha was returned to forest (accounting for 92.14%) and 0.36 Mha was returned to grassland (accounting for 7.86%). Assuming the same fractions of grassland and forest will be restored from the total cropland area, a maximum of 5.58 Mha of cropland can be used for future forest restoration during 2020-2060 (Table S6, S7).

We constrained the maximum extent (slash and suitable land and cropland for forestation) by the key factors including the critical minimum of farmland land area (the so-called *Farmland Red Line*), the demand for urban construction, the implementable rate of reforestation and the rate of survivability of the restored forests. We calculated the annual rate of cropland conversion to urban areas from 2010 to 2019 (based on the *China Statistical Yearbook*) and we assumed that the conversion rates will remain the same over the next decades. The areas available for future urbanization and to maintain the *Farmland Red Line* were subtracted from the current cropland area. The data for the farmland red line was obtained from the National Land Use Outline (2006-2020) Adjustment Plan released in 2016 (Table S8; https://www.ndrc.gov.cn/fggz/fzzlgh/gjjzxgh/201705/t20170517_1196768_ext.html).

According to the recently published *Plan for Major Projects for the Protection and Restoration of Major Ecosystems Nationwide (2021-2035),* China's annual planned area for forestation would be 100 million mu (6.67 million hectares) (https://www.ndrc.gov.cn/xxgk/zcfb/tz/202006/t20200611_1231112_ext.html). According to the statistical data of *China Forestry and Grassland Statistical Yearbook* from 2009 to 2018 (https://data.cnki.net/trade/Yearbook/Single/N2020030029?z=Z010), the average annual area for forestation in China is 6.28 Mha yr^{-1} during 2009-2018, which is basically consistent with the future national planning. Therefore, it is reasonable to assume that reforestation will continue at this rate in the short term (at least 15 years). We use 6.67 Mha yr^{-1} as the rate of reforestation in the future 10 and 40 years.

It should be pointed out that not all reforestation efforts will be successful. Relevant studies have shown that most arid and semi-arid areas in northern China can support relatively low tree cover or shrub forest, especially in areas with high evaporation and transpiration rates [4]. When the soil moisture is insufficient, planted trees will die due to water shortage [5, 6]. According to the changes in vegetation cover, the survival rate of trees after reforestation in the northern regions of China was estimated to be very low (40% and below) [7], especially in the arid and semi-arid areas (only 15%) [8, 9]. The survival rate refers to the ratio of the area with increased vegetation cover due to reforestation to the total reforestation area [7].

This value is 70-85% in other regions. Then the total available areas is adjusted after considering the tree survival rate in each province of reforestation (Extended Data Fig. 2).

Total area available for RF (Mha) = Area of (Slash and suitable for forestry) + Area of (existing cultivated - critical minimum of cultivated land - land needed for urban construction);

Estimated RF area in the future (Mha) = Average annual RF area (Mha/yr)* time of duration (yr);

Actual RF area (Mha) = Minimum (total area available for RF, estimated RF area in the future);

Actual viable area for RF (Mha) = Actual RF area * RF survival rate

After considering the limitations, the projected *actual viable area* for *RF* can be determined for each province (using provincial farmland red line)(Table S9, Extended Data Fig. 2&3). Thus, we estimated that an additional 21.68 Mha of area would be restored to forest during the period 2020-2030. Compared to the existing forest area in the 9th Forest Inventory (2014-2018), the total forest area is expected to reach 242.08 Mha in 2030. This is comparable to the historical forest area of China in 1700 (248.13 Mha) [10]. Our estimate of an additional 31.84 Mha of reforestation over the next 40 years (2020-2060) is a modest value and even a conservative target, which is less than 1/3 of the increase in forest area during 1976-2018 (98.4 Mha) (Table S4). It is also slightly lower than the increase in forest area during 2003-2018 (45.5 Mha). A global estimate of the maximum potential forestation area in China is 40.2 Mha [11], which is also a little higher than our estimate. In another study, it was reported to be 58 Mha or 87 Mha based on the indicator system assessment method and the MaxEnt model, respectively [12]. We believe that our estimate is reasonable since it considers the several constraints discussed earlier.

Flux

Carbon flux is affected by location, forest type, tree species, stand age and other parameters [13]. Data of forest type, tree species, and age group structure was obtained from the website of *National Inventory of Forest Resources* (http://www.forestry.gov.cn/gjslzyqc.html). The county-scale area of reforestation was obtained from the *China Forestry Statistical Yearbook*, which was used for selecting forest type and tree species in each province. The provincial scale was determined to be the unit for calculation, considering the available data samples in the literature. The mean carbon flux was calculated for each province based on published literature according to the proportion of forest type, tree species and stand age.

Taking one province (Guangxi Province) as an example, *Betula alnoides*, *Cunninghamia lanceolata (Lamb.) Hook,* and *Pinus massoniana* are the main tree species for reforestation in this province. We calculated the mean flux rate of the three species in an age group weighted by their area proportions, i.e., 10.88%, 45%, and 44.12%, respectively. If no data of carbon flux were found for a specific age group, we used the mean of the adjacent age groups. In the Guangxi case, there were no data for *Betula alnoides* and *Cunninghamia lanceolata (Lamb.) Hook* within 0-10 years, and we therefore used the mean of the stand age of 11 and 13 years (Table S10). Thus, the carbon flux of Guangxi province during 2020-2030 can be calculated as:

Carbon flux (Mg C ha^{-1} yr^{-1}) of 10 years forest in Guangxi province =

$$10.88\%*1.93+45\%*(3.22+4.41)/2+44.12\%*1.73=2.69$$

The carbon flux calculations for different age of forests (10, 20, 30, 40, 60 years old) in other provinces was calculated with the same method (Table S11).

Previous research shows that the carbon sequestration rate of reforestation projects range from 2.38-2.67 Mg C per ha per year within the first 10 years of the projects implementation, such as the Three-North Shelter Forest Program, the Yangtze River and Zhujiang River Shelter Forest Projects, and the Grain for Green Program [14]. As for as our results, the mean carbon flux during the first 10 years is 2.02 ± 0.14 Mg C ha^{-1} yr^{-1}, gradually increasing to 2.55, 3.53, 3.12 and 3.14 Mg C ha^{-1} yr^{-1} as the forest grows to include the age groups of 20, 30, 40, and 60 years.

Carbon sequestration from reforestation

According to the projected actual viable area of reforestation and carbon flux of each province, the maximum annual carbon sequestration potential of each province in 2020-2030 and 2020-2060 were calculated and summed up to the country's total (Table S12). Our study shows that the historical flux of carbon sequestration by reforestation on an area of 44.71 Mha was 246.90 (213.65-282.33) Tg CO_2 yr^{-1} during 2000-2020. The future potential is 76.64 (61.61-93.68) Tg CO_2 yr^{-1} during 2020-2030 and 234.70 (205.47-266.70) Tg CO_2 yr^{-1} during 2020-2060.

Uncertainty for reforestation

The area of reforestation was estimated based on a determined reforestation rate and it is not considered as a source of uncertainty. The estimate of uncertainty only derives from the uncertainty in carbon flux calculations. The means and standard deviation values of carbon sequestration flux were obtained based on the data collected in the literature, and they were calculated by forest age group (0-10, 10-20, 20-30, 30-40, and 40-60 years) in each province (as shown in Table S11). The uncertainty was calculated using a Monte Carlo simulation (100,000 iterations), by fitting the data to a normal distribution [15].

Co-benefits from reforestation

Reforestation has great impacts on regional biodiversity, water use, soil fertility, and air quality [16]. Some studies show that reforestation can increase surface soil moisture, decrease runoff and alleviate floods [17, 18]. Tree density in reforestation should be determined according to the original forest ecosystems (e.g. for a dryland forest in a semi-arid region). The conversion of grassland and cultivated land to forest can increase carbon storage and reduce soil erosion [19]. As trees can intercept water and access and transpire water from considerable depths in the soil, they are able to regulate surface runoff and groundwater recharge, and to reduce soil erosion. In addition, the existing reforestation projects in China (such as Grain for Green Project, Natural Forest Conservation Program) have been reported to facilitate the restoration of biodiversity [20-22].

Marginal abatement costs for reforestation

According to the data in the White Paper "*Returning Farmland to Forest and Grassland in Twenty Years*" issued by the Forestry Administration of China, the subsidy for returning farmland to forest is paid in five years, totaling 24,000 CNY/ha (including 6,000 CNY/ha for planting seedlings and 18,000 CNY/ha for living and grain subsidies) [3]. According to the data in the '*Measures for the Administration of Forestry Subsidies from the Central Finance*', the subsidy standard for reforestation in suitable forest land, barren hills and wasteland, sandy wasteland, virgin land and low-yield and low-efficiency forest land is 1,500-3,000 CNY/ha [23] (subsidies to reforestation agents). We used the mean value of 2,250 CNY/ha (converted to 2015 USD) to calculate the reforestation investment cost and estimated a best-fit (exponential) equation for provincial data points and used that equation to estimate the abatement levels of carbon sequestration achievable at the three carbon prices (USD 10, 50, and 100 per Mg CO_2, respectively). We used the discount rates of 3% and 5% to represent the change of carbon price in the future estimate. The discount rate was not considered when making the MAC curve for the historical period of 2000-2020 (Fig. S1, Table S13).

Comparison with previous studies

The maximum carbon sequestration of reforestation in China was 247 Tg CO_2e yr^{-1} from an area of 44.71 Mha during 2000-2020. The future NCS potential by reforestation in the United States is estimated to be 307 Tg CO_2 yr^{-1} on a larger area of 63 Mha during 2010-2025 [24] (Extended Data Fig. 7). China and the United States have roughly an equal amount of carbon sequestration per Mha of reforestation. The NCS potentials by reforestation in Canada (-

2.9~24.90 Tg CO_2 during 2020-2050) is much lower than those in China, with 76.64 and 234.70 Tg CO_2 yr^{-1} over 10 and 40 years, respectively. The lower mitigation potential is due to the initial slow tree growth and a delayed implementation scenario to allow time to develop planting stock as well as the smaller area (3.8 Mha) [25]. In contrast, the max mitigation potential of reforestation for China in the global study (2010s-2030) by Griscom et al. [26] is 1256.71 Tg CO_2 yr^{-1}, which is much higher than our values (Extended Data Fig. 7). This is because the global carbon flux in the Griscom et al. research was 4.14 Mg C ha^{-1} yr^{-1}, while the mean value of carbon flux calculated by weighting the reforestation area in each province of China is 0.96 (0.78-1.18) Mg C ha^{-1} yr^{-1} over 10 years and 1.51 (1.30-1.72) Mg C ha^{-1} yr^{-1} over 20 years. Therefore, the NCS potential at 100 USD from Griscom or the Nature Conservancy (TNC), by assuming a 30% of the maximum potential, is also higher than our estimate.

Pathway 2: Avoided forest conversion (AVFC)

Deforested lands generally undergo the process of natural restoration if it is not transformed in the short term into other land use types. The maximum carbon sequestration potential of avoided forest conversion was estimated by calculating the carbon emission resulting from changing land types after deforestation. The carbon loss mainly includes the loss from biomass and soil carbon stock when forest conversion occurs.

Area

According to the Global Forest Watch data (https://www.globalforestwatch.org/), the areas of forest land converted to cultivated land and construction land were 7,903.02 ha and 2,742.38 ha each year, respectively, culminating in an annual forest loss by deforestation of 10,645.39 ha. Using the China Land Use Data in the 1980s and 2010-2015 [27, 28], the proportions of forest converted to cultivated land and construction land were estimated in the six regions of China (see Table S14 for details), as their soil carbon data was available in the literature. In recent years, the conversion of forest land to cultivated land mostly occurred in Northeast China, accounting for 40% of the total conversion, followed by Northwest China, and the conversion of forest land to construction land mostly occurred in South China.

Flux

According to the data from 2001 to 2019 obtained from Global Forest Watch (https://www.globalforestwatch.org/) [29], the carbon loss from aboveground biomass was 3.27 Tg CO_2 yr^{-1} (95% CI: 0.92-5.62 Tg CO_2 yr^{-1}) (Table S15). To estimate the carbon loss from the soil, we first calculated the area of deforestation (persistent conversion to cultivated land or construction land) during 2001-2019. Then the carbon loss in soil was determined by the initial soil organic carbon (SOC) content (in 0-1 m) and the loss rate. The 0-1 m forest SOC in the six regions of China have been summarized in several review papers [30, 31]. According to previously published results [32, 33], the SOC decreased by 30.3% ± 2.4% on average 10 years or more after forest conversion to farmland. Similarly, according to the research results of [34-39], we found that the 10-year loss rate of soil carbon after the conversion of forest land to construction land was 55% ± 4.1%. We assumed that the SOC would decrease by about 59% during 2020-2060 after the conversion from forest land to cultivated land, as suggested by a meta-analysis [40], and that there would be a SOC loss rate of 40% during 2020-2060 after the conversion of woodland to construction land. On a longer time scale, the level of urban SOC can even increase, higher than that of non-urban areas, due to the input of municipal solid waste and the influence of human management measures [37],[41].

Based on the provincial forest area data in the 8th and 9th National Forest Inventories (2009-2018) (Table S4), the ratio of each province's forest area to the national forest area was calculated and the ratio was used as a coefficient to calculate the carbon emission that could be reduced by avoiding forest conversion in each province.

Reduced CO_2 emission by avoided forest conversion

Accordingly, avoided forest conversion could reduce carbon loss through biomass loss by 3.27 (95% CI: 0.92-5.62) Tg CO_2 yr^{-1} and soil carbon loss by 2.26 (95% CI: 1.87-2.62) Tg CO_2 yr^{-1}, a total loss of 5.54 Tg CO_2 yr^{-1} (95% CI: 2.92-8.01 Tg CO_2 yr^{-1}) during 2020-2030 (Table S16). In the period 2020-2060, avoided forest conversion could reduce carbon loss through biomass loss by 3.27 (95% CI: 0.92-5.62) Tg CO_2 yr^{-1} and soil carbon loss by 3.45 Tg CO_2 yr^{-1}, a total loss of 6.72 Tg CO_2 yr^{-1} (95% CI: 4.12-9.08 Tg CO_2 yr^{-1}) (Table S17).

Uncertainty for avoided forest conversion

Biomass loss was estimated from 19 years of data during 2001 to 2019 obtained from the Global Forest Watch with a mean and standard deviation of 3.27 ± 1.20 Tg CO_2 yr^{-1}. Soil carbon loss was calculated from the rate of soil carbon loss after the conversion and the SOC in the six regions. The uncertainty of soil carbon loss in each region was estimated from the loss rates of soil carbon (30.3% ± 2.4% after conversion to farmland and 55% ± 4.1% after conversion to construction land) using the IPCC Approach 1. The uncertainty for results of soil loss for the whole of China was estimated by Monte Carlo simulation (100,000 iterations). The overall uncertainty was combined using Monte Carlo simulation [15].

Co-benefits for avoided forest conversion

Researches at different scales show that land use change has a significant impact on ecosystem services, including biodiversity, water, soil, and air [42, 43]. Forest conversion is one of the greatest threats to biodiversity [42, 44]. The loss of forest eliminates the habitat or habitat corridor of indigenous species [45], and furthermore, changes the local climate conditions in the surrounding areas when converted into farmland or built-up area [46-48], which further affects the living environment of the original species. Similarly, the change in vegetation type can dramatically affect soil aggregate stability, with the forested soil potentially having a greater resistance to soil erosion regardless of the rain conditions [49]. The aggregate stability of soil may decrease when natural forests are converted to cropland [50]. Avoiding forest conversion can therefore protect the habitats of species, maintains biodiversity and enhances soil stability. In addition, forests play a vital role in the hydrological regulation and air quality improvement in the local area. Forest watersheds can regulate and stabilize water runoff to balance river flow over the seasons. Furthermore, forests can retain soil and hence decrease silt runoff into rivers [51]. This is conducive to the use of hydroelectric power in the basin. Forests improve air quality by affecting air pollutants. Compared with cultivated land and urban areas, the concentration of particulate matters in forest areas is significantly reduced and atmospheric visibility is better [52, 53].

Marginal abatement costs for avoided forest conversion

Using an analysis horizon of 20 years, Golub et al. [54] estimated the total average annual forest carbon supply of China for seven carbon price points (ranging from USD 5 to USD 500 per Mg CO_2) for combined changes (increasing carbon stocks by afforesting non-forested lands or preventing conversion of current forest lands (i.e., avoided deforestation). We used a best-fit (R^2 = 0.96) equation for seven data points (Extensive Margin) [54] to estimate the carbon benefits at three carbon price points (USD 10, 50, 100 per Mg CO_2) (Fig. S2, Table S18).

Comparison with previous studies

The rate of avoided forest conversion is estimated to be 0.011 Mha yr^{-1} and it will bring a carbon mitigation potential of 5.54 Tg CO_2 yr^{-1} during 2020-2030 and 6.72 Tg CO_2 yr^{-1} during 2020-2060 [24]. The implement area of avoided forest conversion in USA is 0.38 Mha yr^{-1}, which will bring a carbon mitigation potential of 38 Tg CO_2 yr^{-1}. Our result is lower than that of the United States (Extended Data Fig. 7), partly due to the smaller area of avoided forest conversion, although we had a higher flux rate per unit area from our inclusion of carbon loss from both biomass and soil carbon (soil carbon is not considered in the U.S. study). Besides, the loss of biomass is also reduced proportionally according to the difference of harvest and residue, namely the emission factor, resulting in a low carbon loss. The area of avoided forest conversion in Canada is 0.02 Mha yr^{-1}, which will bring a average value of carbon mitigation potential of 2.63 Tg CO_2 yr^{-1} during 2021-2030 [25]. Their result is lower than that of this study because their study considered the loss of greenhouse gas (GHG) emission from forest conversion as well as the changes in albedo due to land-cover change.

A study shows that the deforestation rate of Xishuangbanna in China was 13722 ha yr^{-1} during 1976-2003, resulting in a biomass carbon loss of 5.87 Tg CO_2 yr^{-1} [55]. The carbon loss per unit area of biomass was estimated to be 427.78 Mg CO_2 ha^{-1}. According to the data of Global Forest Watch we used, the carbon loss per unit area of biomass caused by deforestation is 307.44 Mg CO_2 ha^{-1} at the national scale, which is reasonable.

Pathway 3: Improved plantations (IMP)

Reducing harvest and improving the treatment of logging residue disposals are the main approaches to improved plantation and reducing carbon emission. According to the data of the *National Statistical Yearbook* from 2000 to 2019 (http://www.stats.gov.cn/tjsj/ndsj/), the timber harvest volume has increased from 47.24 million m^{-3} yr^{-1} to 100.459 million m^{-3} yr^{-1} over the last 20 years. The average timber production in the last 10 years was 83.31 million m^{-3} yr^{-1}. We used this value as the baseline value and assumed that this timber demand would be maintained at this level in the next decades.

Assuming a linear increase, the average timber harvesting volume in 2020-2030 is predicted to be 89.73 million m^{-3} yr^{-1}, an increase of 6.42 million m^{-3} yr^{-1} (7.706%) relative to the baseline production. In 2020-2060, the average timber harvesting volume is predicted to be 96.1 million m^{-3} yr^{-1}, a relative increase of 12.78 million m^{-3} yr^{-1} (15.345%). The annual carbon emission caused by timber harvesting was as high as 34.25 Tg C yr^{-1} (of the 83.31 million m^{-3} yr^{-1}) [56]. A reduced carbon emission will come from a reduction in timber harvesting. The carbon sequestration potential can be calculated as follows:

$$\text{Annual C sequestration potential (2020-2030)} = 7.71\%*34.25=2.64 \text{ Tg C yr}^{-1} =9.68 \text{ Tg CO}_2 \text{ yr}^{-1}$$

$$\text{Annual C sequestration potential (2020-2060)} = 15.34\%*34.25=5.25 \text{ Tg C yr}^{-1} =19.27 \text{ Tg CO}_2 \text{ yr}^{-1}$$

In addition to reducing the harvested amount, improved disposal of the logging residues can also reduce carbon emission. There are four ways to deal with the remaining timber: 1) cutting only the stem and leaving the rest of the timber in place (Stem Only, abbreviated SO), 2) the removal of all above-ground timber, including branches, leaves, and other aboveground parts (Floor Removed, FR), 3) removing the whole harvested tree (Whole Tree Harvest, WH) and 4) removing dry timber after cutting down the trees and burning the remaining aboveground parts (Stem Only and Burning, SB). Compared to untreated management for logging residues, the additional average annual carbon sequestration rates are 2.36, 2.03, 1.96, 1.91 Mg C ha^{-1} yr^{-1} using the four ways (SO>FR>SB>WH), respectively under poor site conditions, and the average values are 5.73, 4.91, 4.76, 4.53 Mg C ha^{-1} yr^{-1} (SO>FR>SB>WH), respectively, under good site conditions. The mean value of additional carbon sequestration rate under poor and good site conditions are used in our calculation [57] (Table S19). According to the data from 2001 to 2019 obtained from Global Forest Watch (https://www.globalforestwatch.org/) [29], the annual area of forest harvesting was estimated to be 466584.30 ha in China. Based on the existing treatment methods of logging residues, more reasonable treatment methods of logging residues are assumed to be adopted in the future. We assume that the annual timber cutting in the next decade is increasing at the rate of the past two decades [58].

The proportion of timber harvest volume in each province was calculated based on the timber harvest volume data recorded in the National Statistical Yearbook from 2010 to 2019. The proportion was used as a coefficient to calculate the carbon emission that could be reduced by reducing wood harvesting and changing the methods of treatment of forest residues in each province.

Carbon sequestration through improved management of plantations

Collectively, the carbon sequestration potential is contributed by reducing the amount of harvest by 9.68 Tg CO_2 yr^{-1} (95% CI: 4.66-14.70Tg CO_2 yr^{-1}) and changing the methods of treatment of forest residues by 7.37 Tg CO_2 yr^{-1} (95% CI: -1.92-14.03 Tg CO_2 yr^{-1}), with a total maximum carbon sequestration potential of 17.05 Tg CO_2 yr^{-1} (95% CI: 9.58-24.52Tg CO_2 yr^{-1}) during 2020-2030. For the period 2020-2060, the carbon sequestration potential due to reducing the amount of harvest is 19.27 Tg CO_2 yr^{-1} (95% CI: 5.84-32.70Tg CO_2 yr^{-1}) and changing the methods of treatment of forest residues 29.48 Tg CO_2 yr^{-1} (95%CI: -7.68-56.12 Tg CO_2 yr^{-1}), with a total maximum carbon sequestration potential of 48.75 Tg CO_2 yr^{-1} (95% CI: 20.81-76.69Tg CO_2 yr^{-1}).

Uncertainty for improved plantations

The mean value and standard deviation of reducing the amount of harvest is 9.68 ± 2.56 Tg CO_2 yr^{-1} during 2020-2030 and 19.27 ± 6.85 Tg CO_2 yr^{-1} during 2020-2060. The mean value and standard deviation of mitigation potential contributed by the forest residue treatment methods is 7.37 ± 4.74 Tg CO_2 yr^{-1} during 2020-2030 and 29.48 ± 18.96 Tg CO_2 yr^{-1} during

2020-2060. Based on the mean values and standard deviations of increased carbon sequestration from reduced harvesting and improved plantation management practices, we used a Monte Carlo simulation with 100,000 iterations and fitted the resultant data to a normal distribution, to obtain a combined uncertainty estimate for both improving factors and to estimate its 95% CI.

Co-benefits for improved plantations

Animals that depend on the forest for survival (such as birds) are vulnerable to logging. Logging can reduce animal abundance and even have lasting effects on their populations [59]. Therefore, improved plantation management may enrich the biodiversity by decreasing logging intensity. The method of removal of logging residues has no effect on the arboreal community, but it may increase the richness, diversity and evenness of the understory species [60]. Logging residues are one of the most important sources of exogenous nutrients in the forest logging area. In the process of decomposition of logging residues, a large amount of nutrients are released, which improves the physical and chemical properties of the soil [57, 61].

Marginal abatement costs for improved plantations

Using an analysis horizon of 20 years, Golub et al. [54] estimated the total average annual timber supply of China for seven carbon price points (ranging from USD 5 to USD 500 per Mg CO_2) for combined changes in forest management and aging ("Intensive Margin"). We used a best-fit equation (Polynomial fitting, $R^2 = 0.98$) for seven data points [54] to estimate abatement at the three carbon price points (USD 10, 50, 100 per Mg CO_2) (Fig. S3) (Table S20).

Comparison with previous studies

Different methods of plantation management lead to the incompatibility of carbon sequestration estimates. In the USA, improved plantation focused on a limited extension of economically optimal crop rotation length [24, 26]. As for methods of treatment of forest residues in Canada, they modeled a 10% reduction of slash burning following clearcut (in regions with slash burning) and used up to 50% of post-harvest residues for bioenergy production. The area of 139 Mha (only 10% reduction of slash burning) will bring a mitigation potential of 2 Tg CO_2 yr^{-1} in the first 10 years [25]. Our results of with the methods described above is 7.37 Tg CO_2 yr^{-1} during 2020-2030.

Pathway 4: Natural Forest Management (NFM)

In China, natural forest management has been carried out in conjunction with the Natural Forest Protection Programme (NFPP) since 1998. For the period 1998-2015, the forest areas in most of the upper reaches of the Yangtze River and the Yellow River, and a large forest area in northeastern China has been gradually protected, with measures including bans and/or restrictions on logging and intensive forest regeneration. The aim is to recover natural forests and the environment in the key watersheds and protected areas. During this period, 50.2% of the country's natural forests were under protection through reduced harvesting [62,63]. During 2015-2020, more strict protective measurements for natural forests were launched. Logging has been prohibited in all natural forests in Northeast China [62]. Finally on July 1, 2020, the newly revised *Forest Law of the People's Republic of China* came into effect. China has abolished the quota for commercial logging of natural forests nationwide. This law ensures that the natural forest management will remain in effect in China in the future and that forest rotation will be extended indefinitely in China's natural forests.

As China's harvestable natural forest resources were almost depleted after decades of exploitation prior to the implementation of the NFPP in 1998, the amount of harvesting was greater than the increase in stockpiles in terms of harvestable resources [62]. Therefore, the calculation of the maximum mitigation potential only included the carbon sequestered by the increase in forest carbon density due to the cessation of logging, but not the CO_2 emission from annual harvesting under a business-as-usual scenario. The mitigation capacity under the natural forest management pathway is the annual maximum area of managed natural forest multiplied by the annual increase in natural forest carbon density ($Flux_{NFM}$) within that area.

Area

According to the Fifth National Forest Inventory (1994-1998), there were 79.10 Mha of timber and charcoal forests in China's natural forests [64]. We assume that the area under natural forest management increased linearly from 0 to 79.10 Mha from 2000 to 2020 (equivalent to 41.24 Mha counting a mean flux rate of different age groups). And after 2020 all of the 79.10 Mha of natural forests will be prevented from logging.

Flux

The $Flux_{NFM}$ is the annual natural forest carbon density increment in the NFM area, which is defined here as the increase in carbon density due to the natural recovery of the natural forest with age. We calculated the difference between the carbon densities of the natural forests of different age groups, divided by the number of years required to grow to the different age groups, respectively, to obtain the fluxes.

$$Flux_{NFM,age\ group\ n} = (Carbon\ density_{age\ group\ n} - Carbon\ density_{age\ group\ n-1})/(Age_{age\ group\ n} - Age_{age\ group\ n-1})$$

Forest age. The major tree species in China were classified into five age groups: young, middle-aged, pre-mature, mature and over-mature, according to the Forestry Industry Standards of the People's Republic of China. The average age boundaries and average ages of each age group were calculated using the age group boundaries of the major tree species (Table S21). The area of natural forests under management (timber and charcoal forests) by age was derived from the forestry inventory data of 1994-1998. The national average age of the managed natural forests was 43 years in 2010, calculated as a weighted average of the area of each age group and average ages of each age group (Table S21). As there were relatively fewer sites with data for young, pre-mature and mature forests, the young and middle-aged groups were combined. The groups pre-mature and mature forests were also combined. There are three age groups after these combinations, i.e., young & middle-aged, pre-mature & mature and over-mature (Table S22). $Flux_{NFM,\ age\ group\ n}$ represents the flux when the managed natural forests grows from the $(n-1)^{th}$ to the n^{th} age group.

Carbon density. We collected site-specific data from the papers published during 1992-2020 to calculate the average carbon density of the different age groups in China. The data were compiled from sites with one or more plots [65-105]. Carbon density consists of two parts: vegetation carbon density of living trees (Extended Data Fig. 4), shrubs and herbs; and carbon density of the floor layer, mainly composed of woody debris and litter. Biomass density is converted to carbon density by multiplying the carbon fraction by 0.5. For the sites that contained only aboveground biomass carbon density data, we estimated the belowground biomass carbon density by multiplying it with a coefficient of 0.25 [106] and summed to obtain the total carbon density of the whole tree layer. Due to the limited data available for estimating the change in soil carbon density, soil carbon sequestration was not included in our analysis.

We investigated the non-linear relationship between carbon density and age in the tree layer of the collected site-specific data (Extended Data Fig. 4). We found that the three stages can roughly characterize the change of forest carbon density growth, i.e., the increasing rate of forest carbon density is highest at young and middle-aged groups, lower at pre-mature and mature age groups, and lowest in the over-mature age group.

Forest carbon density was separately calculated for six regions including the East, North, Northeast, Northwest, South Central and Southwest of China [105, 107]. For the tree layer and the floor layer, Monte Carlo simulations were used to estimate the mean and standard deviation of carbon density levels for each age group within each region (100,000 simulations), and the resultant data fitted to a normal distribution. Shrubs and herbs in the vegetation layer were combined into two parts for the north (North, Northeast, Northwest) and the south (East, South Central, Southwest) of China because of the lower data availability from these regions.

Carbon density$_{\text{over-mature}}$ is the weighted average from the area of the managed natural forest and carbon density of over-mature forest in the six regions, that is, the carbon density when all the area was over-mature forest (139 Mg C/ha, Table S22 for detailed figures). The calculated vegetation carbon density levels in the young and middle-aged forest groups in each region were on average 42% of those in the over-mature forests. The vegetation carbon density levels in the pre-mature and mature forest groups were on average 74% of those in the over-mature forest (Table S22). Thus, the relative carbon density in the young & middle aged, and the pre-mature & mature groups were calculated as follows:

$$Carbon\ density_{\text{young \& middle−aged}} = Carbon\ density_{over-mature} \times 42\%$$

$$Carbon\ density_{\text{pre−mature \& mature}} = Carbon\ density_{over-mature} \times 74\%$$

According to Zhang et al. [108], the forest carbon density in the middle-aged and mature forest groups accounts for 43% and 78% of the forest carbon density in the over-mature group, respectively, which are similar to the values observed in this study. The information including the number of plots in the site, age and the mean and standard deviation of carbon density were summarized in Tables S21, S22, S23 and Extended Data Fig. 4. The annual carbon density increment under different age groups in natural forest management area is indicated in Table S24.

The maximum mitigation potential of natural forest management

The historical flux of carbon sequestration by natural forest management during 2000-2020 was 189.01 (109-269) Tg CO_2e yr^{-1} (95% CI). The future potential is 335.88 (0-738.90) Tg CO_2e yr^{-1}(95% CI) during 2020-2030 and 2020-2060.

Uncertainty for natural forest management

The area of the natural forest management is obtained from the Forest Resource Statistics of China, and therefore, considered as determined and not a source of uncertainty. The uncertainty of $Flux_{NFM}$ is considered which originates from the uncertainty of carbon density estimation for the different age groups. Data from Monte Carlo simulations with 100,000 iterations and fitted to a normal distribution was used to combine the uncertainty of vegetation and floor carbon density across the different age groups.

Marginal abatement costs for natural forest management

We referred to two analyses that estimated the MAC for natural forest management in China. Golub et al. [54] estimated the cost of forest carbon sequestration in China through modified management (such as longer harvest rotation). They used seven carbon price points (ranging from USD 2 to USD 200 Mg CO_2^{-1}) with a 20-year analysis horizon and a discount rate of 5%. Austin et al. [109] estimated the cost of the carbon sequestered by forest management and rotation in China for six carbon price points (from USD 5 to USD 100 Mg CO_2^{-1}) under 1% and 3% discount rate scenarios for an analysis period up to 2055 (Fig. S4). We developed best-fit functions for the results of these two studies, respectively, and used the mean values of the three discount rates to calculate how much carbon sequestration can be achieved at USD 10, 50 and 100 Mg CO_2^{-1}. When the MAC estimates exceeded our biophysical analysis, the final MAC estimates were determined using our estimates. For example, the estimated MAC at USD 50 Mg CO_2^{-1} in year 2015 was 220.42 Tg CO_2 yr^{-1}, which exceeded our biophysical estimate, so this final MAC estimate was determined to be 189.01 Tg CO_2 yr^{-1} (Fig. S4, Table S25).

Co-benefits for natural forest management

The implementation of NFM can benefit water, soil and biodiversity. A study shows that assisted natural regeneration in China can trigger positive feedback among soil and water conservation and substantially increase plant diversity [110]. Conversely, when logging intensity increases, stream flows and flooding increase, the species richness of invertebrates, amphibians and mammals decreases. The soil quality and productivity also declines due to the removal of woody debris [111-113].

Pathway 5: Forest Fire Management (FM)

Wildfire can induce large carbon emissions. Usually, there are two ways to reduce the probability of wildfire: 1) prescribed fires applied to consume the fuel, and 2) fire control or prevention practices. In China, the occurrence of forest fire is mainly distributed in six forest ecoregions, including boreal, temperate, mixed temperate-subtropical, subtropical and tropical forests (Fig. S5). The annual mean burnt area was 891,062.42 ha/yr during 1949-1999 and it declined to 120,971.78 ha/yr during 2000-2017 (Extended Data Fig. 5) (Forestry Knowledge Service System, http://forest.ckcest.cn/zh/lytjsjfx.html). In China, fire prevention is the most effective measure to eliminate forest fires and prescribed fires are rarely applied [114-119]. The large reduction in burnt area since 1987 was mainly due to fire prevention. We quantified the net carbon sequestration from applying fire management.

Area

The reduced burnt area from 2000 to 2020 was calculated by subtracting the average annual fire area from 1949 to 2000 from the average annual fire area from 2000 to 2017 (Extended Data Fig. 5). We assumed that the burnt area in 2000-2020 is the area that needs to be managed in 2020-2060. The total decline in area was obtained by multiplying the reduced annual mean area (ha/yr) by the fire cycle (yr).

Due to the lack of burnt area data for the two fire management methods, we assumed that fire prevention and prescribed fire accounted for 90% and 10% of the total burnt area during 2000-2020, respectively [120]. We also assumed that the total burnt area would be the same as that in the past twenty years under the current fire management regimes but that prescribed fire would be implemented on a larger scale (30% of total area) and fire prevention on 70% of the total area during 2020-2060. For the future scenario (2020-2060), the fire management would be implemented incrementally (50% of the area will be managed during 2020-2040 and 50% of the area in 2040-2060).

Reduced CO_2 flux

By clarifying the fire type and burnt area, ecosystem productivity, and carbon emission, the carbon balance by fire disturbance in a certain period can be obtained as follows [121]:

$$C_{balance} = NEP_{WF} + NEP_{Rx} - E_{WF} - E_{Rx}$$

where $C_{balance}$ represents the carbon balance in a given area. NEP_{WF} and NEP_{Rx} represent the net ecosystem productivity with wildfire (WF) and fire management (Rx), respectively. E_{WF} and E_{Rx} represent the carbon emission caused by wildfire and fire management, respectively. We focused on the CO_2 emission reduction ($E_{reduced}$) from prescribed fire or fire control practices, which is the discrepancy of $C_{balance}$ between un-managed wildfire and prescribed fire (or fire control). It is calculated from the following equation:

$$E_{reduced} = \sum A * B * P * ef * T * \mathrm{R}$$

where A represents the annual burnt area; B represents the combustible biomass; P represents the difference in the max proportion (%) of biomass loss between wildfire and prescribed fire (or fire control); ef represents the carbon emission ratio of CO_2 during the combustion process [121]; T represents the fire cycle (yr); R represents the fraction of carbon in the biomass (0.5).

The long-term dynamics of carbon banks can help us understand the potential of emission reduction by fire management. The occurrence of wildfire and ecosystem recovery are directly related to the change in biomass of the ecosystem. In fact, this process is complex considering the biomass loss caused by fire and the biomass accumulation during post-fire regeneration. A simplified diagram was constructed to depict the change in biomass in this disturbance-recovery process (Fig. S6, the numbers in the figure correspond to the proportions of aboveground biomass lost under wildfire and prescribed fire in the case of temperate forest). The proportion of annual recovery was calculated by the ratio of reduced biomass to the cycle period of fire, assuming that biomass is recovered in the period of a fire cycle. According to previous research, the cycle of wildfire in China is about 20 and 10 years in temperate and subtropical/tropical forests, respectively [118, 122]. It is 15 years for temperate-subtropical mixed forests. The frequency of prescribed fire in the subtropical/tropical forests is commonly referred to be 5 years [117, 123], whereas for temperate-subtropical mixed forests it is 7.5 years and 10 years for the boreal forest in northern China. Taking the example of a temperate forest, the discrepancy of biomass and the $C_{balance}$ becomes zero at the 20th year (the biomass is represented with a relative biomass range from 0 to 100%; where 100% indicates the initial state before burning) (Fig. S6). In this case, the initial aboveground biomass loss due to wildfire and prescribed fire are 10.5% and 5.25%, respectively (i.e., the remaining biomass is 89.5% and 94.75% of its initial value, reduced biomass = initial biomass × combustion efficiency). The emission reduction was calculated by using the mean discrepancy of biomass over a fire cycle. For example, the mean value is equal to the area between the red line and blue line shown in Fig. S6. In that example, the accumulated difference is 52.5%, so the mean value per year of the difference is 2.625%).

The proportion of emission reduction from aboveground or underground biomass was calculated for the six forest ecoregions separately according to the diagram (Table S26). The combustion efficiency and the proportion of carbon emission of wildfire for the six forest ecoregions were obtained from Lu et al. [124]. We assume that the rate of recovery is the same for wildfire and prescribed fire, and the combustion efficiency (the ratio of the total burnt biomass to the total flammable biomass) of prescribed fire is half that of wildfire. These same procedures were used in the calculation of belowground biomass CO_2 reduction. The calculation procedures were also the same for fire prevention and other forest types with different values of the fire parameters (Table S26, S27, S28). The aboveground biomass data of the forest was obtained from ChinaBiomass (data source [125]). The belowground biomass was calculated based on the root-to-shoot ratio.

Mapping Province-level Mitigation

With reference to the maps of forest biomass and forest distribution (Fig. S5), we calculated the mean forest biomass for each province and the reduced burnt area of each province were summed. We calculated the difference in the max proportion (%) of biomass loss between wildfire and prescribed fire (or fire control) for each forest type with consideration of their fire cycle length.

The maximum mitigation potential of fire management

The reduced CO_2 emission by fire management was of 9.92 (4.83-15.01) Tg CO_2e yr^{-1} (95% CI) during 2000-2020 and the future potential is 0.73 (0.35-1.11) Tg CO_2e yr^{-1} (95% CI) during 2020-2030 or 2020-2060.

Uncertainty for forest fire management

The burnt area was obtained from statistical data and was not considered a source of uncertainty. The data of means and SDs of combustion efficiency and emission factors of forest fire were obtained from the literature [124] (Table S27, S28). The uncertainty of the two parameters were combined together using Monte Carlo simulations with 100,000 iterations and assuming normal distributions.

The diagram of biomass change by prescribed fire or fire control practices is an ideal state. It is to reduce the fuel amount below the level that can trigger a wildfire. From Fig. S6 we can see that the higher the carbon storage is kept after a prescribed fire, the larger the reduction in carbon emission. However, the closer the carbon storage is maintained to the initial state, the more prone the forest is to wildfires. Therefore, a trade-off exists between the intensity of the prescribed fire and the possibility of wildfire in management practices.

Co-benefits for forest fire management

Fire management can provide other ecosystem services beside mitigating climate change, including the facilitation of soil and water conservation [119], preserving biodiversity [114-119], decreasing air pollution [126, 127] and enhancing the carbon cycle [128].

Marginal abatement costs for forest fire management

Few studies have estimated the economic cost of fire management. Generally, topography, traffic, and other conditions directly affect the cost of fire management measures [26], making the implementation of fire management costly and variable. Griscom et al. [26] set 30%, 60%, and 90% as low, medium, and high costs of emission reduction, respectively (corresponding to 10, 50, 100 USD Mg CO_2^{-1}). Prescribed fires are still in the exploratory stage in China and existing studies mainly focus on their technical aspects [129-131]. As for fire suppression, the cost of their implementation could be very large. We assumed the maximum emission reductions in fire management are 30%, 50%, and 70% of the total emission reductions at low, medium, and high costs, respectively (Table S29).

Comparison with previous studies

This work provides the potential for emission reduction of China's fire management, including fire prevention and prescribed fire. The emission reduction from prescribed fire in this study is significantly lower than the value in the U.S. (18.1 Tg CO_2 yr^{-1}) [24]. The discrepancy is derived from the burnt area (17 Mha in the U.S. vs. 2.45 Mha in China). The flux rate of emission reduction is relatively close, however, with 0.29 Mg CO_2 $ha^{-1}yr^{-1}$ in the US and 0.23 Mg CO_2 $ha^{-1}yr^{-1}$ in China. The flux rate for fire prevention is 0.43 Mg CO_2 $ha^{-1}yr^{-1}$ in China.

Pathway 6: Biochar (BIOC)

Biochar, the solid product of biomass pyrolysis, can be an important natural climate solution to mitigate global warming. Agricultural and forest waste biomass can be used to produce biochar. The biochar produced by pyrolysis of crop residues could be incorporated into the soil to achieve stable carbon storage [132]. The application of biochar can significantly increase the soil carbon in croplands by improving the soil aggregation and physical protection of aggregate-associated SOC from microbial attack, keeping the SOC at a low decomposition rate and substantial negative priming by increasing the pool of recalcitrant organic substrates [133-135].

In this study, we calculated the amount of biochar from the crop residues available for pyrolysis, assuming that this would form the bulk of the biomass resource for any biochar industry [24, 26, 136]. Crop residue availability for biochar in 2030 and 2060 was estimated as the proportion of total crop residue production, the fraction of residue that would be left in croplands to increase SOC, the residue utilization rate and biochar production rate (2010-2017). The available crop residue for biochar production in the past decade were calculated as follows:

$$CR_{biochar\_t} = CRP_{2010-2017} \times \alpha_t \times \frac{CR_{biochar(2010-2017)}}{CRP_{(2010-2017)}}$$

where $CR_{biochar\_t}$ is the crop residue amount for biochar production in year t; $CRP_{2010\text{-}2017}$ is the total crop residue production during that period; α_t refers to the residue utilization rate (%); $CR_{biochar\,(2010\text{-}2017)}$ refers to the crop residue amount for biochar production during the 2010-2017 period.

In China, the mean total amount of crop residue that could be collected and utilized was 708 million tons per year in 2010-2020 and the utilization rate reached 86.72% in 2020. However, the average biochar production was only 0.24 million tons during 2010-2017 according to the China Agricultural Statistical Report, corresponding to a 0.034% production rate. A previous study reported that the biochar yields of rice, wheat, corn and soybean were 32.14%, 31.17%, 30.34% and 25.43%, respectively [137]. Here, we converted the biochar production to the amount of crop residue (0.82 million tons, accounting for 0.11% of the total available national crop residue) by using the fraction of 30% to adjust the estimate of crop residue biomass for biochar production.

For the future projection, we assumed that the proportion of crop residue to produce biochar remains stable during 2020-2060. The Ministry of Agriculture and Rural Affairs of China reported that an improved crop residue collection, storage, and utilization system would be established by 2030 and an industrial pattern of straw comprehensive utilization with reasonable layout and diversified utilization will be achieved. We assume that the utilization rate will increase to 100% by 2030. The carbon sequestration from biochar can be calculated as:

$$CS_{biochar} = CR_{biochar} * CR_{carbon} * Biochar_{carbon} * C_{stable}$$

where $CS_{biochar}$ is the carbon sequestration rate in soil from biochar per Mg crop residue (Mg CO_2e $MgCe^{-1}$); $CR_{biochar}$ is the amount of crop residue for biochar production; CR_{carbon} is the mass conversion rate from crop residue to biochar (%); $Biochar_{carbon}$ is the carbon content in biochar (%); C_{stable} is the stable carbon content in biochar (%). Following previous studies, CR_{carbon} and $Biochar_{carbon}$ is 45% and 50%, respectively [138-140]. C_{stable} is 79.6%, which equals to the fraction of biochar in one hundred years. Based on the three key parameters, we can calculate $CS_{biochar}$ (0.186 Mg Ce). The offset of pyrolysis process to fossil fuel use and the second order effects of biochar on soil organic matter were not considered in our estimation [141].

Uncertainty for biochar

The uncertainties of carbon sequestration from biochar include the amount of crop residue and mitigation potential per unit dry mass (dm). We first calculated the average and SD of the proportion of crop residue (0.11 ± 0.02% of total crop residue) for biochar production during 2010-2017, according to the records from the China Agricultural Statistical Report. For the uncertainty of biochar carbon sequestration rate ($CS_{biochar}$), a range of 18.7 ± 2.0% was used [26]. We used the Mont Carlo simulation to combine the uncertainties of $CS_{biochar}$ and crop residue. Our results showed that the potential mitigation is 0.50 (0.42-0.64), 0.08 (0.06-0.1) and 0.08 (0.06-0.1) Tg CO_2 yr^{-1} for the periods of 2000-2020, 2020-2030 and 2020-2060, respectively.

Marginal abatement costs for biochar

Due to the unavailability of cost data for the application of the biochar pathway, we used the fractional values in the references to calculate the achievable mitigation under the cost 10 USD $MgCO_2^{-1}$ (95%), 50 USD $MgCO_2^{-1}$ (95%), and 100 USD $MgCO_2^{-1}$ (100%) [24, 26].

Co-benefits for biochar

Biochar is often cited to provide important benefits through carbon sequestration. Biochar can help prevent soil erosion through its impacts on soil hydrology, soil wet aggregate stability and water runoff [142, 143]. Because of its porous structure and large surface area, biochar applications can increase the soil field capacity, nutrient availability, efficiency of fertilizer and the cation exchange capacity [144-146].

Comparison with previous studies

Yang et al. [132] reported that the carbon mitigation potential would be more than 8,600 Mt CO_2 yr^{-1} (i.e., 86 Tg CO_2 yr^{-1}) by assuming 73% of national crop residues were used to produce biochar. The biochar pathway estimation from Griscom et al. [26] also needs more than 98 Tg of crop residue. However, according to our investigation, the crop residue utilized to produce fertilizer, forage, fuel, base and raw materials accounted for more than 90% in 2020, and this ratio is still increasing gradually. Therefore, the amount of crop residues for biochar production is actually very small. We provide a conservative estimation for the utility of the biochar pathway in this study.

Pathway 7: Cropland Nutrient Management (CNM)

By implementing cropland nutriment management measures (e.g., reducing the application of N fertilizers), N_2O emissions from croplands can be reduced. Moreover, CO_2, CH_4 and N_2O emission can be also reduced in the fertilizer production process by improving the production technology (e.g., reducing the CO_2 emitted during ammonia production and the excess nitrous oxide during nitric acid production). Zhang et al. [147] reported that total greenhouse gas emission could be reduced to 206 million ton by 2030 with the use of innovative technology, the optimization of fertilizer production and its application in China.

The total consumption of nutrient fertilizer in China reached the historical maximum (24.00 Tg N yr^{-1}) in 2012 and decreased to 19.30 Tg N yr^{-1} in 2019, according to the National Bureau of Statistics (Extended Data Fig. 6, http://www.stats.gov.cn/tjsj/ndsj/). We assumed that China started to improve management of the cropland fertilizer application in 2012. The reduction in N_2O emission due to the decrease in nutrient fertilizer applications during 2012-2020 was regarded as a contribution to climate mitigation during this period. The decrease in N fertilizer application (4.70 Tg N yr^{-1}) accounted for 24% of total fertilizer applications in 2019.

For the future projections until 2030 and 2060, we derived the amount of cropland N fertilizer to be applied from Gu et al. [148], who projected the total reactive nitrogen amount from 2010 to 2050 by designing a reasonable change in diet, nutrient use efficiency, and nutrient recycling. They reported that N fertilizer use would decrease by 16.4 Tg N during 2010-2050, accounting for a 70% reduction in the total applied in 2010. We used the trend described in Gu et al.'s [148] results and projected the amount of N fertilizer to be applied in 2030, 2050 and 2060. Compared with 2020, the total amount of N fertilizer in 2030 and 2060 would be reduced by 2.47 Tg N yr^{-1} (13% of total fertilizer application in 2020) and 9.40 Tg N yr^{-1} (49% of total fertilizer application in 2020), respectively. We used the value of 2.54% (11.9 $MgCO_2e$ per MgN^{-1}) for the emission factor of translating N fertilizer to N_2O emission following Davidson et al. [149]. The total direct emission from cropland N fertilizer can be calculated as:

$$E_{NF} = M_{NF} * EF_{NF}$$

where E_{NF} is the direct N_2O emission from N fertilizer; M_{NF} is the amount of N fertilizer; EF_{NF} is the emission factor.

It is known that fertilizer production itself is a significant source of greenhouse gas emission. We used an overall upstream emission (including N_2O, CO_2, and CH_4) of 4 $kgCO_2e$ kg N^{-1} to estimate the GHG emission of this process [150] in the future scenarios. We assumed that the application of new technology in N fertilizer production envisaged in Zhang et al. [147] will reduce the GHG emissions by 10%. Subsequently, the upstream emission of fertilizer will decrease to 3.6 kgCO_2e kgN^{-1}, and the saved in N_2O emission from this process can be calculated as:

$$E_{NF\text{-}saving} = M_{NF} * EF_{NF}$$

where $E_{NF\text{-}saving}$ is the saved N_2O, CO_2, and CH_4 emission from upstream production of N fertilizer; and M_{NF} is the difference in amount of N fertilizer between base year and projection year (i.e., 2030 and 2060); and EF_{NF} is the emission factor.

The total N_2O emission from N fertilizer application would decrease by 45.95 (34.83-57.08) and 153.29 (111.0-195.58) Tg CO_2e yr^{-1} in 2020-2030 and 2020-2060, respectively. We only considered the uncertainty of the emission factor EF_{NF} (11.9 ± 4.5 Mg CO_2e Mg N^{-1}) of N fertilizer application, which was retrieved from Griscom et al. [26]. Compared with the upstream emission (CO_2, N_2O, CH_4) factor (11.3 Mg CO_2e Mg N^{-1}) used in Zhang et al. [147], our estimation is also conservative for the upstream N_2O emission.

Marginal abatement costs for cropland nutrient management

In China, low or negative costs are associated with avoiding the unnecessary use of excessive fertilizers because the regulations have created perverse subsidies for excessive fertilizer applications [26]. We used 50%, 60% and 95% as the fractional achievable CO_2e emission reduction at 10, 50, and 100 USD Mg CO_2e^{-1}, respectively [24, 26].

Co-benefits for cropland nutrient management

Cropland nutriment management can benefit biodiversity, water, soil and air [151-157]. The positive effects on soil and water of managing cropland nutrients are often cited as important co-benefits with reduced N_2O emission. Better cropland nutrient management can protect soil fertility, reduce freshwater eutrophication, and improve air quality [151]. A clean water ecosystem can be restored by boosting the national nutrient recycling rate in China [158].

Comparison with previous studies

GHG emissions associated with the N fertilizer chain in croplands can decrease by 49-249 Tg CO_2e yr^{-1} during 2010-2030 according to Zhang et al. [147]. Our study used a similar projection of improved manufacturing technologies and controlled N use and obtained a lower estimates in mitigation potential for the same period (84.57-164.57 Tg CO_2e yr^{-1}). TNC and Griscom et al. (Extended Data Fig. 7) reported that nutrient management pathway with a total mitigation potential of 192.86 Tg CO_2e yr^{-1} for the period of 2010-2030 in China. Our estimation is a little lower because we did not account for the mitigation potential from manure application.

Pathway 8: Cover crops (CVCR)

Conservation Agriculture is a farming system that can prevent losses of arable land and regenerating degraded lands. The major principle of conservation agriculture, such as tillage management, residue-return and cover crops, is minimum mechanical soil disturbance, maintaining permanent soil organic cover, and species diversification (FAO, https://www.fao.org/conservation-agriculture/en/). The positive effects of planting cover crops in fallow periods on the soil organic carbon have been reported in many studies [159, 160].

There is high potential to plant cover crops in winter fallow fields in South China [161]. The planting area of cover crops was only 4.49 Mha in 2020, but the potential maximum planting area for the cover crops was 25.66 Mha. We assumed that the planting of cover crops will utilize the maximum planting area (25.66 Mha) by 2030. The total carbon sequestration of cover crops can be calculated as follows:

$$CS_{ca} = LA_{ca} * CSR_{ca}$$

where CS_{ca} is the carbon sequestration in soil from cover crops; LA_{ca} is the potential planting area for cover crop; CSR_{ca} is the soil carbon sequestration rate. We used a carbon sequestration rate of 0.32 Mg C yr^{-1} to estimate the total carbon sequestration potential as suggested by Poeplau and Don [159]. Tillage management was not considered because the effects of no-tillage are still uncertain.

Uncertainty for cover crops

As the area available for cover crop planting was based on statistical data it was not considered as a source of uncertainty. Following Poeplau and Don [159], we used a sequestration rate in the range of 0.16-0.48 Mg C ha^{-1} yr^{-1} (95% CI) for the uncertainty estimate using Monte Carlo simulations (100,000 iterations assuming a normal distribution).

Marginal abatement costs for cover crops

The mitigation by cover crops is 5.27 (2.64-7.91) Tg CO_2 yr^{-1} during 2000-2020, and the future potential is 24.86 (12.43-37.29) and 24.86 (12.43-37.29) Tg CO_2 yr^{-1} during 2020-2030 and 2030-2060, respectively. We assumed 0% mitigation is possible at 10 USD $MgCO_2^{-1}$, 10% mitigation at 50 USD Mg CO_2^{-1} and 100% mitigation at 100 USD Mg CO_2^{-1}.

Co-benefits for cover crops

The co-benefits of climate mitigation for cover crops are mainly associated with their benefits to water and soil [151, 162]. Cover crops can help improve soil fertility through capturing excess nutrients and increasing soil organic matter [163, 164]. Moreover, cover crops also can raise the soil moisture holding capacity, reduce soil erosion, improve water quality and enhance biodiversity [165-167].

Comparison with other studies

The cover crops practice is an essential agricultural management practice to improve cropland soil organic carbon. In the United States, about 88 Mha of cropland can implement cover crops practice and the carbon mitigation potential is 103 Tg CO_2 yr^{-1} [24, 26]. Our results show that about 25 Mha of cropland can be used for cover crops in China, and the carbon mitigation potential is 24.86 Tg CO_2 yr^{-1} during 2020-2060.

Pathway 9: Improved rice cultivation (IMRC)

Much of the rice is planted in standing water, leading to methane CH_4 emission under anaerobic conditions. CH_4 emission can be reduced by implementing alternate wetting and drying drainage and mid-season drainage to shorten the time that the rice crop is in an anaerobic state [168]. Also, the management of fertilizer application, residue and tillage can reduce the amounts of nitrogen and carbon emission [169].

The U.S. Environmental Protection Agency (EPA) provides a consistent and comprehensive set of historical and projected estimates of emissions, and technical and economic mitigation estimates of non-CO_2 GHG for 195 countries from 2015 to 2050 [169]. They used the DeNitrification-DeComposition (DNDC) model to estimate the global CH_4 mitigation potential from rice production by analyzing 26 mitigation scenarios. For China, the EPA reported that the total CH_4 emission are 203 and 185 Mt CO_2e yr^{-1} with maximum mitigation potentials of 25 and 19 Mt CO_2e yr^{-1} in 2030 and 2050, respectively [169]. We used linear interpolation of this data and estimated the maximum mitigation to be 13 Mt CO_2e yr^{-1} in year 2060. The co-benefits of climate mitigation for improved rice cultivation are mainly associated with water [168, 170].

Uncertainty for improved rice cultivation

We estimated the uncertainty of CH_4 emission reduction by combining uncertainties of the CH_4 emission flux and rice planted area. For the flux uncertainty, we reviewed the previous studies focusing on improved water management and found that the average emission reduction was ± 12% [24]. To estimate the uncertainty for the rice planted area, we obtained the annual planted rice acreage from the National Bureau of Statistics of China (http://www.stats.gov.cn/english/). During 2011-2020, the total rice planted area ranged from 29.69 to 30.78 Mha. We used the Monto Carlo method to combine the two uncertainties, resulting in the estimated uncertainty of 12.09%.

Marginal abatement costs for improved rice cultivation

The potential mitigation of improved rice cultivation is estimated to be 33.0 (29.0-37.0) and 44.0 (38.7-49.3) Tg CO_2e yr^{-1} during 2020-2030 and 2020-2060, respectively. We assumed an 50% mitigation is possible at 10 USD $MgCO_2e^{-1}$, 80% mitigation at 50 USD $MgCO_2e^{-1}$, and 80% mitigation at 100 USD $MgCO_2e^{-1}$ [24].

Co-benefits for improved rice cultivation

The positive effects on water of improved rice cultivation are often cited as important co-benefits of its CH_4 reduction. For example, improved rice cultivation can reduce crop water consumption through irrigation management measures (e.g., mid-season drainage and alternate wetting and drying) [171, 172].

Comparison with previous studies

Previous studies reported that the total CH_4 emission from rice paddy land in China ranged from 4.80-28.00 Tg CH_4 yr^{-1} (120-700 Tg CO_2e yr^{-1}, if GWP_{100}=25) [173-176]. The large range of CH_4 emission can be explained by the estimation methods, including (1) extrapolating averaged emission over all rice types, (2) calculation of emission as a fraction of net primary production (NPP) and (3) emissions derived from model simulations [176]. Though the EPA estimation is conservative and has some uncertainties, it gives a reasonable magnitude of national CH_4 emission for China and can be used as reference for rice CH_4 emission reduction. The mitigation potential of improved rice cultivation is estimated to be 30.85 Tg CO_2e yr^{-1} by TNC (Extended Data Fig. 7), which is close to our estimation (29.0-37.0 Tg CO_2e yr^{-1}).

Pathway 10: Avoided Grassland Conversion (AVGC)

We only focused on conversion from grassland to cropland and the other types of conversions were not considered (e.g., grassland to built-up area). As aboveground biomass of grassland is usually removed by burning annually or grazing and aboveground biomass of croplands is harvested every year, we only considered the avoidable emission from belowground biomass and soil organic carbon.

Area

We obtained the area and spatial distribution of grassland conversion to cropland based on land cover data (2000 to 2018, 30m resolution) [177]. We calculated the mean conversion rate of 0.51 ± 0.12 (SD) Mha yr^{-1} of the four time periods: 2000-2005, 2005-2010, 2010-2015 and 2015-2018. Similarly, the conversion rates of temperate grassland and alpine grassland were determined to be 0.506 ± 0.119 and 0.007 ± 0.001 Mha yr^{-1}, respectively. We assume that the conversion rates will be the same in the following decades.

Flux

Belowground biomass

We assumed that all root biomass would be lost when converting grassland to cropland. We used empirical models to estimated belowground biomass (BGB) based on the relationship between mean annual precipitation (MAP) and belowground biomass [178]. Alpine grasslands and temperate grasslands were estimated separately using the empirical models as they have different empirical parameters. We extracted the spatial distribution of alpine and temperate grassland from the vegetation type map of China (1000m resolution, http://www.resdc.cn/) based on the spatial location of the converted area. The precipitation data (during 1982 to 2015, spatial resolution 1000 m) were obtained from the China Meteorological Data Service Center. We calculated the average BGB loss, using a coefficient of 0.45 to convert vegetation biomass density to C density [179]. The average biomass loss by grassland conversion in temperate grasslands and alpine grasslands was estimated to be 4.25 ± 1.02 and 2.71 ± 0.72 Mg C ha^{-1}, respectively (the SDs were obtained from each of the pixels).

Soil organic carbon

We considered soil organic carbon losses to a depth of 1 m soil depth and in different durations of cropping. The percent loss of SOC in the top 1 m of converted grassland was estimated to be 13.8 to 28.0% according to the a previous study [180], which calculated the difference in SOC between agricultural plots and paired remnant native vegetation plots across the globe. Another study showed that SOC decreased in soil depths of 0–60 cm after grassland conversion, but no significant differences were found at depths deeper than 60 cm [181]. SOC may also decline significantly with time and become constant after 20 years of grassland cropping [181]. We assume that the average percent loss of soil organic carbon from the top 1 m after conversion with grass cropping to be 25.57% within a short period (~10 year; (N=11, 95% CI: 12.99-38.15%), and 21.71% after a longer period (~20-40 year) with grassland cropping (N = 36, 95% CI: 16.99-26.43%) [182-199].

According to the spatial location of conversion of grassland to cropland, we obtained the data of initial SOC stocks in the areas where grassland conversion occurred based on the SoilGrids250m v.2 soil carbon database [200]. We applied the loss rates of short-time and long-time cropping to the initial SOC to get the national maps of potential soil carbon emission. We calculated the SOC loss as:

$$CL_{SOC} = SOC_{initial} * R * 10$$

where CL_{SOC} is the SOC loss after conversion (Mg C ha^{-1}), $SOC_{initial}$ is the initial soil organic carbon stocks (kg m^{-2}) and R is the average percent loss of SOC from the top 1 m (%). The average soil carbon loss was estimated to be 26.19 ± 11.78 Mg C ha^{-1} and 22.24 ± 10.01 Mg C ha^{-1} (the SDs were obtained from each of the pixels) during 2020-2030 and 2020-2060, respectively.

The maximum mitigation potential of avoided grassland conversion

The total mitigation potential from avoided carbon loss of belowground biomass and soil organic carbon in temperate and alpine grasslands was 57.42 Tg CO_2 yr^{-1} and 49.96 Tg CO_2 yr^{-1} during 2020-2030 and 2020-2060, respectively (Table S30).

Uncertainty for avoided grassland conversion

We estimated the uncertainties for area and flux. We used Monte Carlo simulations to combine the uncertainties and calculated the 95% CI, yielding a result of 57.42 (8.36-106.2) Tg CO_2 yr^{-1} for 2020-2030 and 49.96 (8.51-91.61) Tg CO_2 yr^{-1} for 2020-2060.

Co-Benefits for avoided grassland conversion

Avoided grassland conversion has the potential to produce strong co-benefits. Increasing the proportion of permanent grassland can increase cereal yields under certain conditions [201]. Grasslands can intercept precipitation and have high permeability and water retention capacity, which is important for water conservation. The permanent grassland has higher permeability because of its developed fine root system, which is mostly distributed in the topsoil layer. The abilities to conserve soil water and prevent soil erosion are also higher than that of cropland [202]. Many plants in the grassland have the ability to absorb some toxic gases in the air [203]. In addition, the grassland ecosystem contains abundant biological resources, is an important habitat for animals and microorganisms, and is a gene bank that stores a large amount of genetic material [204].

Marginal abatement costs for avoided grassland conversion

We used cost data in the *Returning Farmland to Forest and Grassland in Twenty Years in China (1999-2019)*[3]. The standard of this policy was to provide subsidies for retired lands based on the equivalent to 2250 kg ha^{-1} yr^{-1} of raw grain in the Yangtze River basin and southern region, and 1500 kg ha^{-1} yr^{-1} of raw grain for the retired land in the Yellow River basin and northern region. The raw grain subsidy was calculated at 1.4 CNY/kg. Direct subsidies for retired land were given to the farmers who were retired from farming. The subsidy standard was 1575 CNY ha^{-1} yr^{-1} in the Yangtze River Basin and southern areas, and 1050 CNY ha^{-1} yr^{-1} in the Yellow River Basin and northern areas, with an additional 300 CNY ha^{-1} yr^{-1} for living expenses for two years after land retirement. Since most of our grassland conversion areas were identified to be located in the northern regions, we used a subsidy based on the subsidy in the northern regions. Thus, the cost per hectare of avoided grassland conversion to cropland in the northern region can be calculated as:

$$\text{Cost} = (1500*1.4+300)*2+(1050+300)*2=7500 \text{ CNY/ha}$$

We adjusted payments to 2015 USD. We calculated the carbon sequestration potential and cost of carbon sequestration by province, arranged the data in descending order of carbon sequestration potential and then used the cumulative value of carbon sequestration potential and cost to create a MAC curve. The curves were drawn at 3% and 5% discount rates, respectively (Fig. S7).

Comparison with previous studies

We estimated a rate of grassland conversion to cropland in China of 0.51 Mha yr^{-1}, approximately twice as high as that in Canada (0.25 Mha yr^{-1}) [25]. For soil carbon flux, we considered soil carbon loss to a depth of 1 m, but only the top 30 cm soil carbon loss during the conversion of grassland to cropland was considered in Canada (Extended Data Fig. 7). These differences made our maximum mitigation potential much greater than Canada's. We have a closer grassland loss rate to the U.S. (0.69 Mha yr^{-1}), but the average percentage soil carbon loss (28%) in the 1 m soil depth in the U.S. is higher than ours (22%) [24]. In addition, the U.S. study also considered the loss of shrub biomass, including aboveground biomass, belowground biomass and litter, which resulted in their higher maximum mitigation potential.

Pathway 11: Grazing optimization (GROP)

Area

The Chinese government launched a national conservation program "Returning Grazing Land to Grassland (RGLG)" in 2003. Fencing management and pasture sowing are two major options to increase plant productivity and enhance soil carbon accumulation in degraded grasslands. According to the data provided by the National Forestry and Grassland Administration, the total area of fencing management and pasture sowing was increased during 2003-2020, reaching up to 99.56 Mha in 2020, mainly within 13 provinces (Fig. S8). The RGLG program ended in 2020, but management measures such as fencing and pasture sowing are still included in the "Major Projects for the Protection and Restoration of Important Ecosystems (2021-2035)" released in 2020 [205]. According to the outline of the 14th Five-Year Plan for Forestry and Grassland Protection and Development, 230 million mu of degraded grassland will be restored in China by 2025 [206], which means that the average annual grassland restoration area will be 3.07 Mha. According to the Report on the status of China's land greening in 2021, 1.56 million hectares of grassland ecological restoration will be carried out in China in 2021 [207]. These restoration programs included fencing, reseeding and other management measures. To conservatively estimate the future carbon sequestration potential of fencing and pasture sowing measures, we assumed 1.56 Mha per year will be managed for grassland recovery during 2020-2030 and 2030-2060. According to the main data bulletin of the third National Land Survey, the existing grassland area in China is 264.53 Mha [208], 70% of which is degraded to different degrees (i.e., 185.17 Mha) [206]. According to the assumptions, 15.60 and 62.40 Mha of degraded grassland will be restored by 2030 and 2060, respectively.

Carbon flux

The carbon sequestration rate (Mg C ha^{-1} yr^{-1}), including aboveground biomass, belowground biomass and soil organic carbon, was estimated according to Xiong et al. [209], which presented data of 462 and 457 sampling sites inside and outside the fencing areas by carrying out an extensive field survey covering the main project areas. The differences of the carbon stocks in aboveground biomass (0.06 ± 0.003 Mg CO_2 ha^{-1} yr^{-1}), root biomass (0.43 ± 0.02 Mg CO_2 ha^{-1} yr^{-1}), and soil carbon (0.42 ± 0.03 Mg CO_2 ha^{-1} yr^{-1}) are the additional carbon fluxes of the managed compared to the unmanaged sites. We used these values to calculate the future carbon sequestration potential (Table S31), assuming that carbon sequestration rate would remain the same during 2020-2030 and 2020-2060. The calculation used the following formula:

$$CSR_i = (CD_{INi} - CD_{EXi})/T$$

where CSR_i was the carbon sequestration rate in province i, CD_{INi} was the carbon density inside the project area in province i, CD_{EXi} was the carbon density outside the project area in province i, and T was the duration of the project (y).

The total carbon sequestration potential (Mg C yr^{-1}) was calculated as:

$$Carbon\ sequestration = \left(\sum_{i=1}^{p} \sum_{j=2003}^{2020} A_{ij} * CSR_i\right)/T$$

where p is the number of provinces in the project (p=13), CSR_i is the carbon sequestration rate in province i, A_{ij}, the total project area in province i in year j, and T is the duration of project implementation (y).

The maximum mitigation potential of grazing optimization

The total mitigation potential of grazing optimization was 59.08 (53.29-64.20) Tg CO_2 yr^{-1} during 2000-2020, and it is projected to be 7.83 (7.11-8.49) and 29.17 (26.60-32.06) Tg CO_2 yr^{-1} during 2020-2030 and 2020-2060, respectively.

Uncertainty for grazing optimization

The area of the grazing optimization measure was obtained from the National Forestry and Grassland Administration, and was not considered a source of uncertainty. Using the Monte Carlo method, we combined the uncertainties associated with the three carbon fluxes to get the overall uncertainty of climate mitigation by grazing optimization.

Co-benefits for grazing optimization

Grazing optimization has the potential to produce strong co-benefits. The biodiversity of soil animals can be improved with fencing management [210]. Fencing management obviously improved the soil water-retention capacity, and significantly enhanced the total coverage and average height of the plant community [211]. Reseeding can markedly increase species richness and group densities [212], as well as promote the recovery of vegetation in degraded grassland [213]. There are also debates about the effects of fencing management. The positive or negative effects largely depend on the initial state of the fencing on the grassland and time of fencing. Studies suggest that fencing on degraded grassland can promote biodiversity and carbon sequestration, but have negative impacts if applied to well-conditioned grasslands. Four to eight years of fencing is preferable for the recovery of severely overgrazed area, followed by fence removal for the benefits of wildlife [214-220].

Marginal abatement costs for grazing optimization

We used province-level average payments per hectare and the carbon sequestration potential to create the MAC curves of grazing management. The financial investment data of each province were obtained from the National Forestry and Grassland Administration. During 2003-2010, the average land compensation for fencing management and pasture sowing was 211.10 CNY per hectare (including subsides for fence construction, supplementary sowing of grass seeds and feed grain, not including payment for other items such as labor), and we adjusted payments to 2015 USD. We ranked the data of different provinces in descending order of carbon sequestration potential, and then used the cumulative values of carbon sequestration potential and cost for curve fitting with 3% and 5% discount rates, respectively (Fig. S9).

Comparison with previous studies

A previous global study found that the climate mitigation of "grazing-optimal intensity" pathway in China was only 25.04 Tg CO_2 yr^{-1} [221]. Our estimate of mitigation potential for grazing optimization in China was higher, i.e., 59.08 Tg CO_2 yr^{-1} during the 2000-2020 periods (Extended Data Fig. 7). The difference is partly due to the method in consistency. The earlier global study defined the "optimum" as the maximum forage production and predict the management effect using a modeling approach (the Century model) [222]. Our study considered the carbon sequestration in aboveground biomass, belowground biomass and soil carbon, and thus, obtained higher estimates of the mitigation potential.

Pathway 12: Grassland Restoration (GRR)

Restoration area

The croplands, which are not suitable for farming (e.g., steep slope cropland (>15 degrees), rocky desertification cropland, and desertification cropland), are required to be restored to forests or grasslands in the Grain for Green project since 1999 in China. We identified 5.80 Mha area of grassland restoration (i.e., conversion from cropland to grassland) during 2000-2020 using the land use and cover data obtained from the Data Center for Resources and Environmental Sciences, Chinese Academy of Sciences (RESDC) [177].

According to the 'Measures for the inspection and acceptance of a new round of Grain for Green project', the types of returned farmland include slope farmland > 25 degrees, severely desertified farmland, and slope farmland of 15-25 degrees in important water sources, excluding basic farmland. We extracted the croplands with a slope greater than 15 degrees based on the land use map of 2018 and the Digital Elevation Model in China. This amounted to 6.93 Mha (including potential restoration to grasslands or forests). This number is very close to the estimation constrained by *the farmland red line* (7.90 Mha) (Table S6). According to the White Paper issued by the National Forestry and Grassland Administration of China [3], the proportion allocated for the restoration to grassland during 2014 to 2019 accounted for 7.86% of the total restoration area (i.e., 92.14% was for forest restoration). We assumed that 7.86% of the total potential restoration area (0.54 Mha) would be converted into grasslands in the next decades. The 3rd National Land Survey provided a relatively higher number for the sloping farmland (11.96 Mha) (http://www.mnr.gov.cn/dt/ywbb/202108/t20210826_2678340.html). Using the fraction of 7.86%, the maximum area for grassland restoration from sloping farmland would be 0.93 Mha. We used the conservative value of 0.54 Mha in our calculation considering the constraint of *the farmland red line*. The government of the People's Republic of China issued a planning document, which declared that all unsuitable croplands should be restored before 2030 [223]. Thus, we assumed that the 0.54 Mha of cropland would be restored by 2030.

Carbon flux

We considered carbon sequestration in soil and root biomass. Aboveground biomass is annually harvested, grazed or decomposed within a few years, and therefore, is not considered in our calculations.

For soil carbon sequestration, we assume the average increase of soil carbon stocks in the top 1 m to be 0.91 ± 0.40% per year after restoration. This estimate was calculated based on published studies, including 27 observations in China [224-232]. The soil carbon stock data was obtained from the SoilGrids250m data set [200]. The average SOC sequestration rate was estimated to be 3.35 Mg CO_2 ha^{-1} yr^{-1} (SD = 2.56) during 2000 to 2020, and 4.28 Mg CO_2 ha^{-1} yr^{-1} (SD=1.49) during 2020 to 2030.

We assume that the perennial root biomass become constant over 60 years after restoration and the annual increase is in a linear fashion [233]. We used the empirical model of below-ground biomass as the function of the mean annual precipitation (MAP) [178]. We estimated the average accumulation of root biomass per hectare on the location of cropland that could be returned to grassland, under the assumption that the precipitation in these areas is consistent in the future. The precipitation data (during 1982 to 2015) was obtained from the China Meteorological Data Service Center:

(http://data.cma.cn/data/cdcdetail/dataCode/SURF_CLI_CHN_MUL_DAY_V3.0.html). The conversion coefficient of 0.45 was used to convert vegetation biomass density to C density

[179]. The average rates were 0.29 (SD = 0.11) and 0.48 Mg CO_2 ha^{-1} yr^{-1} (SD = 0.12) for root biomass carbon during 2000-2020 and 2020-2030, respectively.

$$\text{SOC rate (Mg C ha}^{-1}\text{ yr}^{-1}) = SOC_{initial} * 0.91\% * 10$$

$$C_{RB}\text{ rate (Mg C ha}^{-1}\text{ yr}^{-1}) = \frac{1.3551 * MAP + 304.2}{60} * 0.45 * 0.01$$

$$\text{Mitigation potential (Tg CO}_2\text{ yr}^{-1}) = (C_{RB}\text{ rate} + \text{SOC rate}) * \text{Area} * 3.67$$

The total sequestration rates were 3.64, 4.77 and 4.77 Mg CO_2 ha^{-1} yr^{-1} during 2000-2020, 2020-2030 and 2020-2060, respectively.

The maximum mitigation potential of grassland restoration

The historical mitigation flux of grassland restoration is estimated to be 21.09 (95% CI: -7.94-50.37) during 2000-2020 and the future potential is 2.59 (95% CI: 0.49-6.52) Tg CO_2 yr^{-1} during 2020-2030 (and 2020-2060).

Uncertainty for grassland restoration

The restoration area during 2003-2020 was obtained from the land use data and determined as a constant, and the uncertainty of the mitigation capacity is only associated with the carbon flux. For the future mitigation potential during 2020-2030 and 2020-2060, uncertainties are associated with both restoration area and flux. We used Monte Carlo simulation to combine the uncertainties of soil carbon sequestration rate and the root biomass sequestration rate, as well as restoration area (0.94 Mha as the upper boundary).

Co-benefits for grassland restoration

Grassland restoration has the potential to produce strong co-benefits. Soil chemical and microbiological properties can be significantly improved after cropland abandonment [234] and runoff and soil erosion can be reduced in the early stages of restoration following the cropland abandonment [235]. Grassland restoration can also improve biodiversity [236].

Marginal abatement costs for grassland restoration

We used province-level averages per hectare payments and total mitigation potential to create the MAC curves. The ecological compensation for conversion from cropland to grassland was 7500 CNY per hectare (the same as in Pathway 10: Avoided Grassland Conversion (AVGC)) [3], and we converted it to 2015 USD. The curves were calculated at 3% and 5% discount rates (Fig. S10).

Comparison with previous studies

The higher carbon sequestration rate of 3.64 Mg CO_2 ha^{-1} yr^{-1} (including belowground biomass and soil organic carbon) and the larger restoration area of 0.54 Mha observed in our calculations indicates that grassland restoration in China has a higher carbon sequestration potential compared to Canada [25] (Extended Data Fig. 7) where the assessment considered only soil organic carbon. As a result, by 2030, a rate of 2.59 Tg CO_2 yr^{-1} is predicted to be achieved in China compared to 0.7 Tg CO_2 yr^{-1} in Canada. In the Canadian study, a sequestration rate of 2.55 Mg CO_2 ha^{-1} yr^{-1} and a restoration area of 0.27 Mha were used. In contrast, in the U.S., grassland restoration with a sequestration rate of 4.37 Mg CO_2 ha^{-1} yr^{-1} (including soil organic carbon and root biomass) on an area of 2.1 Mha will sequester 9 Tg CO_2 yr^{-1} by 2030. The carbon sequestration potential of grassland restoration from cropland in the three countries is relatively small and the difference mainly comes from differences in the areas and the evaluation methods used, where the factors considered in the carbon sequestration rate varied.

Pathway 13: Avoided Coastal Impacts (AVCI)

The coastal wetlands contain important ecosystems such as mangrove forests, saltmarshes, and seagrass beds, which are key blue carbon sinks and have been reduced globally. In recent years, the mangroves have been protected and restored in China with a series of actions and policies. However, the protection of saltmarshes and seagrass beds in China is still inadequate. Avoiding losses of these ecosystems in the coastal wetlands, which has been mainly due to human activity, is an opportunity to enhance CO_2 sequestration and reduce emissions of CO_2 and other GHGs.

Area

We assumed that future potential losses of the saltmarsh and seagrass ecosystems will be of the same magnitudes as those during 2000-2015. The area of saltmarshes in 2015 was 2,979 km^2 according to the literature [237]. For the area in 2000, we used the average estimated area (4,613 km^2) by subtracting the area of mangroves [238] from that of the coastal wetlands [239] given in the same period. The mean annual loss rate of saltmarshes from 2000 to 2015 was 10,894.97 ± 131.42 ha yr^{-1}. Due to the lack of seagrass area data in China, we determined the mean annual loss rate of seagrass beds (241.04 ha yr^{-1}) as the average of the global loss rate (ranging from 0.4-7%) [240].

Flux

The ecosystem carbon stock and the percent of committed emission after disturbance were used to calculate the avoided CO_2 flux. The ecosystem soil carbon stocks were 935.85 Mg CO_2 ha^{-1} for saltmarshes and 396.36 Mg CO_2 ha^{-1} for seagrass beds [241]. According to the estimated half-life of 7.5 years [242, 243], the estimated committed emission were 60% of the soil carbon stock in the first 10 years and 97% of the soil carbon stock in the first 40 years. Hence, the mitigation potential of avoided costal wetland conversion can be projected for different time periods (Table S32).

Uncertainty for avoided coastal impacts

The 95% confidence intervals of area and carbon flux were calculated for saltmarshes and seagrassbeds using Monte Carlo modeling, and then the uncertainties of the total were combined according to the IPCC Approach 1. The total climate mitigation potential of AVCI were estimated to be 6.21 ± 1.32 Tg CO_2 yr^{-1} during 2020-2030 and 10.04 ± 2.13 Tg CO_2 yr^{-1}during 2020-2060.

Co-benefits for avoided coastal impacts

Avoided coastal impacts have the potential to produce strong co-benefits. Coastal wetlands can improve the water and air quality of estuaries by acting as a sink for abundant matters such as nitrogen and heavy metals. In addition, they can provide indispensable habitats for juvenile fish, shellfish, and crustaceans [244, 245]. Land use close to existing wetlands often involves the oxidization of acid sulfate soils that either are or were once part of a wetland, causing the flushing of acid from the soil. Avoiding disturbance of wetlands can conserve soil from erosion [246].

Marginal abatement costs for avoided coastal impacts

There are very limited studies about the cost of avoided coastal wetland loss in China. Hence, we used the MAC of avoided mangrove loss in the global studies [26, 247], which included the estimate of the cost of avoided coastal wetland loss in China. We assumed that protecting a large area of coastal wetland is possible at low cost. 60%, 75%, and 90% of climate mitigation from coastal wetland protection were determined under the cost of 10, 50, and 100 USD $MgCO_2^{-1}$ [247]. This corresponds to 3.72, 4.65 and 5.59 Tg CO_2 yr^{-1} during 2020-2030, and 6.02, 7.53, and 9.03 Tg CO_2 yr^{-1} during 2020-2060, respectively.

Comparison with previous studies

Our estimate (0.09 Tg CO_2 yr^{-1} in 2020-2030) of avoided CO_2 emission from seagrass is close to that of Canada (0.1 Tg CO_2 yr^{-1})[25], but lower than that of the U.S. (7 Tg CO_2 yr^{-1})[24], largely due to the lower rate seagrass bed area loss in China used in this study (estimated as 241 ha yr^{-1} in China; 20,000 ha yr^{-1} in the U.S.). However, as the protection of seagrass bed is difficult, only a low portion of the total mitigation potential can be achieved under a cost of 100 USD $MgCO_2^{-1}$. There is still large uncertainty in the estimates for avoided seagrass impacts in China due to the lack of accurate surveys on the current and historical areas of seagrass.

Pathway 14: Avoided Peatland Impacts (AVPI)

Peatlands are widely distributed in China. A large amount of carbon can be released when peatlands are degraded or converted to other land types. The climate mitigation from this pathway is regarded as reduced or avoided carbon emission from vegetation and soil carbon stocks due to protection of peatlands from human disturbances.

Area

There is very limited data and large uncertainty about the peatland area in China. After a careful comparison of the available literature, the data of peatland area from a comprehensive investigation (17,523.5 km^2) was determined as the reference of the peatland area in 1990 [248]. From Mao et al. [249], the areas of swamp and marsh were 7,760.7 km^2 and 157,304.4 km^2 in 1990, and 7,923.7 km^2 and 139,552.1 km^2 in 2010, respectively. Considering the slow rate of peat accumulation (it usually takes hundreds of years to form a sizeable peatland area), we assumed that the area of forested peatland is constant although the swamp area increased. Consequently, a peatland area of 15,638.8 km^2 in 2010 was used, assuming that the future loss rate of peatlands is in the same magnitude as that in the past decades.

Flux

As carbon emission of peatland varies with different climatic conditions, we calculated the avoided emission in each of the climatic zones: tropical, subtropical, temperate, and plateau climate zone in China (http://geodata.pku.edu.cn, Fig. S11). The annual peatland loss rates and avoided emission rates were used to determine the total avoided emission fluxes in each climate zone. We assumed that the proportion of peatland in the inland marsh in each climate zone is the same.

According to the literature, we assumed that 100% of the biomass carbon and 92% of the soil organic carbon would be released after peatland loss [250]. We calculated the carbon density of the peat biomass [251] and soil carbon [252] in the four climate zones, from which the mean and SD of potential carbon emission could be determined (Table S33).

Mapping Province-level Mitigation

Based on the mitigation potential in each climatic zone and the proportion of marsh area in each province [253], the avoided CO_2 emission from peatland protection was estimated on the provincial scale. For the provinces that cover more than one climate zones, we classified them into the climate zone that contained most of the land area in that province. For Sichuan Province, we considered the combined mitigation potential in subtropical and plateau climate zones.

Uncertainty for avoided peatland impacts

There is a large uncertainty about the peatland area in China. We found another two records of Chinese peatland area [254, 255] for determining the uncertainty range of Chinese peatland area, assuming that the areas' uncertainty range for each climate zone were the same as the national range (78%). Based on estimates of peatland areas and carbon stock from different studies, we calculated 95% confidence intervals of the mitigation potential by Monte Carlo uncertainty modeling and combined the overall uncertainties. The estimated avoided CO_2 emission of peatland conversion in China would be constant at 23.97±13.67 Tg CO_2 yr^{-1} (95% CI) in the next decades (2020-2060).

Co-benefits for avoided peatland impacts

Peatlands play vital roles in regulating the global carbon cycle, maintaining biodiversity, as well as storing and purifying water [256]. Because of their rich plant diversity, peatlands harbor a multitude of characteristic microorganisms, insects, birds and other animals [257]. The exposure of peat soil to the air causes it to become fully oxidized and leached, resulting in a mineral soil after drainage [258], and the increased risk of peat fires can lead to future air pollution [259].

Marginal abatement costs for avoided peatland impacts

The cost for avoided peatland impacts was estimated using the same method as that of avoiding coastal wetland loss since no other data can be used. We assumed that 60%, 75%, and 90% of climate mitigation from avoided peatland impacts could be achieved under the cost of 10, 50, and 100 USD $MgCO_2^{-1}$, respectively.

Comparison with previous studies

This study showed the great climate mitigation potential from avoided peatland impacts in China. The estimated max potential (24 Tg CO_2 yr^{-1}) was twice as that for Canada (10.1 Tg

CO_2 yr^{-1}) (Extended Data Fig. 7). Although the area of avoided peatland impacts in China (0.01 Mha yr^{-1}) accounted for only 1% of the global estimate (0.78 Mha yr^{-1}), its achieved potential under the cost of 100 USD $MgCO_2^{-1}$ (14 Tg CO_2 yr^{-1}) reached 2% of the global potential (678 Tg CO_2 yr^{-1}). This disproportionate result was partly due to the higher carbon storage in peat soils in China relative to the global average. Specifically, peat soils in China contain 17,439.3 Mg C ha^{-1} in the tropics, 11,78.9 Mg C ha^{-1} in the subtropics, 889.4 Mg C ha^{-1} in temperate zones and 608.3 Mg C ha^{-1} in plateau climate zone. For comparison, the global averages for peat soil carbon contents are 217.5 Mg C ha^{-1} in the tropics, 141.9 Mg C ha^{-1} in temperate zones, and 56.6 Mg C ha^{-1} in boreal zones.

Pathway 15: Coastal Wetland Restoration (CWR)

We considered the mitigation potential of restoring mangroves, saltmarshes, and seagrass beds in China. Wetland restoration by re-wetting can capture more carbon in the vegetation and soil. Here only CO_2 sequestration by vegetation and soil of mangrove forests and by the soil of saltmarshes and seagrass beds were considered. The CH_4 emission during the re-wetting process was not considered.

Area

In recent years, much attention has been paid to mangrove restoration, which currently increased to occupy 29,227 ha [237]. Based on the planned mangrove area (9,375 ha) that will be restored in 2020-2025 [260, 261] (Table S34), we first assumed that the area for mangrove restoration in 2020-2030 will be more than that in 2020-2025. The maximum restoration area for mangrove plantation is estimated to be 16,220 ha in 2020-2030 and 14,457.2 ha in 2030-2060, according to the National Mangrove Source Survey [262] (Table S35). We assumed that the maximum restoration area of saltmarshes and seagrass beds was the extent of historical losses. According to the current occupied areas (297,937 ha for saltmarshes and 8,765 ha for seagrass beds) [237, 263] and the percentage loss in area (57% for saltmarshes and 74% for seagrass beds) [264], the calculated maximum restoration area was 320,422.81 ha for saltmarshes and 24,946.54 ha for seagrass beds. We assumed that saltmarshes and seagrass beds would be restored at an even rate from 2020 to 2060, and therefore, 25% of the maximum potential area can be restored in 2020-2030.

Flux

Carbon accounting for the coastal wetland restoration contains both an avoided emission component and a sequestration component. The carbon stock references used were 1303.77 Mg CO_2 ha^{-1} for mangroves, 935.85 Mg CO_2 ha^{-1} for saltmarshes and 396.36 Mg CO_2 ha^{-1} for seagrass beds [241]. Considering the large area of coastal wetland loss before 1980s and the estimated carbon stock half-life of 7.5 years [242, 243], we estimated a release of 84% of the original carbon stock in the first 20 years after the loss of the wetlands, and that the remaining 16% of the carbon stock will be lost in the following years (by 2060 for our study) (Table S36). Therefore, restoring the wetlands can retain the remaining carbon from being released. The mean emission rate is 0.27%$\cdot$yr^{-1}.

Also, restoring the degraded wetlands can sequester additional carbon in soil and/or biomass. The carbon sequestration potential in restored saltmarshes and seagrass beds were calculated based on their carbon sink rates, i.e., 6.09 Mg CO_2 ha^{-1} yr^{-1} [265] and 5.06 Mg CO_2 ha^{-1} yr^{-1} [266], respectively. We considered the carbon sequestration in soil and biomass for the carbon sink potential of restored mangroves. Although some mangrove restoration projects were started before 2020, these mangrove ecosystems are still unstable. Hence, for the carbon sequestration potential of the restored mangroves at different periods, we collected the data of ecosystem carbon contents and calculated the carbon sequestration potential of soil and biomass [267-270] (Fig. S12). According to the literature [267], the biomass carbon content of mangroves restored more than 15 years will be relatively stable, but its SOC content remains much lower than that of the initial mangrove ecosystem.

Uncertainty for coastal wetland restoration

It was difficult to directly estimate uncertainty due to the limited data available. Therefore, we refer to the uncertainty percentage (21%) of avoided coastal wetland impacts. The total climate mitigation potentials of coastal wetland restoration were estimated to be 1.44 ± 0.31 Tg CO_2 yr^{-1} during 2020-2030 and 3.56 ± 0.76 Tg CO_2 yr^{-1} during 2020-2060.

Co-benefits for coastal wetland restoration

The creation or restoration of large coastal ecosystems can provide several benefits, including flood defense and water quality improvement [244]. In China, the restoration project conducted in a degraded coastal wetland has proved to be successful with increased biota species richness and habitat quantity with desalination of the soil [271].

Marginal abatement costs for coastal wetland restoration

Very limited information was available on the costs of restoration projects in China [272]. We used the global cost proportion of mangroves and salt marsh restoration reported in the literature [26], which was based on more than 50 studies mostly conducted in developed countries. This may cause the overestimate on the associated costs of restoration in this study. Generally, the construction of seagrass beds is expensive, and no successful case has been reported yet in China, so we assumed that it is impossible to implement at a cost of 100 USD $MgCO_2^{-1}$ or less.

Comparison with previous studies

The total area of suitable land available for mangrove plantation is very small in China (7202 ha). Therefore, the estimated potential of mangrove restoration in China (0.21 Tg CO_2 yr^{-1}) accounted for only a small part of on the global total [26] (11 Mha, 179 Tg CO_2 yr^{-1} in 2020-2030 under the cost of 100 USD $MgCO_2^{-1}$) (Extended Data Fig. 7). In terms of the mitigation potential from salt marsh restoration, the estimation of China (0.41 Tg CO_2 yr^{-1}) was much lower than that of the U.S. [24] (7 Tg CO_2 yr^{-1}) in 2020-2030, which mainly reflects the lower recovery rate (0.08 ha yr^{-1} in China and 0.48 Mha yr^{-1} in the U.S.) and the lower carbon sequestration rate (2.3 Mg C ha^{-1} in China and 6.7 Mg C ha^{-1} in the U.S.). As seagrass beds restoration remains a worldwide problem, it is challenging to restore under the cost of 100 USD $MgCO_2^{-1}$ for both developed and developing countries [24, 26].

Pathway 16: Peatland Restoration (PTR)

Peatland restoration by re-wetting can reduce CO_2 emission and dissolved organic carbon (DOC) loss, and increase the biomass carbon stock. However, it also raises CH_4 emission. As the biomass of non-forested peatlands becomes stable quickly after restoration, we only included reduced CO_2 emission, DOC loss and increased CH_4 emission for estimating the mitigation potential of drained peatlands in this study. The 100-year global warming potential (GWP) of 25 for CH_4 was used.

Area

Due to the lack of historical peatland area data in China, we refer to the peatland area in 1990 as the maximum historical area, and only the change in area of non-forested peatland since then (Table S37) [231,232]. Therefore, a maximum restorable area in China was estimated to be 188,459.6 ha. We assume that the lost peatland area will be restored at an even rate during 2020-2060, and 25% of the lost area would be restored during 2020-2030 (47,114.9 ha) (Table S37).

Flux

The published data of peatlands in China have focused in the northeastern area (temperate zone) and the Zoiga plateau (plateau climate zone). The mean CO_2 emission rate from the drained peatlands in the plateau climate zone is 28.82 Mg C ha^{-1} yr^{-1} [273]. Since there are limited studies on the CO_2 emission rate from drained peatlands in the other climatic zones and restored peatlands in all climatic zones, we used the data reported by IPCC [274]. The values of the subtropical, temperate and plateau climate zones in our study used that of the temperate zone in the IPCC report, and the factors *in rich status* were used because almost of the peatlands in China are eutrophic [275]. The DOC loss factors reported by IPCC [274] were also used.

We assumed that CH_4 emission rate from restored (by re-wetting) peatlands is one-tenth of that from natural peatlands since 92% of SOC stock has been lost in drained peatland [250]. We used the average values of the CH_4 emission rate from natural peatlands in the literature [273, 276-282], i.e., 0.36 Mg CH_4 ha^{-1} yr^{-1} in the temperate zone and 0.37 Mg CH_4 ha^{-1} yr^{-1} in the plateau climate zone. Due to the lack of observed data, the emission rate from restored peatlands in the tropical and subtropical regions was estimated to be one-tenth of the natural peatlands in tropical and temperate regions [274]. The mean emission rate from the drained peatlands was estimated to be 0.02 Mg CH_4 ha^{-1} yr^{-1} for the plateau climate zone based on literature [273, 283, 284], and the values used for the other regions were obtained from the IPCC report.

Mapping Province-level Mitigation

Based on the mitigation potential in each climatic zone and the published proportion of marsh area in each province [253], we estimated the mitigation potential for each climate zone (Table S38). For the province that covers more than one climate zone, we classified that province into the climate zone that contains most of the land area in that province. For Sichuan Province, we considered the combined mitigation potential in subtropical and plateau climate zones.

Uncertainty for peatland restoration

We found another two records of Chinese peatland area [254, 255] for determining the uncertainty range of Chinese peatland area, assuming that uncertainty range for each climate zone area were the same as the national range. Based on estimates of peatland areas and carbon fluxes from different studies, we calculated the 95% confidence intervals of potential in each climatic zone by Monte Carlo uncertainty modeling. The climate mitigation potential of peatland restoration is 3.61 (-0.83~8.05) Tg CO_2e yr^{-1} (95% CI) during 2020-2030 and 14.47 (-3.23~32.17) Tg CO_2e yr^{-1} (95% CI) during 2020-2060.

Co-benefits for peatland restoration

Regeneration of peatlands reestablishes diverse biological communities [285, 286]. According to previous studies, the longer the time peatland is allowed to restore, the greater the accumulation of its plant residues and organic matter, which help to improve soil properties [287]. The peatland restoration in the high-altitude region of China would maintain high altitude peatland functions such as downstream water supply and biodiversity conservation [286]. In addition, peatland rehabilitation will reduce the likelihood of peat fires [258], which help to reduce the risk of damage to human health from exposure to air pollutants [259].

Marginal abatement costs for peatland restoration

The cost of peatland restoration in China is assumed to be the same as that in the global study [26], in which the achievable percentage are 18% and 48% under the cost of 10 and 100 USD Mg CO_2e^{-1}, respectively. The achievable percentage under the cost of 50 USD Mg CO_2e^{-1} is assumed as the mean of the percentage (33%) under the cost of 10 and 100 USD Mg CO_2e^{-1}.

Comparison with previous studies

As most peatlands are located in the tropics or high latitudes, the potential of peatland restoration in China (2 Tg CO_2e yr^{-1}) only accounted for a very small part of the global potential (394 Tg CO_2e yr^{-1}) during 2020-2030 under the cost of 100 USD Mg CO_2e^{-1}. Compared with the potential of this pathway estimated by other studies on the country level under the cost of 100 USD Mg CO_2e^{-1} in the future decade, the potential of China (2 Tg CO_2e yr^{-1}) was greater than that of Canada (0.1 Tg CO_2e yr^{-1}), but lower than that of the U.S. (9 Tg CO_2e yr^{-1}) (Extended Data Fig. 7). This was mainly due to the differences in recoverable peatland areas (0.3 Mha in Canada, 0.05 Mha in China, and 3 Mha in the U.S.). In addition, the higher costs for peatland restoration in China (48% of max potential could be achieved under the cost of 100 USD Mg CO_2e^{-1}) was also one of the reasons for the lower carbon sequestration potential compared with that in the U.S. (where almost 100% of max potential could be achieved at 100 USD Mg CO_2e^{-1}). Under the cost of 100 USD Mg CO_2e^{-1}, the potential of China in 2020-2060 (7 Tg CO_2e yr^{-1}) was closer to the potential of the U.S. in 2025 (9 Tg CO_2e yr^{-1}).

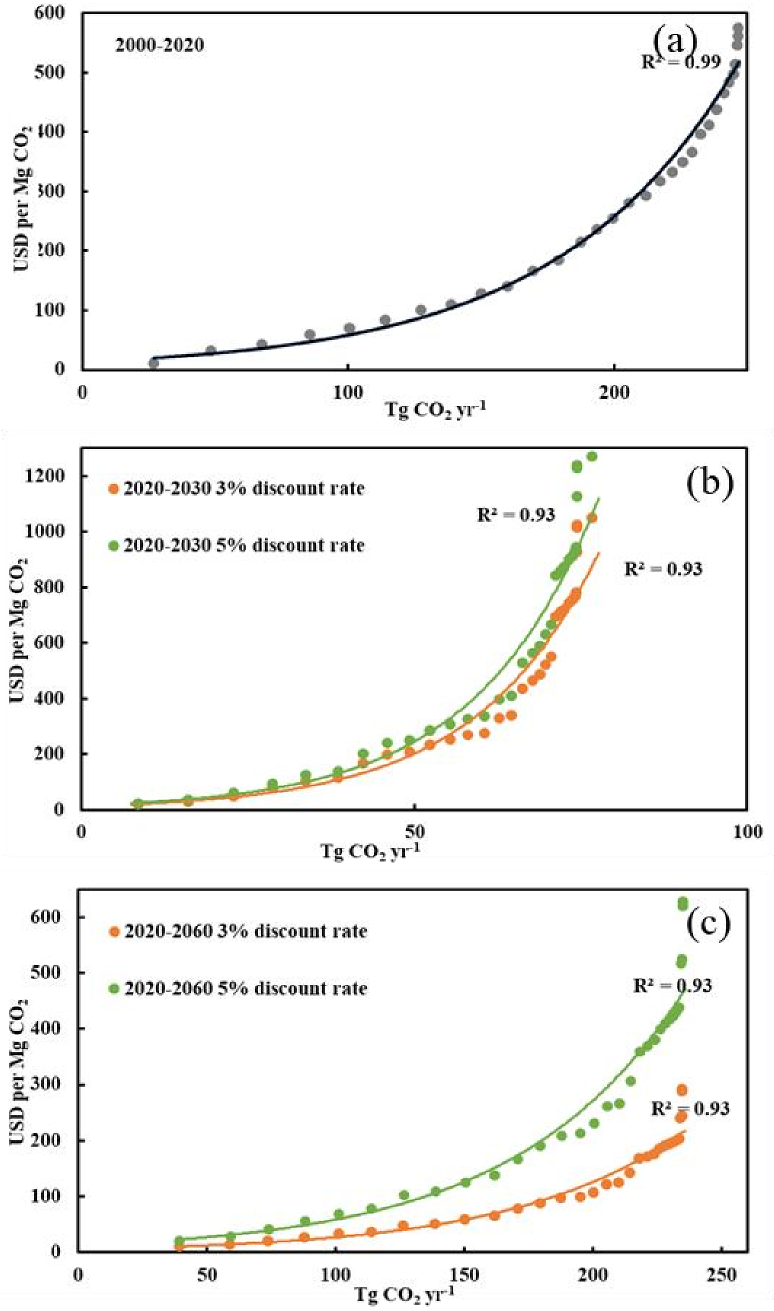

Fig. S1. The MAC curve for carbon sequestration through reforestation.

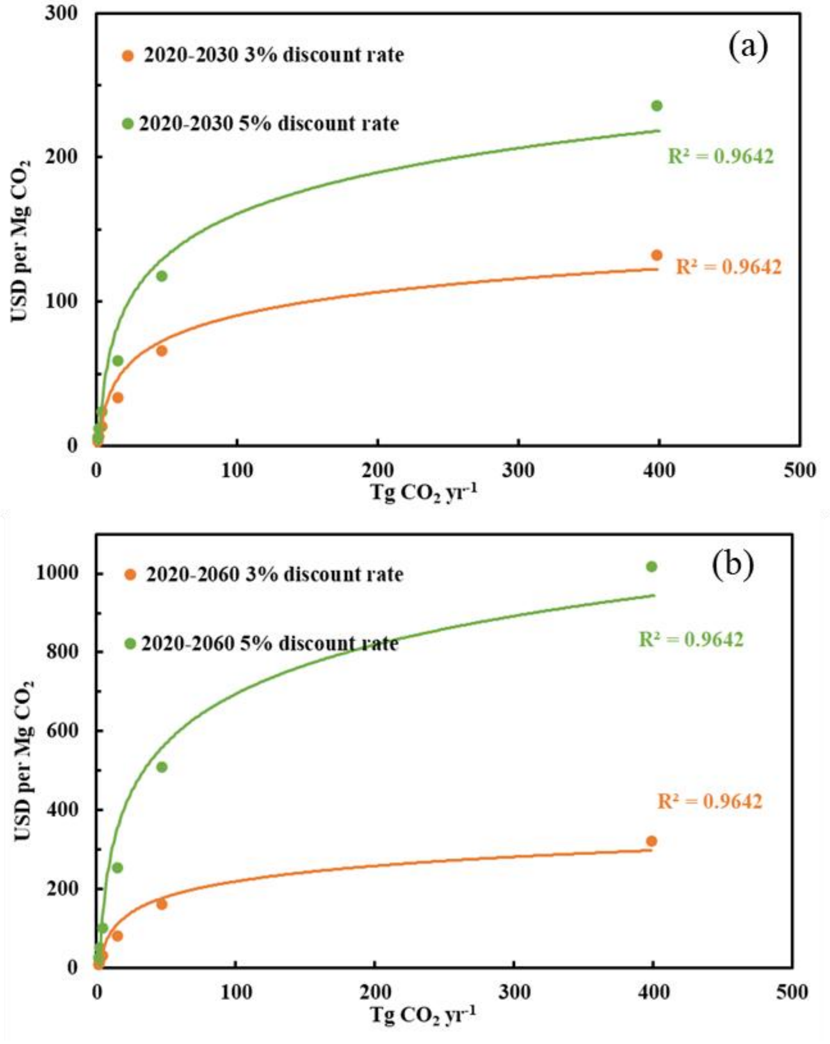

Fig. S2. The MAC curve for carbon sequestration through avoided forest conversion.

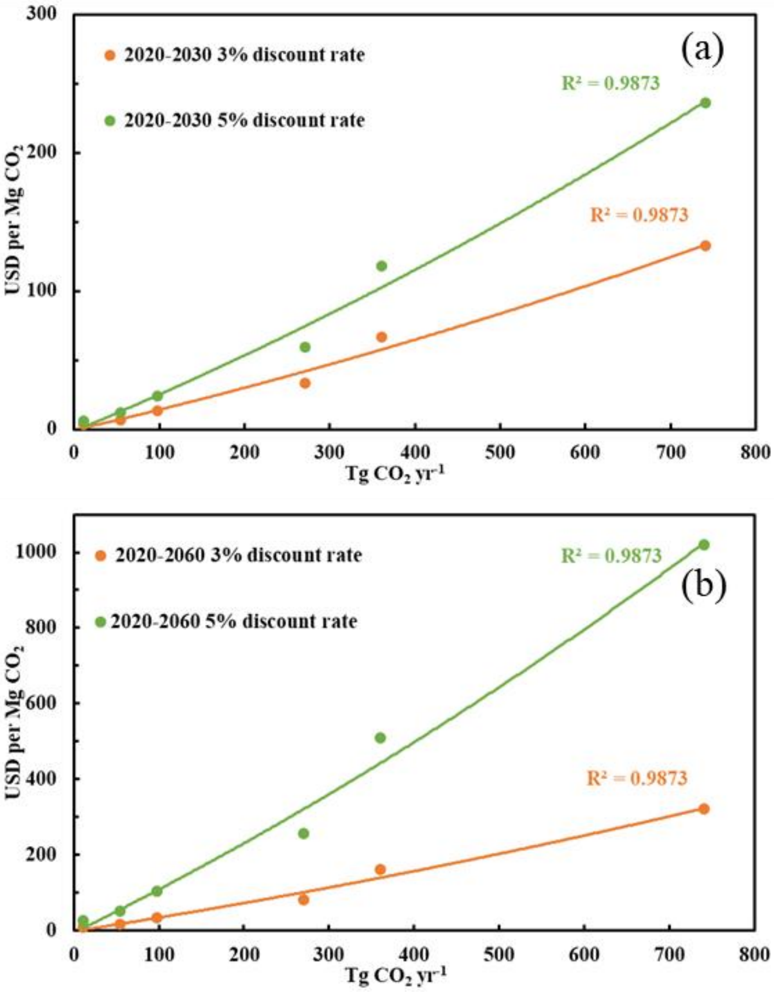

Fig. S3. The MAC curve for carbon sequestration through improved plantations.

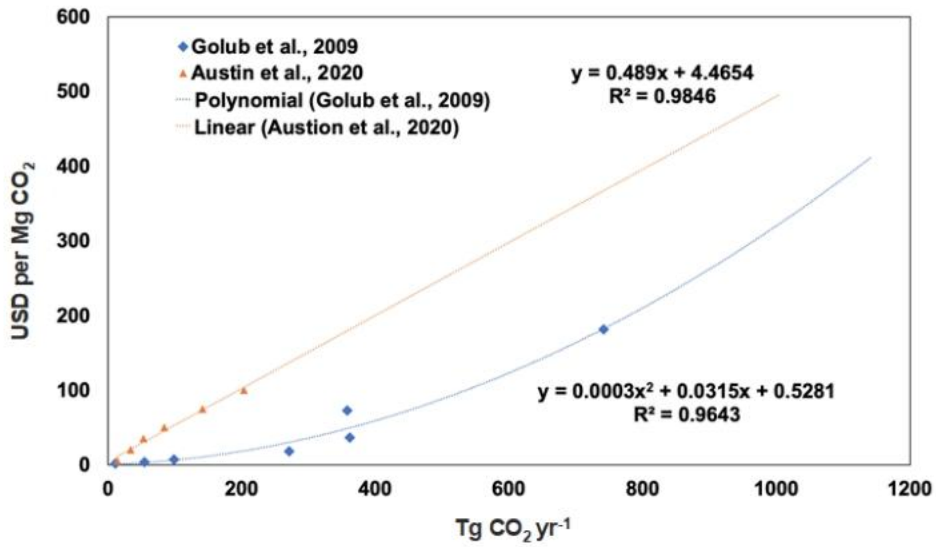

Fig. S4. The MAC curve for carbon sequestration through natural forest management in China after Golub et al. [54] and Austin et al. [109].

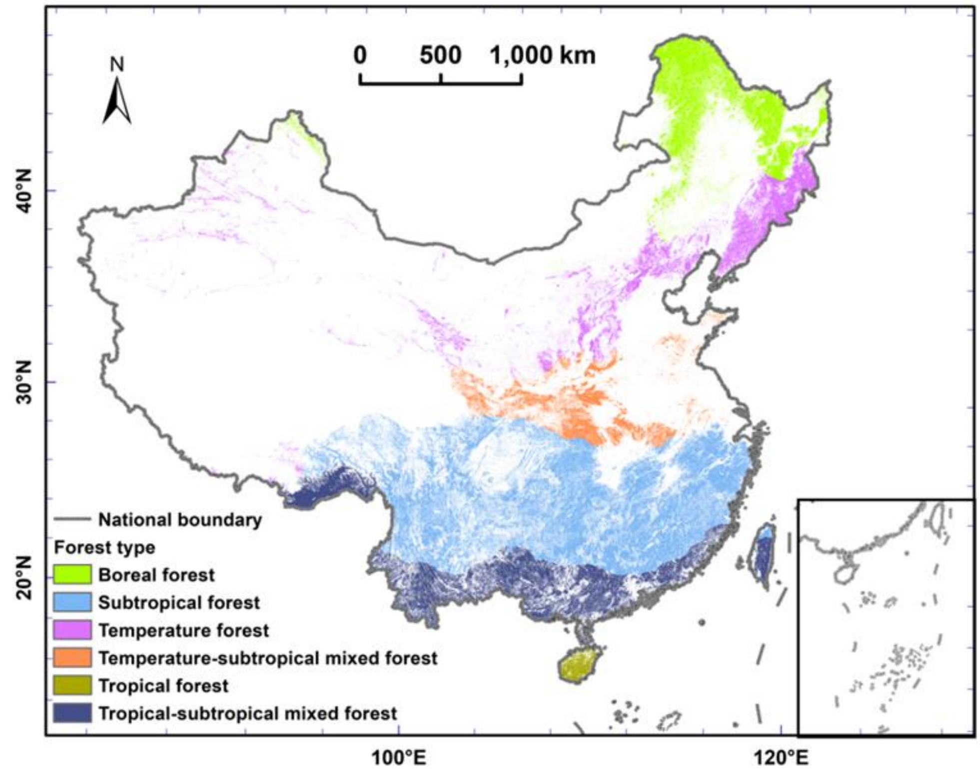

Fig. S5. The distribution of forest types in China. Data derived from Resource Environment and Data Science Center (http://www.resdc.cn/data.aspx?DATAID=98).

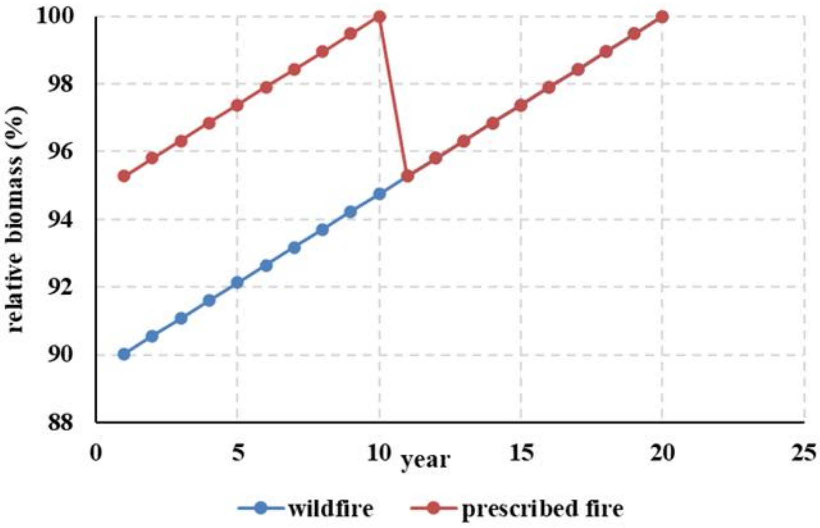

Fig. S6. A simplified diagram for the biomass change after fire disturbance (the values are for the case of temperate forest for aboveground biomass). The discrepancy of biomass under wildfire and prescribed fire means the capacity of fire management to reduce CO_2 emission.

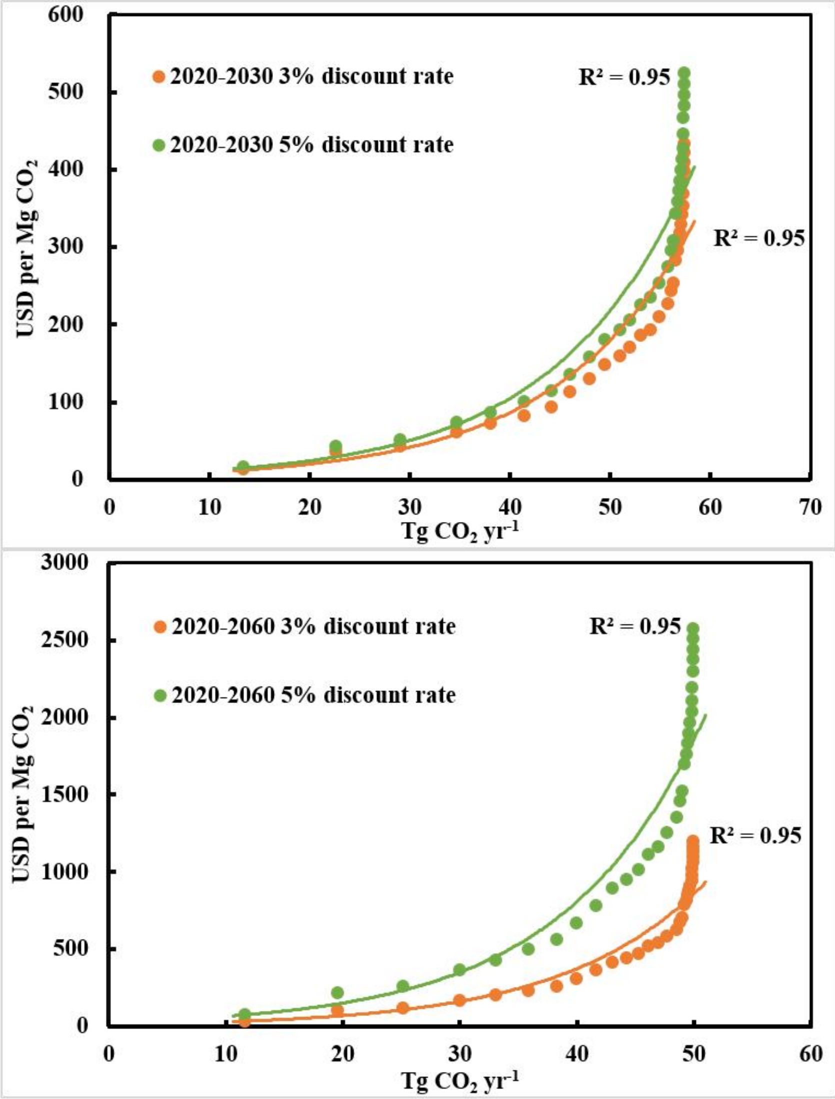

Fig. S7. The MAC curve for carbon sequestration through avoided grassland conversion.

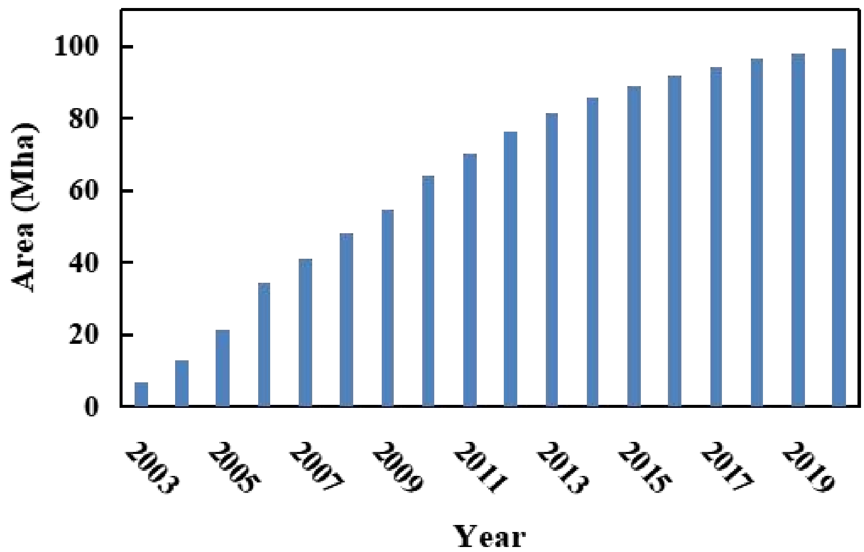

Fig. S8. The accumulated area for grassland fencing and sowing from 2003 to 2019 (Data source: the National Forestry and Grassland Administration).

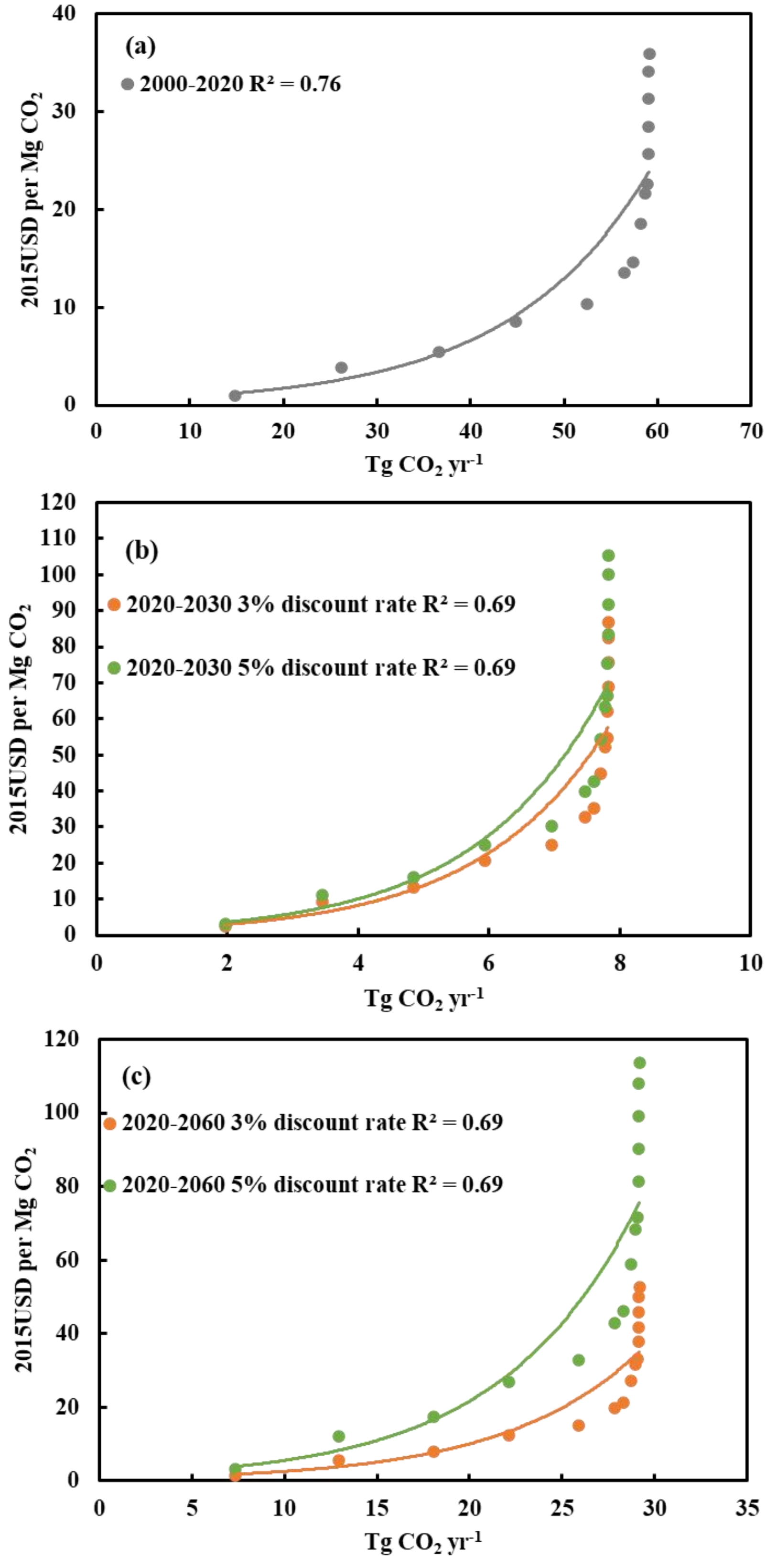

Fig. S9. The MAC curve for carbon sequestration through grazing optimization during 2000-2020 (a), 2020-2030 (b), and 2020-2060 (c).

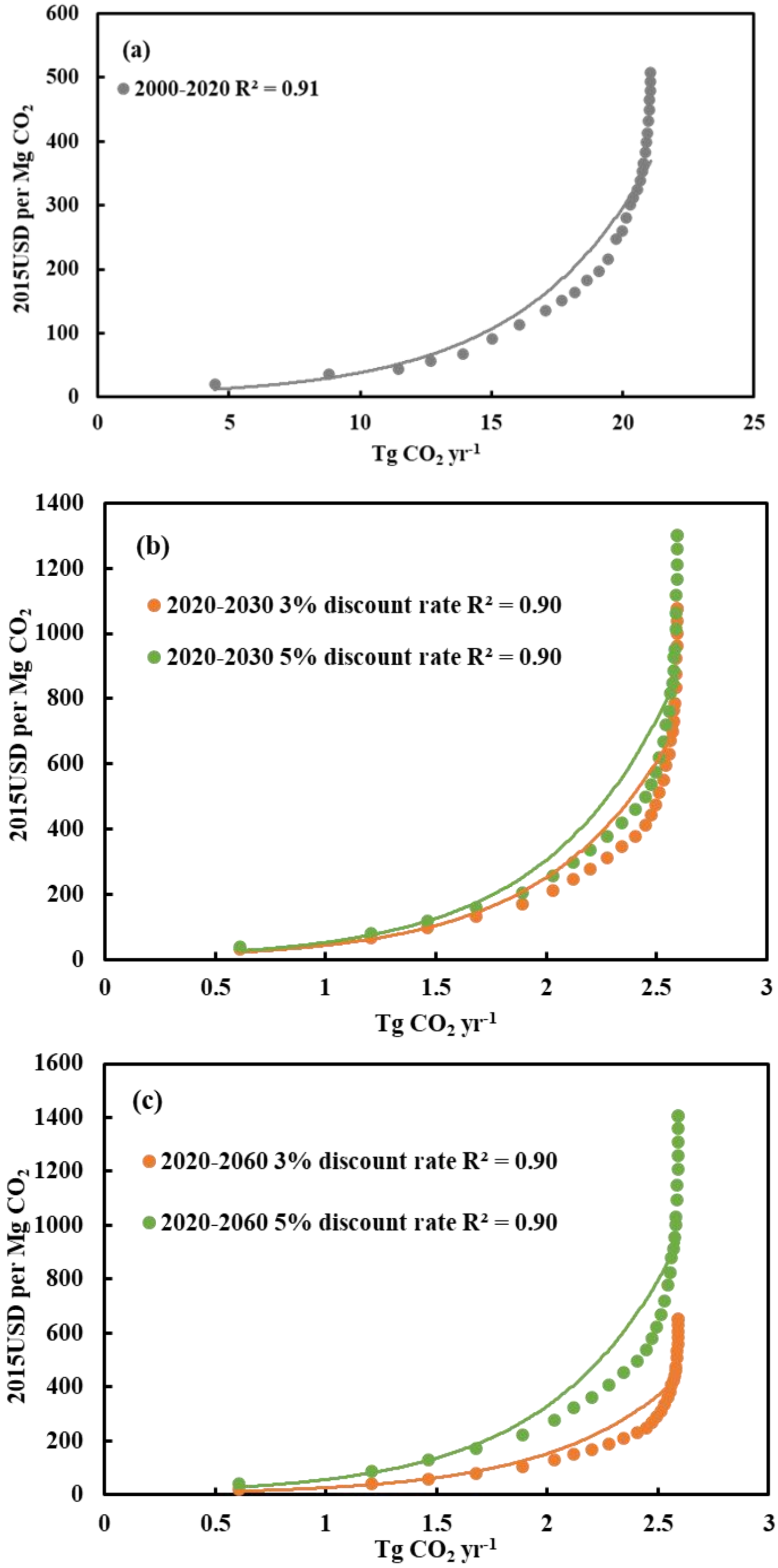

Fig. S10. The MAC curve for carbon sequestration through grassland restoration during 2000-2020 (a), 2020-2030 (b), and 2020-2060 (c).

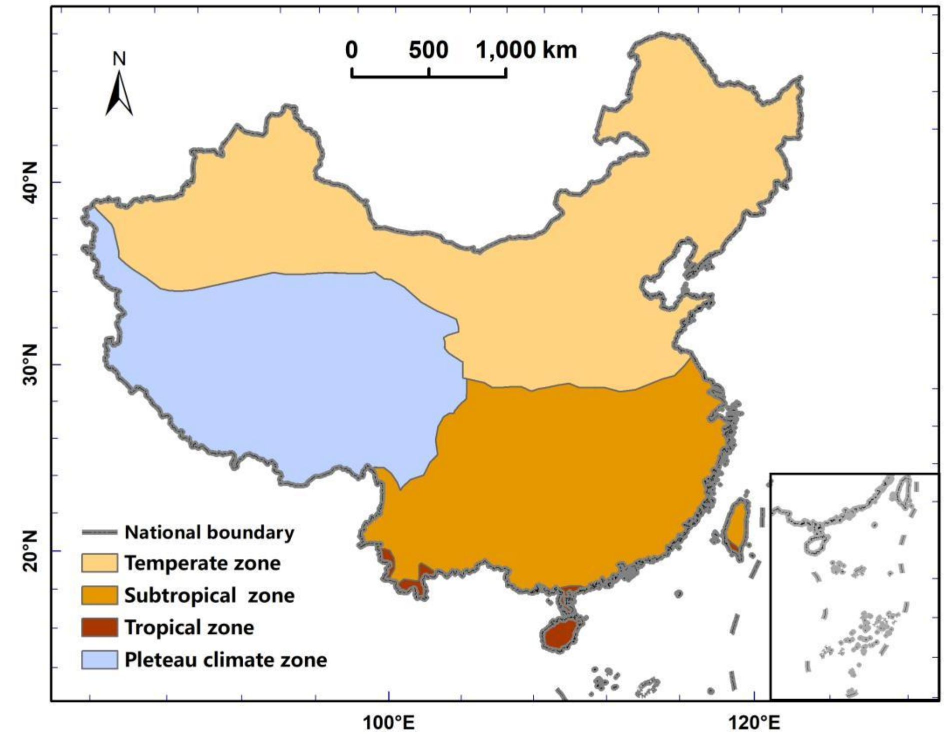

Fig. S11. The classification of Chinese climate zone in estimating reduced carbon emission from avoiding peatland impacts (Data is obtained from http://geodata.pku.edu.cn)**.**

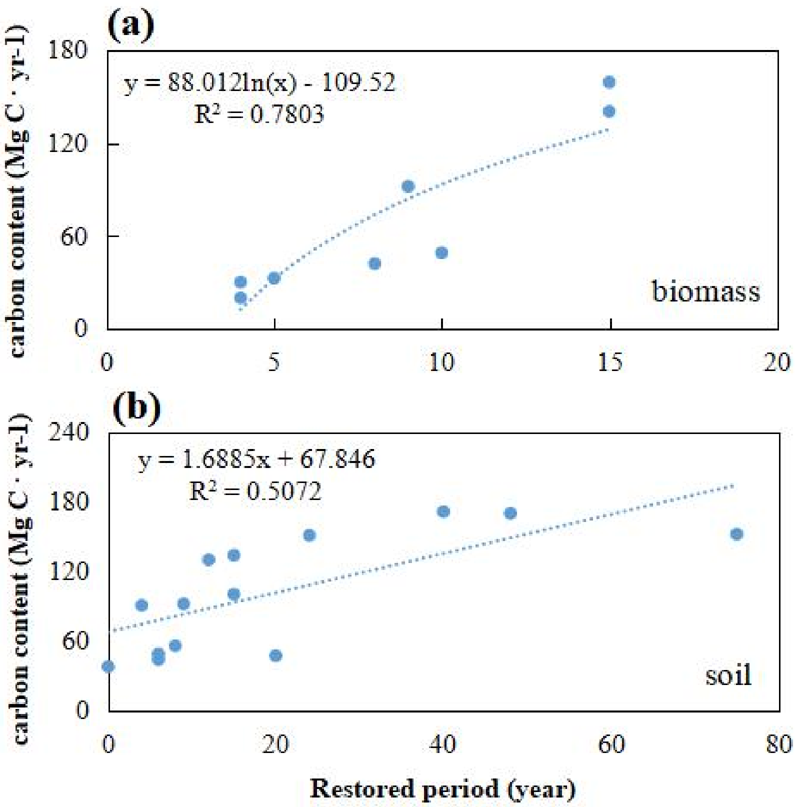

Fig. S12. The rates of change in biomass (a) and soil organic carbon (b) in restoring mangroves.

Table S1. Definition of NCS pathways.

Pathway name	Pathway description	Pathway type	Consideration for avoiding double-counting
Reforestation (RF)	Additional CO_2 sequestration potential from converting non-forest (including slash land, barren land and mountain, sloping cropland) to forest.	Restoration	In order to avoid double counting, the area suitable for mangrove planting has been removed from the total area of slash/suitable land
Avoided Forest Conversion (AVFC)	Avoided carbon emission resulting from changing forestland types after deforestation (to cropland or urban area). The carbon loss mainly includes the loss of biomass and the carbon stored in soil when forest conversion occurs.	Protection	Forest conversion is estimated based on the area of forested land using the latest land use data, avoiding the double calculation of paths such as avoiding grassland conversion.
Improved Plantations (IMP)	Reducing harvest and improving the disposal of logging residues of plantations are the main approaches to improve plantation management and reducing carbon emission. As the commercial logging of natural forests will be canceled nationwide since the implementation of the Forest Law of the People's Republic of China in 2020, timber harvest can be only made for artificial plantations.	Management	Efforts to reduce harvest and improve the disposal of logging residues are limited to plantations. Natural forests are not allowed to harvest in the next decades and thus Natural forest management (NFM) is separated with this pathway..
Natural Forest Management (NFM)	The climate mitigation potential provided by natural forest management stems from carbon sequestration through the low cost of natural regeneration of natural forests and the reduction of CO_2 emission to the atmosphere due to the cessation of natural forest logging. Since the Forest Law of the People's Republic of China came into effect on July 1,	Management	According to the Fifth National Forest Inventory (1994-1998), there were 79.10 Mha of timber and charcoal forests in China's natural forests (Chinese Ministry of Forestry, 1999), this figure does not include any planted forests,

	2020, it stipulates that commercial logging of natural forests will be canceled nationwide and all natural forests will be protected.		as well as other natural forests that have been left uncut by people, i.e., shelter forests and special-use forests.
Fire Management (FM)*	Additional CO_2 (other GHG gases are not considered in this study) sequestration by managed forest fire (prescribed fire or fire control) compared to um-managed wildfire. Regeneration of biomass is also included in the theoretical model base on the observed fire frequency.	Management	No double-counting with other pathways.
Biochar (BIOC)*	Amending agricultural soils with biochar can increases the soil carbon pool by converting non-recalcitrant carbon to recalcitrant carbon through pyrolysis. Here, the biochar mainly comes from crop residue. The effects of biochar on emission of N_2O and CH_4 are not considered in this study.	Management	Potential maximum extent assumed to be the total amount of available crop residue.
Cover Crop (CVCR)	Additional soil carbon sequestration by cover crops (i.e., green manure crops). Area suitable for planting cover crops includes cropland already planted with a perennial or winter crop. In China, there are large differences in dominant green manure types in different regions due to the divergence of climate. For example, winter cover crops (e.g., *Astragalus sinicus*, *Vicia villosa*, *Brassica napus*) are mainly planted in southern China, while cover crops like *Vicia sativa*, *Medicago sativa* are planted in northern China[288].	Management	No double-counting with other pathways.

Cropland Nutrient Management (CRNM)*	Improving crop nutrient management can reduce N_2O emission by reducing the overuse of fertilizer and improvement in N fertilizer use efficiency. The total amount of fertilizer use of China had decreased since 2012. Meanwhile, reducing the N_2O emission during N fertilizer production process can also be achieved by improving technology.	Management	Potential maximum extent includes all croplands, except for those already using best nutrient management practices.
Improved Rice Cultivation (IMRC)	Reducing the emission of CH_4 associated with anaerobic decomposition by improving water management regime, residue management, tillage and fertilizer management alternatives of upland or flooded rice lands.	Management	Biochar is not considered in rice management.
Avoided Grassland Conversion (AVGC)	Avoided CO_2 emission of belowground biomass and soil carbon by avoiding the conversion of grassland to cropland.	Protection	No double-counting with other pathways.
Grazing Optimization (GROP)	Additional carbon sequestration in above- and below-ground biomass and soil carbon by grassland fencing management and pasture sowing.	Management	Fencing and sowing management is applied in grassland area, which is not overlapping with the area for grassland restoration pathway.
Grassland Restoration (GRR)	Additional carbon sequestration in below-ground biomass and soil carbon by restoring grasslands from slope croplands. The applied extent was determined by the actual conversion from cropland to grassland during 2000-2020, and the potential extent was determined to be cultivated lands on steep slope (>15°) and other low-quality or polluted croplands.	Restoration	Grassland restored from cropland, which is separated with grassland restoration in the fencing area of pastures.

Avoided Coastal Wetland Impacts (AVCI)	Avoided CO_2 emission from soil carbon stocks by avoiding loss of coastal wetlands including salt-marshes and seagrass beds.	Protection	Including mangroves, salt marshes, and seagrass beds. Mangroves are not include in the Avoided Forest Conversion pathway to avoid double-counting.
Avoided Peatland Impacts (AVPI)	Avoided CO_2 emission of above- and below-ground biomass and soil carbon due to avoided loss of peatlands (in four climatic zones including tropical, subtropical temperate, and plateau climate zone).	Protection	Including all non-tidal non-forested wetlands. Non-tidal Forested wetlands were not considered due to the unchanged trend in recent decades.
Coastal Wetland Restoration (Mangrove, salt marsh and seagrass bed) (CWR)	Avoided oxidation of soil carbon and enhanced ecosystem carbon sink due to soil re-wetting in mangroves, salt marshes and seagrass beds. We consider the changes of carbon burial rates of biomass and soil in mangroves by different restoration time. CH_4 emission during re-wetting process is not considered.	Restoration	Including restoration of mangroves, salt marshes, and seagrass beds.
Peatland Restoration (PTR)	The net out of avoided oxidation and leaching of soil carbon but enhanced methane emission due to soil re-wetting in peatlands.	Restoration	Including all non-tidal non-forested wetlands.

Table S2. The extents of implementing the 16 NCS pathways in different time periods. The extent of NCS implementation is determined either by the maximum area that are assumed to be realized by a certain year or the assumed rate of change. Estimates for biochar and cropland nutrient management are not based on area but the amount of usable agricultural residue and nitrogen fertilizer, respectively.

Pathway name	Extent (10^6 ha if not announced)			Determination or assumption of maximum extent
	2000-2020	2020-2030	2020-2060	
Reforestation (RF)	44.71	21.68	31.84	It is assumed that the rate of RF in the next decades is the almost same to that of 2009-2018 (6.67 Mha/yr, compared with 6.28Mha/yr during 2009-2018) according to the 'Plan for major projects for the protection and restoration of major ecosystems nationwide (2021-2035)'published recently. If the estimated area is larger than the maximum area available for RF in a province, the max area is used. Noting that the projected total area for RF in the next decades include the area of the past two decades, i.e., during 2020-2030 a total of additional 21.68 Mha of area will be forested, and during 2020-2060, a total of 31.84 Mha of area will be forested.
Avoided Forest Conversion (AVFC)	0	0.11	0.43	It is assumed that the rate of forest converting to cultivated land and construction land is constant at 10645.39 ha yr^{-1} (the rate of that in 1998-2020) (https://www.globalforestwatch.org/) during 2020-2060.
Improved Plantations (IMP)	0	4.67	18.68	It is assumed that the rate of the area of implementing harvest residues treatment is constant at 0.467×10^6 ha yr^{-1} (the rate of that in 1998-2020) (https://www.globalforestwatch.org/) during 2020-2060.

Natural Forest Management (NFM)	41.25	79.10	79.10	According to the Fifth National Forest Inventory (1994-1998), there were 79.10 Mha of timber and charcoal forests in China's natural forests (Chinese Ministry of Forestry, 1999). In the recent decades, the scale of commercial deforestation of natural forests allowed by the policy is gradually shrinking. And after July 1, 2020, all commercial logging of natural forests is prohibited by law in China. It is assumed that a total of 79.10 Mha of timber and charcoal forests harvesting in natural forests are linearly reduced to zero from 2000 to 2020, and it will be zero after 2020. Therefore, the actual maximum area protected from deforestation is equivalent to 41.25 Mha during 2000-2020. And it is assumed to be remains at 79.10 Mha from 2020 to 2060.
Fire Management (FM)*	14.08	0.49	1.96	The mean annual burnt area due to wildfire was greatly reduced (0.89 Mha yr^{-1} during 1949-1999 to 0.12 Mha yr^{-1} during 2000-2017) since the implementation of fire prevention policy in 1987 [122], It is assumed that the large reduction is the outcome of fire prevention. In the past 20 years, the total accumulated burnt area is estimated to be 14.08 Mha. It is assumed that the burnt area will be constant at the level of 0.12 Mha yr^{-1} under the current fire control regime in the next decades, of which 30% will be managed by prescribed fire and 70% by fire prevention.
Biochar (BIOC)*	0.64 Tg dry mass	0.23 Tg dry mass	0.23 Tg dry mass	The national total production of biochar during 2010-2017 accounted for 0.11% of total production of crop residue *according to the China Agricultural Statistical Report*. We assume that the proportion of crop residue to produce biochar is stable during 2020-2060, but the the amount of available crop residue will increase. We assume that the utilization ratio of crop residue to produce biochar equals to that during 2010-2017, and the total amount of crop residue is 708 Tg dry mass yr^{-1}. The comprehensive utilization ratio (CUR) of crop residue increased from 78.00% to 86.72% during 2014-2020. The Ministry of Agriculture and Rural Affairs (MARA) reported that the national crop residue collection, storage and utilization system

				would be established by 2030, and most of crop residue can be utilized (https://www.sohu.com/a/270736500_100252878). We assumed that the CUR will increase to 94.08% and 100% with same increasing rate during recent 5 years (from 2016 to 2020) in 2030 and 2060, respectively.
Cover Crop (CVCR)	4.49	25.66	25.66	The planting area of cover crop in China was about 4.49 Mha in 2010s, while it reached maximum extent in 1970s. Here, we assumed that the planting area of cover crops would reach the maximum extent (25.66 Mha) in 2030 and 2060.
Cropland Nutrient Management (CRNM)*	164.81	164.81	164.81	The extent of cropland applied for improved crop nutrient management is 164.81 Mha including multiple cropping. The national total amount N fertilizer use (23.99 Tg N yr^{-1}) reached historical maximum in 2012 and decrease during 2012-2020. N fertilizer use would decrease by 16.4 Tg N in 2050 compared to 2010 [148]. We assume a 13% and 49% reduction of N use in 2030 and 2060, respectively, compared to the 2020. And this reduction will not affect crop yield according to [289]. A decrease of 10.0 % of the N_2O emission is assumed due to the improvement of N producing technology [147].
Improved Rice Cultivation (IMRC)	0	30.45	30.45	The U.S. Environmental Protection Agency (EPA) provides a consistent and comprehensive set of historical and projected estimates of emission and technical and economic mitigation estimates of non-CO2 GHGs for 195 countries from 2015 to 2050. Projected national total emission of China associated with rice cultivation in 2030 and 2050 are estimated to be 203 and 185 $TgCO_2e$ yr^{-1} [169]. We use the national total emission of China associated with rice cultivation from the EPA report. Meanwhile, we assume that the planted area of rice of is consistent with the average planted area during 2011-2020.

Avoided Grassland Conversion (AVGC)	0	5.10	20.40	The rate of grassland converting to cropland is determined according to land use and cover data from 2000 to 2018, we assume that this rate (0.51Mha yr^{-1}) is constant during 2000-2060, of which the loss rates of temperate and alpine grasslands are 0.506 Mha yr^{-1} and 0.007 Mha yr^{-1}, respectively. We assume the average percent loss of SOC from the top 1 m to be 25.57% after short-time (~10 year) conversion, and 21.71% after long-time (~20-40 year) grassland cropping. For the avoided loss of BGB, we used an empirical model based on the relationship between BGB and mean annual precipitation (MAP) [178].
Grazing Optimization (GROP)	99.56	15.60	62.40	The area of 99.56 Mha is probably the maximum area that was implemented with fencing and pasture sowing by 2020, and the data was obtained from the National Forestry and Grassland Administration of the People's Republic of China. According to the Report on the status of China's land greening in 2021, 1.56 Mha of grassland ecological restoration will be carried out in China in 2021. We assumed that 1.56 Mha yr^{-1} is the rate to imply fencing and pasture sowing measures during 2020-2030 and 2020-2060.
Grassland Restoration (GRR)	5.80	0.54	0.54	We identified the area of conversion from cropland to grassland during 2000-2018 according to land use and cover data. We extracted the croplands with slope > 15 degree as total potential restoration area (including restoration to grasslands and forests) based on the land use map in China in 2018 and Digital Elevation Model. According to the white paper issued by National Forestry and Grassland Administration of China (National Forestry and Grassland Administration, 2020), the proportion of restoration to grassland accounted for 7.86% of the total restoration area during 2014 to 2019. We assumed that 7.86% of the total potential restoration area could be converted into grasslands during 2020-2060. China issued a planning document, which declared that all unsuitable croplands be restored before 2030 (National Development and Reform Commission, 2016). It is assumed that this declaration will be realized by 2030.

Avoided Coastal Wetland Impacts (AVCI)	0	0.10	0.41	We assume that the loss rates of saltmarshes (0.01×10^{6} ha yr^{-1}) and seagrass beds (241.04 ha yr^{-1}) in the next decades are the same as that in the past two decades [237-239, 242].
Avoided Peatland Impacts (AVPI)	0	0.09	0.38	We calculate the loss rate in the past two decades in each climatic zone by the changes of Chinese inland wetlands and the proportion of peatlands to inland wetlands. We assume that the loss rate of peatland in the next decades is the same as that in the past two decades [248, 249].
Coastal Wetland Restoration (Mangrove, salt marsh and seagrass bed) (CWR)	0.01	0.10	0.38	We estimate the reconstructed area of mangrove in 2000-2020 based on the literature [237]. The future reconstruction area of mangrove is determined according to the national policy (National Forestry and Grassland Administration, 2020; State Forestry Administration, 2002). We assume that the historical loss of salt marshes[237, 264] and seagrass beds [264] would be restored by 25% by 2030 and completely restored by 2060.
Peatland Restoration (PTR)	0	0.05	0.19	We assume that there is no peatland restoration in 2000-2020 as no data records. The maximum extent of potential restoration is determined by the degraded area in the past two decades in each climatic zone. We also assume that the historical loss of peatland [248, 249] would restore 25% by 2030 and 100% by 2060.

Table S3. The historical capacity (2000-2020) and future maximum mitigation potential of NCS in 2020-2030 and 2020-2060.

Pathway name	Pathway Element	Intensity		Time Horizon	Max (95% CI bounds)	MAC USD		
		Avoidable flux Mg CO_2 ha^{-1} (if not announced) (95% CI bounds)	Additional Sequestration, Mg CO_2 ha^{-1} yr^{-1} (if not announced) (95% CI bounds)	Years until saturation		10	50	100
					Tg CO_2 yr^{-1}			
Reforestation (RF)	Biomass	---	---		---			
	Soil carbon	---	---		---			
			2020: 5.52 (4.78-6.31)	＞70	2020: 247 (214-282)	0	89	136
	All		2030: 3.54 (2.84-4.32)		2030: 77 (62-94)	0	26	39
	References		2060: 7.37 (6.45-8.383)		2060: 235 (205-267)	60	166	211
Avoided Forest Conversion (AVFC)	Biomass	---			2020: 0 2030: 3 (3-4) 2060: 3 (3-4)			
	Soil carbon	2020: 0 2030: 57.95 (36.24-145.15) 2060: 88.21 (48.32-155.70)	---	＞100	2020: 0 2030: 2 2060: 3			

	All *References*	2020: 0 2030: 212.48 (132.88-532.21) 2060: 323.43 (177.17-570.89)			2020: 0 2030: 6 (3-8) 2060: 7 (4-9)	0 3 2	0 6 4	0 6 7
Improved Plantations (IMP)	Reduced harvest	2020: 0 2030: 1.51 2060: 1.51 Mg CO_2 yr^{-1} m^{-3}			2020: 0 2030: 10 (8-11) 2060: 19 (17-21)			
	Treatment of residues	2020: 0 2030: 15.80 (5.64-25.96) 2060: 63.19 (22.54-103.84)	---	＞100	2020: 0 2030: 7 (4-11) 2060: 29 (14-45)			
	All *References*	---			2020: 0 2030: 17 (10-25) 2060: 49 (21-77)	0 17 24	0 17 49	0 17 49
Natural Forest Management (NFM)	Vegetation	---	2020: 4.13 (2.22-6.04) 2030: 3.85 (0-8.89) 2060: 3.85 (0-8.89)	>100	2020: 172 (922-251) 2030: 305 (0-703) 2060: 305 (0-703)			

	Floor		2020: 0.42 (0.13-0.71) 2030: 0.39 (0-1.16) 2060: 0.39 (0-1.16)		2020: 18 (6-30) 2030: 31 (0-92) 2060: 31 (0-92)			
	All *References*		2020: 4.55 (2.62-6.48) 2030: 4.25 (0-9.34) 2060: 4.25 (0-9.34)		2020: 189 (109-269) 2030: 336 (0-739) 2060: 336 (0-739)	72 72 72	189 220 220	189 336 336
Fire Management (FM)*	Fire prevention	---	2020: 0.86 (0.42-1.3) 2030: 1.73 (0.84-2.62) 2060: 0.43 (0.19-0.65)	>40	2000-2020: 9 (5-15) 2020-2030: 1 (0.4-1.1) 2020-2060: 1 (0.4-1.1)	3 0.2 0.2	5 0.3 0.3	7 0.4 0.4
	Prescribed fire		2020: 0.46 (0.21-0.71) 2030: 0.92 (0.42-1.42) 2060: 0.23 (0.11-0.35)		2000-2020: 1 (0.3-0.9) 2020-2030: ~0 2020-2060: ~0	0.2 0 0	0.3 0 0	0.4 0 0
	All		2020: 1.32 2030: 2.65 2060: 0.66		2000-2020: 10 2020-2030: 1 2020-2060: 1	3 0.2 0.2	5 0.4 0.4	7 1 1

Biochar (BIOC)*	All *References*	---	0.18 (0.17-0.21) MgCe Mg dm^{-1}	>100	2020: 0.5 (0.4-0.6) 2030: 0.08 (0.06-0.1) 2060: 0.08 (0.06-0.1)	0 0.08 0.08	0 0.08 0.08	0 0.08 0.08
Cover Crop (CVCR)	All *References*	---	0.32 (0.16-0.48) MgCe ha^{-1}	>50	2000-2020: 5 2020-2030: 25 (12-37) 2020-2060: 25 (12-37)	0 0 0	0 3 3	0 25 25
Cropland Nutrient Management (CRNM)*	All *References*	15.9 Mg CO_2eMg N^{-1}	11.4-19.4 Mg CO_2e Mg N^{-1}	>100	2000-2020: 79 (56-101) 2020-2030: 46 (35-57) 2020-2060: 153 (111-196)	0 23 77	0 28 92	0 44 145
Improved Rice Cultivation (IMRC)	All *References*	---	---	>100	2000-2020: 0 2020-2030: 33 (29-37) 2020-2060: 44 (39-50)	0 17 22	0 26 35	0 26 35

Avoided Grassland Conversion (AVGC)	Temperate biomass loss Alpine biomass loss Soil carbon loss	2020: 0 2030: 15.60 (8.29-22.90) 2060: 15.60 (8.29-22.90) 2020: 0 2030: 9.95 (4.77-15.12) 2060: 9.95 (4.77-15.12) 2020: 0 2030: 96.12 (11.45-180.82) 2060: 81.62 (9.91-153.66)	---	>100	2020: 0 2030: 57 (8-106) 2060: 50 (9-92)	0 9 0	0 31 11	0 41 20
Grazing Optimization (GROP)	Vegetation Soil	---	2020: 0.32 (0.30-0.34) 2030: 0.27 (0.26-0.28) 2060: 0.25 (0.24-0.27) 2020: 0.27 (0.25-0.30) 2030: 0.23 (0.21-0.25) 2060: 0.22 (0.20-0.23)	>50	2020: 32 (28-36) 2030: 4 (3.9-4.5) 2060: 16 (14-17) 2020: 27 (23-31) 2030: 4 (3-4) 2060: 13 (11-16)			

	All *References*		2020: 0.59 (0.57-0.62) 2030: 0.50 (0.48-0.52) 2060: 0.47 (0.45-0.49)		2020: 59 (53-64) 2030: 8 (7-8) 2060: 29 (27-32)	46 4 20	59 8 28	59 8 29
Grassland Restoration (GRR)	Vegetation	---	2020: 0.29 (0.18-0.40) 2030: 0.48 (0.37-0.60) 2060: 0.48 (0.37-0.60)	>50	2020: 2 (0.5-3) 2030: 0.3 (0.1-0.6) 2060: 0.3 (0.1-0.6)			
	Soil		2020: 3.35 (0.78-5.91) 2030: 4.28 (2.79-5.77) 2060: 4.28 (2.79-5.77)		2020: 19 (-10-49) 2030: 2 (1-5) 2060: 2 (1-5)			
	All *References*		2020: 3.64 (1.07-6.20) 2030: 4.77 (3.27-6.26) 2060: 4.77 (3.27-6.26)		2020: 21 (-8-50) 2030: 3 (0.5-7) 2060: 3 (0.5-7)	3 0.2 0.2	11 1 1	15 1 2

Avoided Coastal Wetland Impacts (AVCI)	Salt marsh	2020: 0 2030: 564.46 2060: 912.64			2020: 0 2030: 6 2060: 10	0 4 6	0 5 7	0 6 9
	Seagrass	2020: 0 2030: 239.06 2060: 386.53		>64	2020: 0 2030: ~0 2060: ~0	0 0 0	0 0 0	0 0 0
	All *References*				2020: 0 2030: 6 (5-8) 2060: 10 (8-12)	0 4 6	0 5 7	0 6 9
Avoided Peat Impacts (AVPI)					2020: 0 2030, 2060:	0	0	0
	Tropical	59249.77			1			
	Subtropical	4062.21 (-559.71-8676.74)			6			
	Temperate	3025.90 (-539.50-6585.81)		>100	3			
	Plateau	2075.41 (1738.31-2408.74)			14			
	All *References*				24 (10-38)	14	18	22

Coastal Wetland Restoration (Mangrove, salt marsh and seagrass bed) (CWR)	Mangrove	3.48	2020: 29.81 2030: 40.35 2060: 18.01		2020: 0 2030: 1 2060: 1	0 0 0	0 0.1 0.1	0.1 0.2 0.2
	Salt marsh	2.50	6.09		2020: 0 2030: 1 2060: 3	0 0 0	0 0.2 1	0 0.4 2
	Seagrass	1.06	5.06	> 100	2020: 0 2030: 0 2060: 0	0 0 0	0 0 0	0 0 0
	All *References*				2020: 0 2030: 2 (1-2) 2060: 4 (3-4)	0 0 0	0 0.3 2	0.1 1 2
Peatland Restoration (PTR)	Tropical	7.15 (-0.37-14.67)		>100	2020: 0 2030: 0 2060: 0			

	Subtropical	1.65 (0.09-3.21)			2020: 0 2030: 0 2060: 0			
	Temperate	7.08 (0.05-14.11)			2020: 0 2030: 0 2060: ~0			
	Plateau	102.73 (54.13-151.33)			2020: 0 2030: 4 2060: 14			
	All *References*				2020: 0 2030: 4 (-1-8) 2060: 14 (-3-32)	0 1 3	0 1 5	0 2 7

Table S4. The change of forest area during 1970s to 2018 in China. Data source: the National Inventory of Forest Resources, http://www.forestry.gov.cn.

Rank	Inventory period	Area of forest land (10^2 Mha)	Area of forest (10^2 Mha)	Percentage of forest cover (%)
1	1973-1976	2.58	1.22	12.70
2	1977-1981	2.67	1.15	12.00
3	1984-1988	2.67	1.25	12.98
4	1989-1993	2.63	1.34	13.92
5	1994-1998	2.63	1.59	16.55
6	1999-2003	2.85	1.75	18.21
7	2004-2008	3.06	1.96	20.36
8	2009-2013	3.13	2.08	21.63
9	2014-2018	3.26	2.20	22.96

Table S5. Provincial data of slash and suitable land for forestry according to the 9th National Inventory of Forest Resources (Due to data limitation, Hong Kong, Macao and Taiwan are not included in this study).

Province	Area of forest land (Mha)	Area of forest (Mha)	Area of slash /suitable land (Mha)	% of slash /suitable land	Area of slash/ suitable land (excl. mangroves) (Mha)
National	325.91	220.45	52.65		52.59
Beijing	1.07	0.72	0.02	2.06	0.02
Tianjin	0.20	0.14	0.00	1.57	0.00
Hebei	7.76	5.03	1.47	18.95	1.47
Shanxi	7.87	3.21	2.60	33.00	2.60
Inner Mongolia	44.99	26.15	17.14	38.10	17.14
Liaoning	7.36	5.72	1.06	14.37	1.06
Jilin	9.05	7.85	0.97	10.68	0.97
Heilongjiang	24.54	19.90	4.19	17.08	4.19
Shanghai	0.10	0.09	0.00	0.10	0.00
Jiangsu	1.75	1.56	0.06	3.43	0.06
Zhejiang	6.60	6.05	0.26	3.91	0.25
Anhui	4.49	3.96	0.18	3.99	0.18
Fujian	9.24	8.12	0.48	5.15	0.46

Jiangxi	10.80	10.21	0.15	1.42	0.15
Shandong	3.49	2.67	0.33	9.37	0.33
Henan	5.21	4.03	0.46	8.87	0.46
Hubei	8.76	7.36	0.69	7.93	0.69
Hunan	12.58	10.53	1.27	10.11	1.27
Guangdong	10.80	9.46	0.79	7.32	0.77
Guangxi	16.30	14.30	1.17	7.20	1.16
Hainan	2.18	1.94	0.16	7.39	0.15
Chongqing	4.22	3.55	0.24	5.59	0.24
Sichuan	24.55	18.40	1.19	4.83	1.19
Guizhou	9.28	7.71	1.00	10.76	1.00
Yunnan	25.99	21.06	1.85	7.13	1.85
Xizang	17.98	14.91	0.37	2.04	0.37
Shaanxi	12.37	8.87	1.90	15.36	1.90
Gansu	10.46	5.10	3.68	35.13	3.68
Qinghai	8.19	4.20	3.38	41.27	3.38
Ningxia	1.80	0.66	0.83	46.30	0.83
Xinjiang	13.71	8.02	4.77	34.78	4.77

Table S6. Projections of provincial data of reforestation from cropland for 2020-2030 and 2020-2060 (Mha).

Province	Existing cultivated area	Warning limit of arable land	Land needed for urban construction	Total potential area for cropland restoration	Potential area for restoring cropland to forest	Restoration rate Mha/yr	Max restoration area 2020-2030	Max restoration area 2020-2060
National	134.70	124.33	3.19	7.90	7.25	0.64	3.21	5.58
Beijing	0.21	0.11	0.01	0.09	0.08	0.00	0.03	0.08
Tianjin	0.43	0.33	0.02	0.08	0.08	0.00	0.01	0.03
Hebei	6.49	6.05	0.18	0.26	0.24	0.04	0.24	0.24
Shanxi	4.05	3.84	0.06	0.15	0.14	0.03	0.14	0.14
Inner Mongolia	9.32	7.67	0.15	1.50	1.38	0.05	0.55	1.38
Liaoning	4.95	4.60	0.07	0.28	0.26	0.02	0.16	0.26
Jilin	6.97	6.07	0.05	0.86	0.79	0.01	0.14	0.54
Heilongjiang	15.84	13.87	0.06	1.92	1.77	0.01	0.10	0.39
Shanghai	0.19	0.19	0.01	0.00	0.00	0.00	0.00	0.00
Jiangsu	4.57	4.57	0.13	0.00	0.00	0.00	0.00	0.00
Zhejiang	1.97	1.88	0.12	0.00	0.00	0.01	0.00	0.00
Anhui	5.86	5.82	0.11	0.00	0.00	0.02	0.00	0.00
Fujian	1.34	1.26	0.09	0.00	0.00	0.02	0.00	0.00

Jiangxi	3.09	2.93	0.13	0.03	0.00	0.02	0.00	0.00
Shandong	7.56	7.53	0.18	0.00	0.00	0.02	0.00	0.00
Henan	8.08	8.02	0.19	0.00	0.00	0.02	0.00	0.00
Hubei	5.20	4.83	0.16	0.21	0.20	0.03	0.20	0.20
Hunan	4.16	3.97	0.11	0.08	0.07	0.04	0.07	0.07
Guangdong	2.60	2.48	0.21	0.00	0.00	0.03	0.00	0.00
Guangxi	0.72	0.71	0.02	0.00	0.00	0.02	0.00	0.00
Hainan	4.37	4.36	0.11	0.00	0.00	0.00	0.00	0.00
Chongqing	2.33	1.91	0.07	0.35	0.32	0.02	0.21	0.32
Sichuan	6.72	6.30	0.18	0.24	0.22	0.04	0.22	0.22
Guizhou	4.50	4.19	0.14	0.17	0.15	0.04	0.15	0.15
Yunnan	6.20	5.85	0.17	0.19	0.17	0.04	0.17	0.17
Xizang	0.45	0.39	0.03	0.02	0.02	0.01	0.02	0.02
Shaanxi	3.98	3.61	0.09	0.28	0.26	0.03	0.26	0.26
Gansu	5.37	4.98	0.09	0.30	0.27	0.03	0.27	0.27
Qinghai	0.59	0.55	0.03	0.00	0.00	0.01	0.00	0.00
Ningxia	1.29	1.17	0.04	0.09	0.09	0.01	0.08	0.09
Xinjiang	5.29	4.29	0.21	0.79	0.73	0.02	0.20	0.73

Table S7. Projections of the total area available for reforestation of 31 provinces in China.

Province	Area of slash and suitable land (Mha)	RF area from cultivated land during (Mha)		Total area available for RF during (Mha)	
		2020- 2030	2020- 2060	2020-2030	2020-2060
National	52.59	3.21	5.58	55.81	58.17
Beijing	0.02	0.03	0.08	0.05	0.10
Tianjin	0.00	0.01	0.03	0.01	0.04
Hebei	1.47	0.24	0.24	1.71	1.71
Shanxi	2.60	0.14	0.14	2.74	2.74
Inner Mongolia	17.14	0.55	1.38	17.69	18.52
Liaoning	1.06	0.16	0.26	1.21	1.32
Jilin	0.97	0.14	0.54	1.10	1.51
Heilongjiang	4.19	0.10	0.39	4.29	4.58
Shanghai	0.00	0.00	0.00	0.00	0.00
Jiangsu	0.06	0.00	0.00	0.06	0.06
Zhejiang	0.25	0.00	0.00	0.25	0.25
Anhui	0.18	0.00	0.00	0.18	0.18
Fujian	0.46	0.00	0.00	0.46	0.46

Jiangxi	0.15	0.00	0.00	0.15	0.15
Shandong	0.33	0.00	0.00	0.33	0.33
Henan	0.46	0.00	0.00	0.46	0.46
Hubei	0.69	0.20	0.20	0.89	0.89
Hunan	1.27	0.07	0.07	1.34	1.34
Guangdong	0.77	0.00	0.00	0.77	0.77
Guangxi	1.16	0.00	0.00	1.16	1.16
Hainan	0.15	0.00	0.00	0.15	0.15
Chongqing	0.24	0.21	0.32	0.45	0.56
Sichuan	1.19	0.22	0.22	1.41	1.41
Guizhou	1.00	0.15	0.15	1.15	1.15
Yunnan	1.85	0.17	0.17	2.03	2.03
Xizang	0.37	0.02	0.02	0.39	0.39
Shaanxi	1.90	0.26	0.26	2.16	2.16
Gansu	3.68	0.27	0.27	3.95	3.95
Qinghai	3.38	0.00	0.00	3.38	3.38
Ningxia	0.83	0.08	0.09	0.91	0.92
Xinjiang	4.77	0.20	0.73	4.97	5.50

Table S8. Provincial data of warning limit of cultivated land

Province	Stock of cultivated land (Mha)	Basic cropland conservation area (Mha)	Land used for construction (Mha)
National	124.33	103.07	40.72
Beijing	0.11	0.10	0.37
Tianjin	0.33	0.28	0.44
Hebei	6.05	5.15	2.25
Shanxi	3.84	3.26	1.10
Inner Mongolia	7.67	6.20	1.70
Liaoning	4.60	3.68	1.70
Jilin	6.07	4.92	1.13
Heilongjiang	13.87	11.10	1.69
Shanghai	0.19	0.17	0.32
Jiangsu	4.57	3.90	2.36
Zhejiang	1.88	1.60	1.35
Anhui	5.82	4.92	2.06
Fujian	1.26	1.07	0.88
Jiangxi	2.93	2.46	1.34

Shandong	7.53	6.39	2.91
Henan	8.02	6.80	2.68
Hubei	4.83	3.91	1.78
Hunan	3.97	3.30	1.71
Guangdong	2.48	2.11	2.09
Guangxi	0.71	0.61	0.37
Hainan	4.36	3.65	1.29
Chongqing	1.91	1.62	0.72
Sichuan	6.30	5.20	1.90
Guizhou	4.19	3.50	0.74
Yunnan	5.85	4.89	1.15
Xizang	0.39	0.32	0.16
Shaanxi	3.61	3.06	1.00
Gansu	4.98	3.99	0.95
Qinghai	0.55	0.44	0.37
Ningxia	1.17	0.93	0.34
Xinjiang	4.29	3.54	1.86

Table S9. Projections of surviving area for reforestation of 31 provinces.

Province	Mean rate of RF (Mha/yr)	Max area (Mha)		Actual area (Mha)		Surviving area (Mha)	
		2020-2030	2020-2060	2020-2030	2020-2060	2020-2030	2020-2060
National	6.41	64.13	256.54	33.84	57.45	21.68	31.84
Beijing	0.03	0.28	1.10	0.05	0.10	0.04	0.09
Tianjin	0.01	0.09	0.34	0.01	0.04	0.01	0.03
Hebei	0.43	4.26	17.02	1.71	1.71	1.71	1.71
Shanxi	0.28	2.80	11.19	2.74	2.74	1.92	1.92
Inner Mongolia	0.55	5.50	21.99	5.50	18.52	2.20	7.41
Liaoning	0.16	1.57	6.29	1.21	1.32	0.49	0.53
Jilin	0.14	1.35	5.41	1.10	1.51	0.44	0.60
Heilongjiang	0.10	0.96	3.86	0.96	3.86	0.39	1.54
Shanghai	0.00	0.02	0.10	0.00	0.00	0.00	0.00
Jiangsu	0.05	0.47	1.89	0.06	0.06	0.05	0.05
Zhejiang	0.05	0.53	2.13	0.25	0.25	0.21	0.21
Anhui	0.16	1.60	6.41	0.18	0.18	0.15	0.15
Fujian	0.18	1.81	7.24	0.46	0.46	0.39	0.39
Jiangxi	0.23	2.35	9.39	0.15	0.15	0.13	0.13

Shandong	0.19	1.85	7.42	0.33	0.33	0.28	0.28
Henan	0.19	1.87	7.49	0.46	0.46	0.39	0.39
Hubei	0.27	2.68	10.71	0.89	0.89	0.76	0.76
Hunan	0.44	4.44	17.75	1.34	1.34	1.14	1.14
Guangdong	0.28	2.75	11.01	0.77	0.77	0.65	0.65
Guangxi	0.20	2.04	8.16	1.16	1.16	0.99	0.99
Hainan	0.02	0.18	0.72	0.15	0.15	0.13	0.13
Chongqing	0.21	2.11	8.43	0.45	0.56	0.38	0.47
Sichuan	0.37	3.69	14.77	1.41	1.41	1.20	1.20
Guizhou	0.41	4.13	16.51	1.15	1.15	0.98	0.98
Yunnan	0.44	4.41	17.63	2.03	2.03	1.72	1.72
Xizang	0.06	0.60	2.39	0.39	0.39	0.33	0.33
Shaanxi	0.30	3.04	12.18	2.16	2.16	1.51	1.51
Gansu	0.27	2.71	10.83	2.71	3.95	1.08	1.58
Qinghai	0.13	1.28	5.12	1.28	3.38	0.90	2.37
Ningxia	0.08	0.77	3.08	0.77	0.92	0.31	0.37
Xinjiang	0.20	1.99	7.97	1.99	5.50	0.80	2.20

Table S10. Carbon flux calculation of reforestation for three tree species in Guangxi province as an example.

Province	Tree species	Stand age (year)	Carbon flux （MgC ha^{-1} yr^{-1}）	References
Guangxi	*Pinus massoniana*	8	1.73	[290, 291]
	Betula alnoides	13	1.93	[291, 292]
	Cunninghamia lanceolata （*Lamb.*） *Hook*	11	3.22	[291, 293]
	Cunninghamia lanceolata （*Lamb.*） *Hook*	13	4.41	[291, 294]

Table S11. Provincial carbon fluxes of restored forests in different age classes.

Province	Carbon flux in 10-year-old forest ($Mg\ C\ ha^{-1}\ yr^{-1}$)		Carbon flux in 20-year-old forest ($Mg\ C\ ha^{-1}\ yr^{-1}$)	
	Value	References	Value	References
National	2.02±0.14		2.55±0.16	
Beijing	1.14	[295]	1.23	[291, 296]
Tianjin	2.52±0.55	[297, 298]	2.37	[297, 298]
Hebei	1.17	[291, 296]	1.23	[291, 296]
Shanxi	1.43	[298, 299]	2.95±0.02	[298, 300]
Inner Mongolia	1.71±0.14	[301]	1.87±0.25	[301]
Liaoning	3.35±0.36	[291, 302, 303]	3.18±0.74	[302]
Jilin	1.93±1.87	[304]	2.86±0.23	[304]
Heilongjiang	1.11	[291, 299]	1.27	[305]
Shanghai	2.58	[291, 296]	2.64	[291, 296]
Jiangsu	2.18	[306]	3.12	[307]
Zhejiang	1.77±0.50	[308]	3.28±0.31	[308-310]
Anhui	2.32±0.69	[311]	2.5	[312]
Fujian	2.58±0.46	[291, 313-315]	1.94	[291, 313]
Jiangxi	1.88	[291, 316]	2±0.24	[291, 317]
Shandong	1.17	[291, 296]	1.90±0.32	[318]
Henan	3.43±0.87	[319, 320]	3.75	[321]
Hubei	1.61	[322]	2.8	[322]
Hunan	3.61±0.28	[323, 324]	3.52±0.31	[325]
Guangdong	2.80±0.38	[326-329]	3.41±0.65	[326, 330]
Guangxi	2.69±0.45	[290-294]	5.24±0.55	[290, 291, 331-333]
Hainan	2.47	[291, 299]	2.31	[291, 296]
Chongqing	1.03	[291, 299]	2.64	[291, 296]
Sichuan	3.88±0.37	[334]	3.46	[335, 336]
Guizhou	2.01		2.19±0.53	[336, 338, 339]

Yunnan	1.84	[291, 299]	2.64	[291, 296]
Xizang	1.78	[291, 299]	2.64	[291, 296]
Shaanxi	0.60	[291, 299]	2.21±0.17	[340-342]
Gansu	1.58	[291, 299]	3.93	[343]
Qinghai	1.66	[291, 299]	1.23	[291] [296]
Ningxia	1.44	[291, 299]	1.23	[291, 296]
Xinjiang	1.44	[291, 299]	1.58	[291, 296]

Table S11 (continued):

Province	**Carbon flux in 30-year-old forest (Mg C ha^{-1} yr^{-1})**		**Carbon flux in 40-year-old forest (Mg C ha^{-1} yr^{-1})**		**Carbon flux in 60-year- old forest (Mg C ha^{-1} yr^{-1})**	
	Value	References	Value	References	Value	References
National	3.53±0.20		3.12±0.19		3.14±0.18	
Beijing	4.37±0.20	[344, 345]	2.74±0.43	[346]	3.53	[345]
Tianjin	2.01	[291, 296]	2.04	[291, 296]	2.04	[291, 296]
Hebei	2.52±0.26	[318]	2.42	[347]	3.20	[347]
Shanxi	2.87	[348]	3.24±1.27	[348, 349]	3.53±0.25	[318]
Inner Mongolia	1.93	[350]	1.71	[301]	1.71	[301]
Liaoning	3.68±0.21	[318]	3.64±0.25	[318]	1.87	[302]
Jilin	2.09	[304]	3±0.09	[304]	3±0.09	[304]
Heilongjiang	3.74	[351]	5.52±1.26	[351, 352]	4.71±0.49	[352]
Shanghai	3.42	[291, 296]	3.45	[291, 296]	3.45	[291, 296]
Jiangsu	1.97±0.28	[306, 353]	3.45	[291, 296]	3.45	[291, 296]
Zhejiang	2.58±0.26	[308]	2.93±0.49	[308]	3.72	[308]
Anhui	4.65	[354]	3.57	[354]	3.43±0.35	[291, 311, 312]
Fujian	3.20±0.20	[291, 313]	2.94±0.48	[291, 313, 355]	3.35	[291, 296]
Jiangxi	3.86±0.35	[291, 316]	3.44±0.45	[291, 317]	3.36±0.47	[291, 317]
Shandong	4.42±0.29	[318]	1.46	[356]	2.04	[291, 296]
Henan	4.97	[357]	3.63	[320]	2.04	[291, 296]

Hubei	3.42	[291, 296]	1.43±0.30	[358]	3.45	[291, 296]
Hunan	4.62	[359]	3.45	[291, 296]	5.59±1.26	[324, 360]
Guangdong	5.59±0.90	[361, 362]	3.45	[291, 296]	1.57	[363]
Guangxi	4.44±0.88	[290, 291, 332, 333, 364]	4.71±1.18	[291, 333, 365]	4.02	[331]
Hainan	6.42±1.19	[366, 367]	3.12	[291, 296]	3.12	[291, 296]
Chongqing	3.42	[291, 296]	3.45	[291, 296]	3.45	[291, 296]
Sichuan	3.39±0.60	[318, 335, 336]	2.38	[335, 336]	3	[296, 336]
Guizhou	3.09±0.51	[336-338]	4.02	[339]	3	[296, 336]
Yunnan	3.42	[291, 296]	3.35±0.60	[291, 368]	3.45	[291, 296]
Xizang	3.42	[291, 296]	3.45	[291, 296]	3.45	[291, 296]
Shaanxi	2.50±0.45	[318, 340, 341]	2.54±0.32	[340]	2.53±0.23	[340]
Gansu	5.33	[343]	6.25	[343]	5.86	[369]
Qinghai	2.01	[291, 296]	1.67	[291, 370]	2.04	[291, 296]
Ningxia	3.76	[371]	2.04	[291, 296]	2.04	[291, 296]
Xinjiang	2.36	[291, 296]	2.39	[291, 296]	2.39	[291, 296]

Table S12 Carbon sequestration capacity during 2000-2020 and future potential during 2020-2030 and 2020-2060 of reforestation of 31 provinces.

Province	Area of reforestation (Mha)			Maximum potential (Tg CO_2 yr^{-1})		
	2000-2020	2020-2030	2020-2060	2000-2020	2020-2030	2020-2060
National	44.71	21.68	31.84	246.90	76.64	234.70
Beijing	0.20	0.04	0.09	0.58	0.09	0.61
Tianjin	0.06	0.01	0.03	0.37	0.05	0.21
Hebei	2.93	1.71	1.71	8.58	3.65	9.20
Shanxi	2.50	1.92	1.92	13.38	5.03	14.76
Inner Mongolia	4.99	2.20	7.41	21.82	6.89	39.24
Liaoning	1.23	0.49	0.53	9.84	2.98	5.35
Jilin	0.68	0.44	0.60	3.99	1.56	4.37
Heilongjiang	1.11	0.39	1.54	3.24	0.78	13.16
Shanghai	0.03	0.00	0.00	0.22	0.00	0.00
Jiangsu	0.48	0.05	0.05	3.11	0.20	0.40
Zhejiang	0.24	0.21	0.21	1.51	0.70	1.66
Anhui	0.79	0.15	0.15	4.63	0.65	1.46
Fujian	0.63	0.39	0.39	3.45	1.86	3.08

Jiangxi	1.29	0.13	0.13	6.09	0.45	1.07
Shandong	1.42	0.28	0.28	5.33	0.59	1.82
Henan	1.69	0.39	0.39	14.79	2.47	4.54
Hubei	1.71	0.76	0.76	9.24	2.24	5.15
Hunan	2.19	1.14	1.14	19.06	7.55	12.71
Guangdong	0.80	0.65	0.65	6.06	3.35	7.30
Guangxi	1.18	0.99	0.99	11.46	4.88	12.39
Hainan	0.16	0.13	0.13	0.94	0.58	1.35
Chongqing	1.37	0.38	0.47	6.12	0.71	3.66
Sichuan	3.00	1.20	1.20	26.88	8.51	11.50
Guizhou	2.17	0.98	0.98	11.11	3.61	8.12
Yunnan	3.28	1.72	1.72	17.95	5.79	14.20
Xizang	0.35	0.33	0.33	1.89	1.07	2.72
Shaanxi	2.87	1.51	1.51	9.82	1.65	8.70
Gansu	2.03	1.08	1.58	13.64	3.13	19.79
Qinghai	0.86	0.90	2.37	3.04	2.72	11.38
Ningxia	0.82	0.31	0.37	2.68	0.81	2.27
Xinjiang	1.65	0.80	2.20	6.06	2.10	12.52

Table S13. The MAC estimates for carbon sequestration through reforestation.

Discount rate	USD Mg CO_2^{-1}	Tg CO_2 yr^{-1}		
		2000-2020	2020-2030	2020-2060
3%	10	-	0.00	34.72
3%	50	-	24.54	139.91
3%	100	-	37.16	185.22
5%	10	-	0.00	85.98
5%	50	-	28.11	191.17
5%	100	-	40.73	236.48
mean	10	0	0.00	60.35
mean	50	89.37	26.32	165.54
mean	100	135.89	38.95	210.85

Table S14. The proportion of converting forest to cultivated land and construction land in the six subregions of China.

Subregion	Conversion from forest land to cultivated land			Conversion from forest land to construction land		
	Total rate (ha yr^{-1})	Fraction	Rate in (ha yr^{-1})	Total rate (ha yr^{-1})	Fraction	Rate in (ha yr^{-1})
NEC		0.38	3010.13		0.03	76.14
NC		0.02	143.93		0.17	478.97
EC	7903.02	0.07	575.74	2742.38	0.13	345.69
SC		0.18	1399.33		0.46	1255.73
NWC		0.21	1664.33		0.11	292.92
SWC		0.14	1109.55		0.11	292.92

NEC: Northeast China; NC: North China; EC: East China; SC: South China; NWC: Northwest China; SWC: Southwest China

Table S15. The area of permanent deforestation and carbon loss through biomass from 2001 to 2019.

Year	Rate of permanent deforestation ($ha\ yr^{-1}$)	Biomass loss (Mg)	Carbon loss through biomass ($Mg\ CO_2\ yr^{-1}$)
2001	4170.5	699437.8	1282302.6
2002	4376.0	720094.5	1320173.3
2003	3688.7	628590.6	1152416.1
2004	7941.6	1332923.4	2443692.9
2005	7281.8	1293485.6	2371390.3
2006	10040.3	1753102.9	3214022.0
2007	10734.7	1936904.6	3550991.7
2008	17062.0	3147175.5	5769821.8
2009	14343.3	2546320.6	4668254.4
2010	14039.0	2314585.0	4243405.8
2011	11792.0	2053195.7	3764192.2
2012	14955.1	2607984.3	4781304.5
2013	10407.1	1729134.4	3170079.7
2014	11126.9	1822471.9	3341198.6
2015	9363.0	1553448.8	2847989.5
2016	14100.9	2254260.9	4132811.7
2017	14900.4	2281671.1	4183063.6
2018	11074.1	1644533.5	3014978.1
2019	10864.9	1598272.4	2930166.1
Mean	10645.4	1785136.5	3272750.3

Table S16. Carbon loss of forest to cultivated land and construction land in the six subregions of China during 2020-2030.

Subregion	SOC of forest (0-1m) kg m^{-2}	Conversion from forest to cultivated land			Conversion from forest to construction land		
		Carbon loss rate	Annual conversion rate (ha yr^{-1})	Annual carbon loss (Tg CO_2 yr^{-1})	Carbon loss rate	Annual conversion rate (ha yr^{-1})	Annual carbon loss (Tg CO_2 yr^{-1})
NEC	15.68	30%	3010.13	0.52	55%	76.14	0.02
NC	14.07	30%	143.93	0.02	55%	478.97	0.14
EC	12.08	30%	575.74	0.08	55%	345.69	0.08
SC	12.14	30%	1399.33	0.19	55%	1255.73	0.31
NWC	17.69	30%	1664.33	0.32	55%	292.92	0.10
SWC	26.39	30%	1109.55	0.32	55%	292.92	0.16

Table S17. Carbon loss of forest to cultivated land and construction land in the six subregions of China during 2020-2060.

Subregion	**SOC of forest (0-1m) kg/m²**	**Conversion from forest to cultivated land**			**Conversion from forest to construction land**		
		Carbon loss rate	Annual conversion rate (ha/yr)	Annual carbon loss (Tg CO_2 yr^{-1})	Carbon loss rate	Annual conversion rate (ha/yr)	Annual carbon loss (Tg CO_2 yr^{-1})
NEC	15.68	59%	3010.13	1.02	40%	76.14	0.02
NC	14.07	59%	143.93	0.04	40%	478.97	0.10
EC	12.08	59%	575.74	0.15	40%	345.69	0.06
SC	12.14	59%	1399.33	0.37	40%	1255.73	0.22
NWC	17.69	59%	1664.33	0.64	40%	292.92	0.08
SWC	26.39	59%	1109.55	0.63	40%	292.92	0.11

Table S18. The MAC estimates for carbon sequestration through avoided forest conversion.

Discount rate	USD Mg CO_2^{-1}	Tg CO_2 yr^{-1}		
		2000-2020	2020-2030	2020-2060
3%	10	-	3.20	2.49
3%	50	-	17.78(max 5.54)	5.04
3%	100	-	151.61(max 5.54)	12.20(max 6.72)
5%	10	-	2.65	2.21
5%	50	-	6.95(max 5.54)	2.76
5%	100	-	23.16(max 5.54)	3.64
mean	10	-	2.93	2.35
mean	50	-	12.37 (max5.54)	3.90
mean	100	-	87.38 (max 5.54)	7.92(max 6.72)

Table S19. Annual carbon sequestration under different treatment methods of harvested residues.

Methods	The average of annual total carbon sequestration ($Mg\ C\ ha^{-1}\ yr^{-1}$)		
	Under poor site condition	Under good site condition	Average
Stem Only	2.36	5.73	4.05
Floor Removed	2.03	4.91	3.47
Stem Only and Burning	1.96	4.76	3.36
Whole Tree Harvest	1.91	4.53	3.22

Table S20. The MAC estimates for carbon sequestration through improved plantations.

Discount rate	USD Mg CO_2^{-1}	Tg CO_2 yr^{-1}		
		2000-2020	2020-2030	2020-2060
3%	10	-	72.82 (max17.05)	33.39
3%	50	-	318 (max17.05)	142.62 (max48.75)
3%	100	-	583.04 (max17.05)	270.84 (max48.75)
5%	10	-	43.47 (max17.05)	14.00
5%	50	-	188.11 (max17.05)	49.38 (max48.75)
5%	100	-	352.39 (max17.05)	92.41 (max48.75)
mean	10	-	58.14 (max17.05)	23.69
mean	50	-	253.06 (max17.05)	96.00 (max48.75)
mean	100	-	467.72 (max17.05)	181.63 (max48.75)

Table S21. The number and proportion of forest sites under natural forest management by age group.

Site information	Young	Middle-aged	Pre-mature	Mature	Over-mature
Average age boundaries of each age group	<31	<51	<65	<93	>93
Average ages of each age group	16	41	58	79	122
Tree sites number by age group	88	154	57	98	365
Shrub sites number by age group	37	52	17	9	27
Herb sites number by age group	29	41	16	8	27
Floor sites number by age group	49	81	34	33	63
Area by age group, 1994-1998 (Mha)	27.25	29.66	8.55	8.27	5.36
Area Proportion by age group, 1994-1998 (%)	34	37	11	10	7

Table S22 The specific variable values used in the calculation of carbon sequestration fluxes by nature forest management.

	East	North	Northeast	Northwest	South Central	Southwest	China
Area (Mha)	11	13	21	4	13	17	79
Over-mature vegetation carbon density （Mg C/ha）	150	89	125	113	152	180	139
Over-mature floor layer carbon density （Mg C/ha）	8	9	10	8	8	18	11
Percent of carbon density in young & middle-aged to over-mature forest (%)	43	57	45	43	34	28	42
Percent of carbon density in pre-mature & mature to over-mature forest(%)	83	88	72	65	74	60	74

Table S23. The number of sites and plots for estimating carbon flux of natural forest management.

		Vegetation			Floor
	All	Live tree biomass (aboveground and belowground)	Shrub	Herb	Floor (woody debris and litter)
Sites	762	762	142	121	260
Plots	2363	2363	1202	821	1490

Table S24 The annual carbon density increment (flux) under different age groups in managed natural forest, with standard deviations. unit: Mg C ha^{-1} yr^{-1}

Age group	Young and middle-aged	Pre-mature and mature	Over-mature
	Before 51	52~93	After 94
Vegetation	1.13±0.28	1.05±0.70	0.64±0.76
Floor	0.12±0.04	0.11±0.11	0.07±0.12
All	1.25±0.29	1.16±0.71	0.71±0.77

Table S25. The MAC estimates for carbon sequestration through natural forest management.

Carbon price	Golub et al. [54]	Austin et al. [109]	Mean
2015 USD per Mg CO_2^{-1}	Tg CO_2 yr^{-1}		
10	132.78	11.32	72.05
50	356.97	83.86	220.42
100	525.71	202.61	364.16

Table S26. The proportion of reduced biomass by fire management compared to wildfire.

Forest type	Aboveground biomass (%)	Underground biomass (%)
Fire prevention		
Tropical forest	11.25±2.25	22.5±18
Tropical-subtropical mixed forest	9.675±2.03	22.5±18
Subtropical forest	8.1±1.46	22.5±18
Temperate-subtropical mixed forest	6.53+0.93	23.3±18
Temperate	4.99±0.71	23.75±18
Boreal forest	11.88±4.51	23.75±18
Prescribed fire		
Tropical forest	6.25±1.25	12.5±10.88
Tropical-subtropical mixed forest	5.375±1.125	12.5±10.88
Subtropical forest	4.5±0.8125	12.5±10.88
Temperate-subtropical mixed forest	3.484±0.4982	12.5±10.88
Temperate	2.625±0.375	12.5±10.88
Boreal forest	6.25±2.375	12.5±10.88

Table S27. Combustion efficiency of different forest types in China.

Forest type	**Combustion Efficiency, % [124]**	
	Above Ground	Ground Layer
Tropical forest	25.0(20.0-30.0)	50.0(3.0-90.0)
Tropical-subtropical mixed forest	21.5(17.0-26.0)	50.0(3.0-90.0)
Subtropical forest	18.0(14.5-21.0)	50.0(3.0-90.0)
Temperate-subtropical mixed forest	14.0(12.0-16.0)	50.0(3.0-90.0)
Temperate	10.5(9.0-12.0)	50.0(3.0-90.0)
Boreal forest	25.0(15.0-34.0)	50.0(3.0-90.0)

Table S28. CO_2 emission factors of forest fire of different forest types.

Forest type	Emission Factors, g/kg C [124]
Tropical forest	3476±198
Tropical-subtropical mixed forest	3545±202
Subtropical forest	3614±206
Temperate-subtropical mixed forest	3683±210
Temperate	3752±214
Boreal forest	3590±70

Table S29. The MAC estimates of carbon sequestration through forest fire management.

Year	Fire management	Tg CO_2 yr^{-1} 10	50	100
		MAC USD Mg CO_2^{-1}		
2000-2020	Fire prevention	2.81	4.68	6.55
	Prescribed fire	0.17	0.28	0.39
2020-2030	Fire prevention	0.18	0.30	0.41
	Prescribed fire	0.04	0.07	0.09
2020-2060	Fire prevention	0.18	0.30	0.41
	Prescribed fire	0.04	0.07	0.09

Table S30. The mitigation potential of avoided grassland conversion.

Year	Type	Loss rate (Mha yr^{-1})	Flux (Mg C ha^{-1})	Max (Tg CO_2 yr^{-1})	All (Tg CO_2 yr^{-1})
2020-2030	Alpine Veg	0.007	2.71	0.07	
	Temperate Veg	0.506	4.25	7.91	57.42
	SOC	0.51	26.19	49.44	
2020-2060	Alpine Veg	0.007	2.71	0.07	
	Temperate Veg	0.506	5.25	7.91	49.96
	SOC	0.51	22.24	41.98	

Table S31 Increased carbon fluxes of fenced grassland sites compared to degraded sites in the main areas implemented the Returning Grazing Land to Grassland Program.

Province	Carbon fluxes(Mg CO_2 ha^{-1} yr^{-1})		
	AGB	BGB	SOC
Inner Mongolia	0.04	0.33	0.31
Sichuan	0.13	0.85	0.86
Xizang	0.04	0.26	0.28
Gansu	0.05	0.52	0.48
Qinghai	0.09	0.55	0.51
Ningxia	0.02	0.23	0.23
Xinjiang	0.04	0.28	0.29
Jilin	0.04	0.33	0.31
Liaoning	0.04	0.33	0.31
Heilongjiang	0.04	0.33	0.31
Shannxi	0.05	0.52	0.48
Yunnan	0.13	0.85	0.86
Guizhou	0.13	0.85	0.86

Table S32. Avoiding fluxes and mitigation potential for saltmarshes and seagrass beds.

Year	Saltmarshes		Seagrass beds	
	Avoiding fluxes ($Mg\ CO_2\ ha^{-1}$)	Potential ($Tg\ CO_2\ yr^{-1}$)	Avoiding fluxes ($Mg\ CO_2\ ha^{-1}$)	Potential ($Tg\ CO_2\ yr^{-1}$)
2020-2030	564.46±62.17	6.15±0.68	239.06±58.96	0.06±0.07
2020-2060	912.64±100.51	9.94±1.10	386.53±95.33	0.09±0.1

Table S33. Carbon stocks and conversion rates of peatlands.

Climate zone	Conversion rate	Biomass	SOC	Avoiding flux
	ha yr^{-1}	Mg C ha^{-1}	Mg C ha^{-1}	Tg CO_2 yr^{-1}
Tropical zone	11.10±8.67	100.10	17439.34	0.66±0.51
Subtropical zone	1390.16±1086.39	22.28±31.30	1178.90	5.65±6.03
Temperate zone	1081.56±845.22	6.24±8.63	889.41	3.27±2.57
Plateau climate zone	6940.16±5423.61	5.87±8.63	608.30	14.40±11.34

Table S34. The areas of mangroves in different periods.

Province	**2000** (ha)	**2020** (ha)	**2020-2025** (ha)	**Suitable area** (ha)
Guangdong	9084	12100	5500	22260.6
Guangxi	8374.9	9330	1000	9274
Hainan	3930.3	6300	2000	9609.4
Fujian	615.1	1240	675	12508.6
Zhejiang	20.6	257	200	5195.6
National	22024.9	29227	9375	58848.2
Reference	[372]	[373-375]	[260]	[372]

Table S35. The area available for mangrove restoration.

Province	**2000-2020** (ha)	**2020-2030** (ha)	**2030-2060** (ha)
Guangdong	3016	10160.6	0
Guangxi	955.1	1000	0
Hainan	2369.7	3309.4	0
Fujian	624.9	1350	9918.6
Zhejiang	236.4	400	4538.6
National	7202.1	16220	14457.2

Table S36. The historical flux and future mitigation potential of restored mangroves in China at the provincial level.

Province	2000-2020	2020-2030	2020-2060
	Tg C · yr^{-1}		
Guangdong	0.10	0.44	0.25
Guangxi	0.03	0.07	0.04
Hainan	0.08	0.19	0.11
Fujian	0.02	0.07	0.23
Zhejiang	0.01	0.02	0.10
National	0.24	0.78	0.73

Table S37. The extents of peatland restoration in different periods.

Climate zones	2020-2030 (ha)	2020-2060 (ha)
Tropical zone	55.50	221.98
Subtropical zone	6950.81	27803.23
Temperate zone	5407.80	21631.20
Plateau climate zone	34700.80	138803.19

Table S38. The future mitigation potential of peatland restoration.

Mg CO_2 e ha^{-1} yr^{-1}	CO_2		CH_4		DOC	
Climate zone/Measure	Drained	Re-wet	Drained	Re-wet	Drained	Re-wet
Tropical zone	7.33	0.00	0.15	1.47	3.01	1.87
Subtropical zone	10.27	1.83	0.15	7.20	1.14	0.88
Temperate zone	10.27	1.83	0.15	1.77‡	1.14	0.88
Plateau climate zone	105.67*	1.83	0.48 f	1.85⸙	1.14	0.88

Note: * f ‡ ⸙: These values came from published data; other values came from the IPCC report [241,274].

Reference

1. Liu, Y., Gao, X., Fu, C., Yu, G. & Liu, Z. Estimation of carbon sequestration potential of forest biomass in China based on National Forest Resources Inventory. *Acta Ecol. Sin.*, **39**(11), 4002-4010 (2019).(In Chinese)
2. Liu, G., Fu, B. & Fang, J. Carbon dynamics of Chinese forests and its contribution to global carbon balance. *Acta Ecol. Sin.*, **20**(5),733-740 (2000).(In Chinese)
3. *Returning Farmland to Forest and Grassland in Twenty Years in China (1999—2019)*. (2020); Available from: http://www.forestry.gov.cn/html/main/main_195/20200630085813736477881/file/20200630090428999877621.pdf （In Chinese）.
4. Wang, X., Zhang, C., Hasi, E. & Dong, Z. Has the Three Norths Forest Shelterbelt Program solved the desertification and dust storm problems in arid and semiarid China? *J. Arid. Environ.*, **74**(1),13-22 (2010).10.1016/j.jaridenv.2009.08.001.
5. Cao, S., Chen, L. & Yu, X. Impact of China's Grain for Green Project on the landscape of vulnerable arid and semi-arid agricultural regions: a case study in northern Shaanxi Province. *J. Appl. Ecol.*, **46**(3),536-543 (2009).10.1111/j.1365-2664.2008.01605.x.
6. Wang, Y. & Cao, S. Carbon sequestration may have negative impacts on ecosystem health. *Environ. Sci. Technol.*, **45**(5),1759-60 (2011).10.1021/es200042s.
7. Wang, F. et al. Vegetation restoration in Northern China: A contrasted picture. *Land Degrad. Dev.*, **31**(6),669-676 (2020).10.1002/ldr.3314.
8. Cao, S. Why large-scale afforestation efforts in china have failed to solve the desertification problem. *Environ. Sci. Technol.*, **42**(6),1826-1831 (2008).
9. Su, Y. Review of the 25th anniversary achievements of the three North Shelterbelt. *Tide of Sci. Tech.*, **3**,42-44 (2004).(In Chinese)
10. Ge, Q., Dai, J., He, F., Pan, Y. & Wang, M. Land use changes and their relations with carbon cycles over the past 300 a in China. *Sci China Ser D Earth Sci.*, **51**(6),871-884 (2008).10.1007/s11430-008-0046-z.
11. Bastin, J. F. et al. The global tree restoration pothential. *Science*, **365**,76-79 (2019).
12. Zhang, D., Zuo, X. & Zang, C. Assessment of future potential carbon sequestration and water consumption in the construction area of the Three-North Shelterbelt Programme in China. *Agric. For. Meteorol.*, **303** (2021).10.1016/j.agrformet.2021.108377.
13. Guo, Q. & Ren, H. Productivity as related to diversity and age in planted versus natural forests. *Glob. Ecol. Biogeogr.*, **23**(12),1461-1471 (2014).10.1111/geb.12238.
14. Lu, F. et al. Effects of national ecological restoration projects on carbon sequestration in China from 2001 to 2010. *Proc. Natl. Acad. Sci. U. S. A.*, **115**(16),4039-4044 (2018).10.1073/pnas.1700294115.
15. Frey, C., Penman, J., Hanle, L., Monni, S. & Ogle, S. Chapter 3: Uncertainties, in 2006 IPCC Guidelines for National Greenhouse Gas Inventories (Intergovernmental Panel on Climate Change, 2006).1-66. www.ipcc-nggip.iges.or.jp/public/2006gl/pdf/1_Volume1/ V1_3_Ch3_Uncertainties. pdf (2006).www.ipcc-nggip.iges.or.jp/public/2006gl/pdf/1_Volume1/ V1_3_Ch3_Uncertainties. pdf.
16. Zeng, Y. et al. The impact of secondary forest restoration on multiple ecosystem services and their trade-offs. *Ecol. Indic.*, **104**,248-258 (2019).10.1016/j.ecolind.2019.05.008.
17. Qiu, G. Y., Yin, J., Tian, F. & Geng, S. Effects of the "Conversion of Cropland to Forest and Grassland Program" on the water budget of the Jinghe River catchment in China. *J. Environ. Qual.*, **40**(6),1745-55 (2011).10.2134/jeq2010.0263.
18. Yu, P., Wang, Y., Coles, N., Xiong, W. & Xu, L. Simulation of Runoff Changes Caused by Cropland to Forest Conversion in the Upper Yangtze River Region, SW China. *PLoS One*, **10**(7),e0132395 (2015).10.1371/journal.pone.0132395.
19. Li, Z., Cheng, X. & Han, H. Future Impacts of Land Use Change on Ecosystem Services under Different Scenarios in the Ecological Conservation Area, Beijing, China. *Forests*, **11**(5) (2020).10.3390/f11050584.
20. Hua, F. et al. Opportunities for biodiversity gains under the world's largest reforestation programme. *Nat. Commun.*, **7**,12717 (2016).10.1038/ncomms12717.
21. Liu, J., Li, S., Ouyang, Z., Tam, C. & Chen, X. Ecological and socioeconomic effects of China's policies for ecosystem services. *Proc. Natl. Acad. Sci. U. S. A.*, **105**(28),9477-9482 (2008).
22. Chen, H. L. et al. Assessing the effects of payments for ecosystem services programs on forest structure and species biodiversity. *Biodivers. Conserv.*, **29**(7),2123-2140 (2020).10.1007/s10531-020-01953-3.
23. *Measures for the administration of forestry subsidies from the central finance*. (2014); Available from: http://www.gov.cn/xinwen/2014-05/20/content_2682763.htm （In Chinese）.
24. Fargione, J. E. et al. Natural climate solutions for the United States. *Sci. Adv.*, **4**(11),eaat1869 (2018).
25. Drever, C. R., Cook-Patton, S. C. & Akhter, F. Natural climate solutions for Canada. *Sci. Adv.*, **7**,eabd6034 (2021).
26. Griscom, B. W. et al. Natural climate solutions. *Proc. Natl. Acad. Sci. U. S. A.*, **114**(44),11645-11650 (2017).10.1073/pnas.1710465114.
27. Liu, J. et al. Spatiotemporal characteristics, patterns and causes of land use changes in China since the late 1980s. *Acta Geogr. Sin.*, **69**(1),3-14 (2014).10.11821/dlxb201401001. (In Chinese)
28. Liu, J. et al. Spatio-temporal patterns and characteristics of land-use change in China during 2010-2015. *Acta Geogr. Sin.*, **73**(5),789-802 (2018).10.11821/dlxb201805001. (In Chinese)
29. Curtis, P. G., Slay, C. M., Harris, N. L., Tyukavina, A. & Hansen, M. C. Classifying drivers of global forest loss. *Science*, **361**,1108–1111 (2019).
30. Liu, J., Wang, S., Chen, J., Liu, M. & Zhuang, D. Storages of soil carbon and nitrogen and land use change in China: 1900-2000. *Acta Geogr. Sin.*, **59**(4),483-496 (2004).(In Chinese)
31. Xue, Y. Soil carbon source/sink caused by land use change in the last decades of the last century in Eastern China. *China University of Geosciences (Beijing), Master Dissertation* (2013).(In Chinese)
32. Murty, D., Kirschbaum, M. U. F., Mcmurtrie, R. E. & Mcgilvray, H. Does conversion of forest to agricultural land change soilcarbon and nitrogen? a review of the literature. *Glob. Change Biol.*, **8**,105-123 (2002).
33. Lugo, A. E. & Brown, S. Management of topical soils as sinks of atmospheric carbon. *Plant Soil*, **149**,27–41 (1993).
34. Chen, H. et al. Simulating effects of urban soil sealing on the soil organic carbon pool. *Acta Ecol. Sin.*, **37**(8),2600-2610 (2017).(In Chinese)

35. Luo, S., Mao, Q., Ma, K. & Wu, J. A review of carbon cycling and sequestration in urban soils. *Acta Ecol. Sin.*, **32**(22),7177-7189 (2012).(In Chinese)
36. Zhu, C., Zhao, S. & Zhou, D. Organic carbon storage in urban built-up areas of China in 1997-2006. *Chin. J. Appl. Ecol.*, **23**(5),1195-1202 (2012).10.13287/j.1001-9332.2012.0165. (In Chinese)
37. Churkina, G., Brown, D. G. & Keoleian, G. Carbon stored in human settlements: the conterminous United States. *Glob. Change Biol.*, **16**(1),135-143 (2010).10.1111/j.1365-2486.2009.02002.x.
38. Edmondson, J. L., Davies, Z. G., McHugh, N., Gaston, K. J. & Leake, J. R. Organic carbon hidden in urban ecosystems. *Sci Rep*, **2**,963 | DOI: 10.1038/srep00963 (2012).10.1038/srep00963.
39. Liu, R., Wang, M. & Chen, W. The influence of urbanization on organic carbon sequestration and cycling in soils of Beijing. *Landsc. Urban Plan.*, **169**,241-249 (2018).10.1016/j.landurbplan.2017.09.002.
40. Guo, L. & Gifford, R. M. Soil carbon stocks and land use change: a meta analysis. *Glob. Change Biol.*, **8**(4),345-360 (2010).
41. Vasenev, V. I., Stoorvogel, J. J. & Vasenev, I. I. Urban soil organic carbon and its spatial heterogeneity in comparison with natural and agricultural areas in the Moscow region. *Catena*, **107**,96-102 (2013).10.1016/j.catena.2013.02.009.
42. Brook, B. W., Sodhi, N. S. & Ng, P. K. L. Catastrophic extinctions follow deforestation in Singapore. . *Nature*, **424**,420-423 (2003).
43. Zhou, G. Influences of tropical forest changes on environmental quality in hainan province. *Ecol. Eng.*, **4**,223-229 (1995).
44. Gibson, L. et al. Primary forests are irreplaceable for sustaining tropical biodiversity. *Nature*, **478**(7369),378-81 (2011).10.1038/nature10425.
45. Martensen, A. C., Pimentel, R. G. & Metzger, J. P. Relative effects of fragment size and connectivity on bird community in the Atlantic Rain Forest: Implications for conservation. *Biol. Conserv.*, **141**(9),2184-2192 (2008).10.1016/j.biocon.2008.06.008.
46. Ishiyama, N., Miura, K., Inoue, T., Sueyoshi, M. & Nakamura, F. Geology-dependent impacts of forest conversion on stream fish diversity. *Conserv. Biol.*, **35**(3),884-896 (2020).10.1111/cobi.13655.
47. Schmidt, M., Jochheim, H., Kersebaum, K.-C., Lischeid, G. & Nendel, C. Gradients of microclimate, carbon and nitrogen in transition zones of fragmented landscapes – a review. *Agric. For. Meteorol.*, **232**,659-671 (2017).10.1016/j.agrformet.2016.10.022.
48. Williams-Linera, G., Dominguez-Gastelu, V. & Garcia-Zurita, M. Microenvironment and floristics of different edges in a fragmented tropical rainforest. *Conserv. Biol.*, **12**(5),1091-1102 (1998).
49. Zeng, Q., Darboux, F., Man, C., Zhu, Z. & An, S. Soil aggregate stability under different rain conditions for three vegetation types on the Loess Plateau (China). *Catena*, **167**,276-283 (2018).10.1016/j.catena.2018.05.009.
50. Duan, L., Sheng, H., Yuan, H., Zhou, Q. & Li, Z. Land use conversion and lithology impacts soil aggregate stability in subtropical China. *Geoderma*, **389**,114953. https://doi.org/10.1016/j.geoderma.2021.114953 (2021).10.1016/j.geoderma.2021.114953.
51. Guo, Z., Li, Y., Xiao, X., Zhang, L. & Gan, Y. Hydroelectricity production and forest conservation in watersheds. *Ecol. Appl.*, **17**(6),1557-1562 (2007).
52. Zhu, Z., Wang, G. & Dong, J. Correlation Analysis between Land Use/Cover Change and Air Pollutants—A Case Study in Wuyishan City. *Energies*, **12**(13),2545. doi:10.3390/en12132545 (2019).10.3390/en12132545.
53. Huang, Z. & Du, X. Urban Land Expansion and Air Pollution: Evidence from China. *J. Urban Plan. Dev*, **144**(4),05018017 (2018).10.1061/(asce)up.1943-5444.0000476.
54. Golub, A., Hertel, T., Lee, H. L., Rose, S. & Sohngen, B. The opportunity cost of land use and the global potential for greenhouse gas mitigation in agriculture and forestry. *Resour. Energy Econ.*, **31**(4),299-319 (2009).10.1016/j.reseneeco.2009.04.007.
55. Li, H., Ma, Y., Aide, T. M. & Liu, W. Past, present and future land-use in Xishuangbanna, China and the implications for carbon dynamics. *For. Ecol. Manage.*, **255**(1),16-24 (2008).10.1016/j.foreco.2007.06.051.
56. Fu, C., Fang, H. & Yu, G. Carbon Emissions from Forest Vegetation Caused by Three Major Disturbances in China. *J. Resour. Ecol.*, **2**(3),202-209 (2011).10.3969/j.issn.1674-764x.2011.03.002.
57. Wang, W. et al. Long term effects of logging treatment on carbon sequestration in Chinese Fir plantation. *Res. Soil Water Conserv.*, **23**(6),198-203 (2016).10.13869/j.cnki.rswc.2016.06.025. (In Chinese)
58. Yang, H., Nie, Y. & Ji, C. Study on China's Timber Resource Shortage and Import Structure: Natural Forest Protection Program Outlook, 1998 to 2008. *For. Prod. J.*, **60**(5),408-414 (2010).Doi 10.13073/0015-7473-60.5.408.
59. Tobias, J. Hidden impacts of logging. *Nature*, **523**,163-164 (2015).
60. Premer, M. I., Froese, R. E., Webster, C. R. & Nagel, L. M. Vegetation response to logging residue removals in Great Lakes aspen forests: Long-term trends under operational management. *For. Ecol. Manage.*, **382**,257-268 (2016).10.1016/j.foreco.2016.09.048.
61. Wu, Y. Effect of Different Logging Residue Clearances on the Growth and Soil Physical-chemical Proper‐ ties of Chinese fir Forest. *Anhui Agri. Sci. Bull.*, **23**(9),105-107 (2017).10.16377/j.cnki.issn1007-7731.2017.09.045. (In Chinese)
62. Dai, L. et al. Opportunities and challenges for the protection and ecological functions promotion of natural forests in China. *For. Ecol. Manage.*, **410**,187-192 (2018).
63. Zhang, K., Song, C., Zhang, Y. & Zhang, Q. Natural disasters and economic development drive forest dynamics and transition in China. *For. Policy Econ.*, **76**,56-64 (2017).
64. Chinese Ministry of Forestry. Forest Resource Statistics of China for Periods 1994–1998. *Department of Forest Resource and Management, Chinese Ministry of Forestry, Beijing.* (In Chinese)
65. Zhu, H. et al. Biomass and carbon storage of communities in secondary karst forests in Mashan county,Guangxi. . *Acta Ecol. Sin.*, **35**(8),2616-2621 (2015).(In Chinese)
66. Zhang, Z. et al. Carbon Storage and Distribution of Pinus massoniana Forest Ecosystem in Tieshanping of Chongqing. . *Sci. Silv. Sin.*, **45**(5),49-53 (2009).(In Chinese)
67. Zhang, Z. et al. Study on the biomass structure and distribution of natural secondary forest of Pinus massoniana. *J. Agri. Univ. Hebei*, **5**,37-43 (2006).(In Chinese)
68. Zhang, Y., Gu, F., Liu, S., Liu, Y. & Li, C. Variations of carbon stock with forest types in subalpine region of southwestern China. *For. Ecol. Manage.*, **300**,88–95 (2013).
69. Zhang, P. et al. Carbon storage and sequestration of tree layer in subtropical evergreen broadleaf forests in Ailao Mountain of Yunnan. *Chin. J. Ecol.*, **29**(6),1047-1053 (2010).(In Chinese)

70. Zhang, L. et al. Biomass and net primary productivity of secondary evergreen broadleaved forest in Huangmian Forest Farm, Guangxi. *Chin. J. Appl. Ecol.*, **11**,2029-2033 (2004).(In Chinese)
71. Zhang, J. et al. Carbon storage and its sequestration potential by ecological service forest in Zhejiang. *Acta Ecol. Sin.*, **30**(14),3839-3848 (2010).(In Chinese)
72. Zhang, G. et al. Analysis of the carbon stock structure in forest plantations with different regeneration methods. *Ecol. Environ. Sci.*, **21**(2),206-212 (2012).(In Chinese)
73. Zeng, L. et al. Effect of altitudinal variation on carbon density in arbor layer and soil layer of Picea crassifolia forest in Qilian Mountains. *Acta Ecol. Sin.*, **38**(20),7168-7177 (2018).(In Chinese)
74. Yao, F. et al. Determination and Evaluation of Biomass of Different Broad-leaf Stand Types in Qingyuan Forest Center. *J. Zhejiang For. Sci. Tech.*, **3**,75-79 (2003).(In Chinese)
75. Yang, L. et al. Carbon and nitrogen storage and distribution in four forest ecosystems in Liupan Mountains， northwestern China. *Acta Ecol. Sin.*, **35**(15), 5215-5227 (2015).(In Chinese)
76. Xian, J., Zhang, Y., Wang, K., Hu, T. & Yang, H. Carbon stock and its allocation in five forest ecosystems in the subalpine coniferous forest zone of western Sichuan Province, Southwest China. *Chin. J. Plant Ecol.*, **33**(2),283-290 (2009).(In Chinese)
77. Wang, Y. et al. Carbon stock and its distribution of three typical forest types in southeastern Guizhou Province, southwestern China. *J. Beijing For. Univ.*, **36**(5),54-61 (2014).(In Chinese)
78. Wang, X., Zhang, J., Pang, H., Zheng, L. & Cui, H. Carbon storage and carbon density of forest ecosystems in Hubei Province. *J. Central South Univ. For. Tech.*, **35**(10),93-108 (2015).(In Chinese)
79. Tong, Z., Chen, Q., Xiong, H., Wang, Y. & Wu, J. Carbon storage and distribution pattern of Pinus yunnanensis forest in Mopan Mountain. *J. Sichuan Agricul. Univ.*, **31**(4),381-385+407 (2013).(In Chinese)
80. Tang, J., Yin, J., Qi, J., Jepsen, M. R. & Lü, X. Ecosystem carbon storage of tropical forests over limestone in Xishuangbanna, SW China. *J. Trop. For. Sci.*, **24**(3),399-407 (2012).
81. Sun, M. et al. Characteristics of Carbon Sink in Black Locust Plantation and Oak Natural Secondary Forest in Loess Hilly Region. *Res. Soil Water Conserv.*, **27**(2),55-61 (2020).(In Chinese)
82. Qiu, Z., Feng, Z., Song, Y., Li, M. & Zhang, P. Carbon sequestration potential of forest vegetation in China from 2003 to 2050: Predicting forest vegetation growth based on climate and the environment. *J. Clean Prod.*, **252**,119715 (2020).https://doi.org/10.1016/j.jclepro.2019.119721.
83. Qiu, F. et al. Carbon storage of evergreen broad-leaved forest, Jinpenshan, Jiangxi province. *J. Central South Univ. For. Tech.*, **40**(1),105-115 (2020).(In Chinese)
84. Pang, H., Wang, X. & Zhang, J. Characteristics of Carbon Storage and Carbon Density of Pinus massoniana Natural Forests in Hubei Province, China. *J. Northeast For. Univ.*, **42**(7),40-43 (2014).(In Chinese)
85. Mou, C., Wan, S., Su, P. & Sun, Z. Biomass distribution patterns of Alnus hirsuta and Betula platyphylla-swamp ecotone communities in Changbai Mountains. *Chin. J. Appl. Ecol.*, **12**,2211-2216 (2004).(In Chinese)
86. Liu, Y., Yu, G., Wang, Q. & Zhang, Y. How temperature, precipitation and stand age control the biomass carbon density of global mature forests. *Glob. Ecol. Biogeogr.*, **23**(3),323–333 (2014).
87. Liu, Y. et al. Studies on biomass and net production of Quercus acutidentata forest in Baotianman Nature Reserve. *Acta Ecol. Sin.*, **9**,1450-1456 (2001).(In Chinese)
88. Liu, Y. et al. Biomass and net productivity of Quercus variabilis forest in Baotianman Natural Reserve. *Chin. J. Appl. Ecol.*, **6**,11-16 (1998).(In Chinese)
89. Lin, F. Biomass Characteristics and Allocation of Castanopsis fargesii Natural Stand in Wuyishan Mountains. *Acta Agri. Univ. Jiangxi*, **1**,74-77 (2006).(In Chinese)
90. Li, Y., Wang, L., Liu, J. & Zhou, H. Changes of Carbon Storage and Carbon Density of Forests in the Kanas National Nature Reserve, Xinjiang. *Arid Zone Res.*, **36**(5),1136-1150 (2019).(In Chinese)
91. Li, S. et al. Changes in biomass carbon and soil organic carbon stocks following the conversion from a secondary coniferous forest to a pine plantation. *PLoS One*, **10**(9),e0135946 (2015). https://doi.org/10.1371/journal.pone.0135946.
92. Huang, Y. et al. Supporting data and code for A global map of root biomass across the world's forests. figshare. Dataset. (2020).https://doi.org/10.6084/m9.figshare.12199637.v1.
93. Hu, Q., Wang, S., Chen, L., Zhang, W. & Gong, C. Biomass and carbon density of main forest ecosystems in Hubei Province. *Chin. J. Ecol.*, **31**(7),1626-1633 (2012).(In Chinese)
94. Guo, C., Wu, Y. & Ni, J. Estimation for vegetation carbon storage in Tiantong National Forest Park. *Chin. J. Appl. Ecol.*, **25**(11),3099-3113 (2014).(In Chinese)
95. Gao, Y., Ding, F., Pan, M., Zhou, F. & Wu, P. Carbon sequestration and distribution characteristics in natural secondary forests of Betula luminifera in west Guizhou. *J. Nanjing For. Univ. (Nat. Sci. Ed.)* **38**(4),51-56 (2014).(In Chinese)
96. Fang, J. Study on Biomass and Productivity of Picea likiangensis var. linzhiensis Forest in Nanyigou of Tibet. *For. Res.*, **25**(5),582-589 (2012).(In Chinese)
97. Ding, F., Pan, Z., Wu, P., Cui, Y. & Zhou, F. Carbon accumulation and distribution characteristics of the evergreen broad-leaved and deciduous broad-leaved mixed forests in East Guizhou. *Acta Ecol. Sin.*, **35**(6),1761-1768 (2015).(In Chinese)
98. Chi, L. et al. Carbon Storage and Density of Pinus tabulaeformis and Quercus liaotungensis Forests in Taiyue Mountain of Shanxi Province, China. *J. Northeast For. Univ.*, **41**(8),32-35 (2013).(In Chinese)
99. Dai, L., Zhang, Y., Wang, L., Zheng, S. & Xu, W. Assessment of carbon density in natural mountain forest ecosystems at Northwest China. *Int. J. Environ. Res. Pub. He.*, **18**(4),1-12 (2021).
100. Deng, K., Shi, P. & Yang, Z. Biomass allocation and net primary productivities and treeline ecotone on the Changbai Mountains. Northeast China. *J. Nat. Resour.*, **6**,942-948 (2006).(In Chinese)
101. Di, Y. et al. Carbon storage and its allocation pattern of forest ecosystems with different restoration methods in sub-tropical China. *Chin. Sci. Bull.*, **57**,1553–1561 (2012).(In Chinese)

102. Zhou, L. et al. Changes in carbon density for three old-growth forests on Changbai Mountain, Northeast China: 1981-2010. *Ann. For. Sci.*, **68**(5),953-958 (2011).
103. Zhou, X. et al. Ecosystem carbon stock and within-system distribution in successional Fagus lucida forests in Mt. Yueliang, Guizhou, China. *Chin. J. Plant Ecol.*, **42**,703-712 (2018).(In Chinese)
104. Zhou, Z. et al. Estimation methods in predicting carbon stock of forest communities in the natural reserve of Baihua mountain. *J. Northwest Agri. For. Univ.*, **40**(11),139-146 (2012).(In Chinese)
105. Zhu, J. et al. Carbon stocks and changes of dead organic matter in China's forests. *Nat. Commun.*, **8**(1),1-10 (2017).
106. FAO. *Global Forest Resources Assessment 2020 Report China (FAO, Rome, Italy)*. (2020); Available at: http://www.fao.org/3/ca9980en/ca9980en.pdf.].
107. Fang, J., Chen, A., Peng, C., Zhao, S. & Ci, L. Changes in forest biomass carbon storage in China between 1949 and 1998. *Science*, **292**(5525),2320–2322 (2001).
108. Zhang, C. et al. Disturbance-induced reduction of biomass carbon sinks of China's forests in recent years. *Environ. Res. Lett.*, **10**(11) (2015). https://doi.org/10.1088/1748-9326/10/11/114021.
109. Austin, K. G. et al. The economic costs of planting, preserving, and managing the world's forests to mitigate climate change. *Nat. Commun.*, **11**(1),1-9 (2020).
110. Yang, Y. et al. Large Ecosystem Service Benefits of Assisted Natural Regeneration. *J. Geophys. Res.: Biogeosciences*, **123**(2),676–687 (2018).
111. Burivalova, Z., Sekercioğlu, C. H. & Koh, L. P. Thresholds of logging intensity to maintain tropical forest biodiversity. *Curr Biol*, **24**(16),1893–1898 (2014).
112. Burton, T. A. Effects of Basin-Scale Timber Harvest on Water Yield and Peak Streamflow. *J Am Water Resour Assoc*, **33**(6),1187–1196 (1997).
113. Jurgensen, M. F. et al. Review Article: Impacts of Timber Harvesting on Soil Organic Matter, Nitrogen, Productivity, and Health of Inland Northwest Forests. *Soc Am For*, **43**(2),234-251 (1997).
114. Gao, Z. et al. Study on reconnaissance of prescribed burning in Anning City. *Fire Sci. Tech.*, **39**(9),1285-1290 (2020).
115. Zhang, W. et al. Effects of prescribed burning on pinusyunnanensis pure forest fuel in Yunnan province. *Fire Sci. Tech.*, **39**(6),2018-2021 (2020).
116. Chen, Y., Cao, J., Zhou, L., Li, F. & Fu, S. Effects of prescribed burning on carbon accumulation in two paired vegetation sites in subtropical china. *For. Ecosyst.*, **6**(1),9 (2019).
117. Du, J., Zhang, J., Guo, Y. & Chen, D. Discussion on the Interval Period of the Prescribed Burning. *For. Sci. Tech.*, **33**(4),2-4 (2008).(In Chinese)
118. Liu, G., Sha, Y. & Liu, G. Study of Prescribed Burning to the Rejuvenation of Populus davidiana and Betula platyphlla Forest Stands and the Wild Edible Vegetables. *For. Prod. Spec. China*, **4**,71-73 (2008).(In Chinese)
119. Zhang, Q. & Zhang, H. A review of the impact of planned burning on forest ecosystems and its application. *East china For. Manage.*, **30**(4),39-42 (2016).(In Chinese)
120. Ma, A. et al. The Overview of Prescribed Burning Effect and Application Research. *Guangdong For. Sci. Tech.*, **25**(6),95-99 (2009).(In Chinese)
121. Wiedinmyer, C. et al. Estimating emissions from fires in North America for air quality modelin. *Atmos. Environ.*, **40**(19),3419-3432 (2006).
122. CHINA NATIONAL BUREAU OF STATISTICS. China statistical yearbook 2019. (2019).(In Chinese)
123. Yoshihara, Y., Koyama, A., Undarmaa, J. & Okuro, T. Prescribed burning experiments for restoration of degraded semiarid Mongolian steppe. *Plant Ecol.*, **216**(12),1649–1658 (2015).
124. Lu, A., Tian, H., Liu, M., Liu, J. & Melillo, M. Spatial and temporal patterns of carbon emissions from forest fires in China from 1950 to 2000. *J. Geophys. Res.*, **111**,D05313 (2006).doi:10.1029/2005JD006198.
125. Wu, B., Zeng, Y. & Zhao, D. Remote sensing based vegetation aboveground biomass data(ChinaBiomass) from AIRCAS, 2000, 2005 and 2010. Described in Remote Sensing Monitoring Algorithms and Dynamic Change Patterns of Ecological Parameters of China. *Beijing: Science Press*, **ISBN 978-7-5088-5688-9** (2019).
126. Chen, J. et al. A review of biomass burning: Emissions and impacts on air quality, health and climate in China. *Sci. Total Environ.*, **579**,1000-1034 (2017).
127. Wang, X., Feng, Z. & Zhuang, Y. CO_2, CO AND CH_4 EMISSIONS FROM FOREST FIRES IN CHINA. *Sci. Silv. Sin.*, **37**(1),90-95 (2001).(In Chinese)
128. Wang, X., Xu, J., Wu, Z. & Shen, Y. Effect of annual prescribed burning of wetlands on soil organic carbon fractions: A 5-year study in Poyang, China. *Ecol. Eng.*, **138**,219-226 (2019).
129. Zhang, Y. Planned burn removal application techniques. *Inner Mongolia For.*, **5**,16-17 (2016).(In Chinese)
130. Dai, H., Xing, J., Guan, Q. & Wang, W. Planned burning research and application. *For. fire prev.*, **1**,52-53 (2000).(In Chinese)
131. Xiao, G., Liu, Z., Li, W. & Shi, H. Forest fire technology for forest management in northeast and Inner Mongolia. *For. Sci. Tech.*, **21**(1),33-35 (1996).(In Chinese)
132. Yang, Q., Zhou, H. & Bartocci, P. Prospective contributions of biomass pyrolysis to China's 2050 carbon reduction and renewable energy goals. *Nat. Commun.*, **12**(1),1-12 (2021).
133. Bai, X. et al. Responses of soil carbon sequestration to climate-smart agriculture practices: A meta-analysis. *Glob. Change Biol.*, **25**(8),2591-2606 (2019).
134. Du, Z.-L., Zhao, J.-K., Wang, Y.-D. & Zhang, Q.-Z. Biochar addition drives soil aggregation and carbon sequestration in aggregate fractions from an intensive agricultural system. *J. Soils Sediments*, **17**(3),581-589 (2017).
135. Weng, Z. H. et al. Biochar built soil carbon over a decade by stabilizing rhizodeposits. *Nat. Clim. Chang.*, **7**(5),371-376 (2017).
136. Yang, Q. et al. Country-level potential of carbon sequestration and environmental benefits by utilizing crop residues for biochar implementation. *Appl. Energy*, **282**,116275 (2021).

137. Li, F. & Wang, J. Estimation of carbon emission from burning and carbon sequestration from biochar producing using crop straw in China. *Trans. Chin. Soc. Agric. Eng.*, **29**(14),1-7 (2013).
138. Spokas, K. A. Review of the stability of biochar in soils: predictability of O: C molar ratios. *Carbon Manage.*, **1**(2),289-303 (2010).
139. Dharmakeerthi, R. S., Hanley, K., Whitman, T., Woolf, D. & Lehmann, J. Organic carbon dynamics in soils with pyrogenic organic matter that received plant residue additions over seven years. *Soil Biol. Biochem.*, **88**,268-274 (2015).
140. Liang, B. et al. Stability of biomass-derived black carbon in soils. *Geochim. Cosmochim. Acta*, **72**(24),6069-6078 (2008).
141. Eggleston, H., Buendia, L., Miwa, K., Ngara, T. & Tanabe, K. 2006 IPCC guidelines for national greenhouse gas inventories. (2006).
142. Blanco-Canqui, H. Biochar and soil physical properties. *Soil Science Society of America Journal*, **81**(4),687-711 (2017).
143. Blanco-Canqui, H. Biochar and water quality. *Journal of Environmental Quality*, **48**(1),2-15 (2019).
144. Atkinson, C. J., Fitzgerald, J. D. & A., H. N. Potential mechanisms for achieving agricultural benefits from biochar application to temperate soils: a review. *Plant Soil*, **337**(1),1-18 (2010).
145. Biederman, L. A. & Harpole, W. S. Biochar and its effects on plant productivity and nutrient cycling: a meta-analysis. *Global Change Biology bioenergy*, **5**(2),202-214 (2013).
146. Chan, K. Y., Van, Z. L. & Meszaros, I. Using poultry litter biochars as soil amendments. *Soil Research*, **46**(5),437-444 (2008).
147. Zhang, W. et al. New technologies reduce greenhouse gas emissions from nitrogenous fertilizer in China. *Proc. Natl. Acad. Sci. U. S. A.*, **110**(21),8375-8380 (2013).
148. Gu, B., Ju, X., Chang, J., Ge, Y. & Vitousek, P. M. Integrated reactive nitrogen budgets and future trends in China. *Proc. Natl. Acad. Sci. U. S. A.*, **112**(28),8792-8797 (2015).
149. Davidson, E. A. The contribution of manure and fertilizer nitrogen to atmospheric nitrous oxide since 1860. *Nat. Geosci.*, **2**(9),659-662 (2009).
150. Snyder, C. S., Bruulsema, T. W., Jensen, T. L. & Fixen, P. E. Review of greenhouse gas emissions from crop production systems and fertilizer management effects. *Agric. Ecosyst. Environ.*, **133**(3-4),247-266 (2009).
151. Smith, P. et al. The role of ecosystems and their management in regulating climate, and soil, water and air quality. *J. Appl. Ecol.*, **50**(4),812-829 (2013).
152. Einheuser, M. D. et al. Modeling the effects of conservation practices on stream health. *Sci. Total Environ.*, **435**,380-391 (2012).
153. Woodward, G. et al. Continental-scale effects of nutrient pollution on stream ecosystem functioning. *Science*, **336**(6087),1438-1440 (2012).
154. Keeler, B. L. et al. Linking water quality and well-being for improved assessment and valuation of ecosystem services. *Proc. Natl. Acad. Sci. U. S. A.*, **109**(45),18619-18624 (2012).
155. Quemada, M., Baranski, M., Nobel-de Lange, M., Vallejo, A. & Cooper, J. Meta-analysis of strategies to control nitrate leaching in irrigated agricultural systems and their effects on crop yield. *Agric. Ecosyst. Environ.*, **174**,1-10 (2013).
156. Carpenter, S. R. et al. Nonpoint pollution of surface waters with phosphorus and nitrogen. *Ecol. Appl.*, **8**(3),559-568 (1998).
157. Bussink, D. Relationships between ammonia volatilization and nitrogen fertilizer application rate, intake and excretion of herbage nitrogen by cattle on grazed swards. *Fertil. Res.*, **38**(2),111-121 (1994).
158. Yu, C. Q., Huang, X. & Chen, H. Managing nitrogen to restore water quality in China. *Nature*, **567**(7749),516-520 (2019).
159. Poeplau, C. & Don, A. Carbon sequestration in agricultural soils via cultivation of cover crops–A meta-analysis. *Agric. Ecosyst. Environ.*, **200**,33-41 (2015).
160. Jian, J., Du, X. & Reiter, M. S. A meta-analysis of global cropland soil carbon changes due to cover cropping. *Soil Biol. Biochem.*, **143**,107735 (2020).
161. Wang, L. & HU YG, Y. G. Carbon fixation by winter cover crops in South China and the effects of WCC on rice yields. *Ecol. Environ.*, **15**(3),616-619 (2006).
162. Derpsch, R., Friedrich, T., Kassam, A. & Li, H. Current status of adoption of no-till farming in the world and some of its main benefits. *Int. J. Agric. Biol. Eng.*, **3**(1),1-25 (2010).
163. McDaniel, M. D., Tiemann, L. K. & Grandy, A. S. Does agricultural crop diversity enhance soil microbial biomass and organic matter dynamics? A meta-analysis. *Ecol. Appl.*, **24**(3),560-570 (2014).
164. Büchi, L., Wendling, M. & Amossé, C. Importance of cover crops in alleviating negative effects of reduced soil tillage and promoting soil fertility in a winter wheat cropping system. *Agric. Ecosyst. Environ.*, **256**,92-104 (2018).
165. De Baets, S., Poesen, J. & Meersmans, J. Cover crops and their erosion-reducing effects during concentrated flow erosion. *Catena*, **85**(3),237-244 (2011).
166. Basche, A. D., Kaspar, T. C. & Archontoulis, S. V. Soil water improvements with the long-term use of a winter rye cover crop. *Agric. Water Manage.*, **172**,40-50 (2016).
167. Abdalla, M., Hastings, A. & Cheng, K. A critical review of the impacts of cover crops on nitrogen leaching, net greenhouse gas balance and crop productivity. *Glob. Change Biol.*, **25**(8),2530-2543 (2019).
168. Sander, B. O. et al. Mitigating greenhouse gas emissions from rice production through water-saving techniques: potential, adoption and empirical evidence. *Clim. Chang. Agric. Water Manage. Devel. Countr.*, **8**,193 (2015).
169. USEPA. Global Non-CO2 Greenhouse Gas Emission Projections & Mitigation Potential 2015–2050. *US Environmental Protection Agency Washington, DC* (2019).
170. Toze, S. Reuse of effluent water—benefits and risks. *Agric. Water Manage.*, **80**(1-3),147-159 (2006).
171. Meijide, A., Gruening, C. & Goded, I. Water management reduces greenhouse gas emissions in a Mediterranean rice paddy field. *Agric. Ecosyst. Environ.*, **238**,168-178 (2017).
172. Wang, H., Zhang, Y. & Zhang, Y. Water-saving irrigation is a 'win-win'management strategy in rice paddies–With both reduced greenhouse gas emissions and enhanced water use efficiency. *Agric. Water Manage.*, **228**,105889 (2020).
173. Cao, M., Dent, J. B. & Heal, O. W. Methane emissions from China's paddyland. *Agric. Ecosyst. Environ.*, **55**(2),129-137 (1995).
174. Li, C., Qiu, J. & Frolking, S. Reduced methane emissions from large-scale changes in water management of China's rice paddies during 1980–2000. *Geophysical Research Letters*, **29**(20),33-1-33-4 (2002).

175. Zhang, W., Yu, Y. & Huang, Y. Modeling methane emissions from irrigated rice cultivation in C hina from 1960 to 2050. *Glob. Change Biol.*, **17**(12),3511-3523 (2011).
176. Wang, Z., Zhang, X. & Liu, L. Estimates of methane emissions from Chinese rice fields using the DNDC model. *Agric. For. Meteorol.*, **303**,108368 (2021).
177. Xu, X. et al. Multi-period Land Use Land Land Cover Remote Sensing Monitoring Dataset in China(CNLUCC).2018.DOI:10.12078/2018070201; Available from: http://www.resdc.cn/DOI., (In Chinese)
178. Yang, Y., Fang, J., Ma, W., Guo, D. & Mohammat, A. Large-scale pattern of biomass partitioning across China's grasslands. *Glob. Ecol. Biogeogr.*, **19**(2),268-277 (2010).10.1111/j.1466-8238.2009.00502.x.
179. Xu, L. et al. Carbon storage in China's terrestrial ecosystems: A synthesis. *Sci Rep*, **8** (2018).
180. Sanderman, J., Hengl, T. & Fiske, G. J. Soil carbon debt of 12,000 years of human land use. *Proc. Natl. Acad. Sci. U. S. A.*, **114**(36),9575-9580 (2017).10.1073/pnas.1706103114.
181. Tang, S. et al. Synthesis of soil carbon losses in response to conversion of grassland to agriculture land. *Soil Tillage Res.*, **185**,29-35 (2019).10.1016/j.still.2018.08.011.
182. Han, X., Tsunekawa, A., Tsubo, M. & Li, S. Effects of land-cover type and topography on soil organic carbon storage on Northern Loess Plateau, China. *Acta Agric. Scandinavica Sec. B-Soil Plant Sci.*, **60**(4),326-334 (2010).10.1080/09064710902988672.
183. Liu, H., Zhang, W. & Wang, K. Effect of reclamation on soil properties of zonal and intrazonal grasslands in agro-pastoral ecotone. *Trans. Chin. Soc. Agric. Eng.*, **25**(10),272-277 (2009).
184. Liu, H., Wang, J., Lv, J. & Wang, K. Response of grasslands conversion to croplands on soil organic carbon in Bashang area of Northern China. *Afr. J. Biotechnol.*, **9**(12),1783-1788 (2010).
185. Liu, X., Li, L., Wang, Q. & Mu, S. Land-use change affects stocks and stoichiometric ratios of soil carbon, nitrogen, and phosphorus in a typical agro-pastoral region of northwest China. *J. Soils Sediments*, **18**(11),3167-3176 (2018).10.1007/s11368-018-1984-5.
186. Meng, F., Kuang, X., Du, Z., Wu, W. & Guo, Y. Impact of land use change and cultivation measures on soil organic carbon (SOC) and its 13C values. *Environ. Sci.*, **31**(8),1733-9 (2010).
187. Qi, Y. et al. Effects of a conversion from grassland to cropland on the different soil organic carbon fractions in Inner Mongolia, China. *J. Geogr. Sci.*, **22**(2),315-328 (2012).10.1007/s11442-012-0929-y. (In Chinese)
188. Qiu, L. et al. Effects of land-use change on soil organic carbon and nitrogen in density fractions and soil delta C-13 and delta N-15 in semiarid grasslands. *Plant Soil*, **390**(1-2),419-430 (2015).10.1007/s11104-015-2435-3.
189. Song, X. et al. The influence of the conversion of grassland to cropland on changes in soil organic carbon and total nitrogen stocks in the Songnen Plain of Northeast China. *Catena*, **171**,588-601 (2018).10.1016/j.catena.2018.07.045.
190. Han, K., Yu, P., Han, D. & Jia, H. Effect of Cultivation Chronosequence on the Dynamics of Soil CarbonPool in Songnen Alkaline Grassland. *Chin. J. Soil Sci.*, **48**(01),127-133 (2017).(In Chinese)
191. Han, X., Wang, S., Song, C. & Qiao, Y. Effect of Land Use and Cover Change on Ecological Environment in Black Soil Region. *Sci. Geogr. Sin.*(02),203-208 (2005).(In Chinese)
192. Liu, M., Chang, Q., Qi, Y. & Sun, N. Soil Organic Carbon and Particulate Organic Carbon under Different Land Use Types on Loess Plateau. *J. Nat. Resour.*, **25**(02),218-226 (2010).
193. Sun, W., Zhu, H. & Guo, S. Soil organic carbon as a function of land use and topography on the Loess Plateau of China. *Ecol. Eng.*, **83**,249-257 (2015).10.1016/j.ecoleng.2015.06.030.
194. Wang, G., Ma, H., Wang, Y. & Chang, J. Impacts of Land Use Change on Environment in the Middle Reaches of the Heihe Rive. *J. Glaciol. Geocryol.*(04),359-367 (2003).(In Chinese)
195. Wang, Z.-P., Han, X.-G. & Li, L.-H. Effects of grassland conversion to croplands on soil organic carbon in the temperate Inner Mongolia. *J. Environ. Manage.*, **86**(3),529-534 (2008).10.1016/j.jenvman.2006.12.004.
196. Yu, X. et al. Effects of land use and cultivation time on soil organic and inorganic carbon storage in deep soils. *J. Geogr. Sci.*, **30**(6),921-934 (2020).10.1007/s11442-020-1762-3. (In Chinese)
197. Geng, Y. et al. Effects of Cultivating and Grazing on Soil Organic Carbon and Soil Inorganic Carbon in Temperate Semiarid Grassland. *J. Agro-Environ. Sci.*, **27**(6),2518-2523 (2008).
198. Zhang, Y., Li, P., Xiao, L., Zhao, B. & Shi, P. Effects of Topography and Land Use on Soil Organic Carbon in Hilly Region of Loess Platea. *Acta Pedol. Sin.*, **56**(05),1140-1150 (2019).(In Chinese)
199. Zhao, W. et al. Impact of land use conversion on soil organic carbon stocks in an agro-pastoral ecotone of Inner Mongolia. *J. Geogr. Sci.*, **27**(8),999-1010 (2017).10.1007/s11442-017-1417-1. (In Chinese)
200. Hengl, T. & Wheeler, I. Soil organic carbon stock in kg/m2 for 5 standard depth intervals (0–10, 10–30, 30–60, 60–100 and 100–200 cm) at 250 m resolution (v0.2) [Data set]. Zenodo. https://doi.org/10.5281/zenodo.2536040., (2018). (In Chinese)
201. Bareille, F. & Dupraz, P. Productive Capacity of Biodiversity: Crop Diversity and Permanent Grasslands in Northwestern France. *Environ. Resour. Econ.*, **77**(2),365-399 (2020).
202. Su, D. The Effects and Position of Natural Grassland on Controlling Soil Erosion and Desertification in Watershed of the Middle and Upper Reaches of Yellow Rive. *Acta Agrestia Sin.*(02),77-81 (2000).(In Chinese)
203. Zhao, T., Ouyang, Z., Zheng, H., Wang, X. & Miao, H. Analyses on grassland ecosystem services and its indexes for assessment. *Chin. J. Ecol.*(06),155-160 (2004).(In Chinese)
204. Ge, Y., Chunxia, L. & Gaodi, X. progress in ecosystem services of grassland. *Resour. Sci.*, **27**(6),172-179 (2005).
205. *Major projects for the protection and restoration of important ecosystems*. (2020); Available from: http://www.forestry.gov.cn/main/72/20200612/093234638407152.html.
206. *China will restore 230 million mu of degraded grassland during the 14th Five Year Plan period*. (2021); Available from: http://www.gov.cn/xinwen/2021-08/20/content_5632429.htm.
207. *Bulletin on China's land greening in 2021*. (2022); Available from: http://www.forestry.gov.cn/main/586/20220311/132243469507944.html.
208. *Main data bulletin of the third national land survey*. (2021); Available from: http://www.gov.cn/xinwen/2021-08/26/content_5633490.htm.

209. Xiong, D. Evaluation on Carbon Sequestration Capacity and Potential of National Program of Returning Grazing Land to Grassland in China's grassland. *The University of Chinese Academy of Sciences* (2016).
210. Donghui, W. U., Wenying, Y. I. N. & Yuefen, L. I. Effects of mowing practice and fencing enclosure on the soil collembola community in an alkalinized grassland of Leymus chinensis in Songnen Plain. *Acta Prataculturae Sinica*, **17**(5),117-123 (2008).
211. Yang, Y. et al. Effects of Fencing Measurement on Vegetation Community Structure and Soil Water-holding Capacity in Batang Alpine Meadow. *Mountain Research*, **34**(5),606-614 (2016).
212. Zheng, H. P., Chen, Z. X., Niu, J. Y. & Gao, Y. H. Effects of interseeding on plant diversity and productivity in Maqu alpine desertified meadow. *Acta Prataculturae Sinica* (2009).
213. Cao, Z. L., Zheng, C. L., Zhao, T. N. & Sun, B. P. Effects of Reseeding on Vegetation Restoration in Desertification Grassland. *Research of Soil and Water Conservation* (2009).
214. Frank, D. A., Kuns, M. M. & Guido, D. R. Consumer control of grassland plant production. *Ecology*, **83**(3),602-606 (2002).
215. Reeder, J. D. & Schuman, G. E. Influence of livestock grazing on C sequestration in semi-arid mixed-grass and short-grass rangelands. *Environmental Pollution*, **116**(3),457-463 (2002).
216. Mekuria, W. & Veldkamp, E. Restoration of native vegetation following exclosure establishment on communal grazing lands in Tigray, Ethiopia. *Applied Vegetation Science*, **15**(1),71-83 (2012).
217. Su, Y. Z., Li, Y. L., Cui, H. Y. & Zhao, W. Z. Influences of continuous grazing and livestock exclusion on soil properties in a degraded sandy grassland, Inner Mongolia, northern China. *Catena*, **59**(3),267-278 (2005).
218. Deng, L., Zhang, Z. & Shangguan, Z. Long-term fencing effects on plant diversity and soil properties in China. . *Soil Tillage Res.*, **137**,7-15 (2014).
219. Liu, J., Bian, Z., Zhang, K., Ahmad, B. & Khan, A. Effects of different fencing regimes on community structure of degraded desert grasslands on Mu Us desert, China. *Ecology and Evolution*, **9**(6),3367-3377 (2019).
220. Sun, J. et al. Reconsidering the efficiency of grazing exclusion using fences on the Tibetan Plateau. *Science Bulletin*, **65**(16),1405-1414 (2020).
221. Griscom, B. W. et al. Natural climate solutions. *Proceedings of the National Academy of Sciences of the United States of America*, **114**(44),11645-11650 (2017).10.1073/pnas.1710465114.
222. Henderson, B. B. et al. Greenhouse gas mitigation potential of the world's grazing lands: Modeling soil carbon and nitrogen fluxes of mitigation practices. *Agric. Ecosyst. Environ.*, **207**,91-100 (2015).10.1016/j.agee.2015.03.029.
223. *Cultivated land grassland and lake recuperation planning (2016-2030)*. (2016); Available from: http://www.gov.cn/xinwen/2016-11/30/content_5140144.htm (In Chinese).
224. Deng, L., Shangguan, Z. & Sweeney, S. Changes in Soil Carbon and Nitrogen following Land Abandonment of Farmland on the Loess Plateau, China. *PLoS One*, **8**(8),e71923 (2013).
225. Han, X. et al. Changes in soil organic and inorganic carbon stocks in deep profiles following cropland abandonment along a precipitation gradient across the Loess Plateau of China. *Agric. Ecosyst. Environ.*, **258**,1-13 (2018).10.1016/j.agee.2018.02.006.
226. Miao, S., Qiao, Y. & Zhang, F. Conversion of Cropland to Grassland and Forest Mitigates Global Warming Potential in Northeast China. *Pol. J. Environ. Stud.*, **24**(3),1195-1203 (2015).
227. Chen, X. et al. Effects of land cover on soil organic carbon stock in a karst landscape with discontinuous soil distribution. *J. Mount. Sci.*, **11**(3),774-781 (2014).10.1007/s11629-013-2843-x.
228. Li, X., Fu, H., Li, X., Guo, D. & Dong, X. Effects of land-use regimes on carbon sequestration in the Loess Plateau, northern China. *N. Z. J. Agric. Res.* (2008).
229. Zhang, L., Zhao, R. & Xie, Z. Response of soil properties and C dynamics to land-use change in the west of Loess Plateau. *Soil Sci. Plant Nutr.*, **60**(4),586-597 (2014).10.1080/00380768.2014.922407.
230. He, S., Liang, Z., Han, R., Wang, Y. & Liu, G. Soil carbon dynamics during grass restoration on abandoned sloping cropland in the hilly area of the Loess Plateau, China. *Catena*, **137**,679-685 (2016).10.1016/j.catena.2015.01.027.
231. Liu, Y., Dang, Z., Tian, F., Wang, D. & Wu, G. Soil Organic Carbon and Inorganic Carbon Accumulation Along a 30-year Grassland Restoration Chronosequence in Semi-arid Regions (China). *Land Degrad. Dev.*, **28**(1),189-198 (2017).10.1002/ldr.2632.
232. Xu, H. et al. Stocks and Stoichiometry of Soil Organic Carbon, Total Nitrogen, and Total Phosphorus after Vegetation Restoration in the Loess Hilly Region, China. *Forests*, **10**(1),27 (2019).
233. Wang, J. & Zhang, X. Vertical distribution of root in different successional stages of grassland on abandoned cropland. *Sci. Soil Water Conserv.* (2010).
234. Wang, B., Liu, G. B., Xue, S. & Zhu, B. Changes in soil physico-chemical and microbiological properties during natural succession on abandoned farmland in the Loess Plateau. *Environ. Earth Sci.*, **62**(5),915-925 (2011).
235. Liu, Y., Fu, B., Lü, Y., Wang, Z. & Gao, G. Hydrological responses and soil erosion potential of abandoned cropland in the Loess Plateau, China. *Geomorphology*, **138**(1),404-414 (2012).
236. Ren, Y., Lu, Y. & Fu, B. Quantifying the impacts of grassland restoration on biodiversity and ecosystem services in China: A meta-analysis. *Ecol. Eng.*, **95**,542-550 (2016).10.1016/j.ecoleng.2016.06.082.
237. Mao, D. et al. National wetland mapping in China A new product resulting from object-based and hierarchical classification of Landsat 8 OLI images. *ISPRS-J. Photogramm. Remote Sens.*, **164**,11-25 (2020).10.1016/j.isprsjprs.2020.03.020.
238. Jia, M., Wang, Z., Zhang, Y., Mao, D. & Wang, C. Monitoring loss and recovery of mangrove forests during 42 years: The achievements of mangrove conservation in China. *Int. J. Appl. Earth Obs. Geoinf.*, **73**,535-545 (2018).10.1016/j.jag.2018.07.025.
239. Niu, Z. et al. Mapping wetland changes in China between 1978 and 2008. *Chin. Sci. Bull.*, **57**(22),2813-2823 (2012).10.1007/s11434-012-5093-3.
240. Waycott, M. et al. Accelerating loss of seagrasses across the globe threatens coastal ecosystems. **106**(30),12377-12381 (2009).
241. IPCC. Coastal Wetlands. In: 2013 Supplement to the 2006 IPCC guidelines for National Greenhouse Gas Inventories. (2013).
242. Pendleton, L. et al. Estimating global "blue carbon" emissions from conversion and degradation of vegetated coastal ecosystems. *PLoS One*, **7**(9),e43542 (2012).10.1371/journal.pone.0043542.

243. Granek, E. & Ruttenberg, B. I. Changes in biotic and abiotic processes following mangrove clearing. *Estuarine, Coastal and Shelf Science*, **80**,555-562 (2008).10.1016/j.ecss.2008.09.012.
244. Temmerman, S. et al. Ecosystem-based coastal defence in the face of global change. **504**(7478),79-83 (2013).
245. Salem, M. & Mercer, D. The Economic value of mangroves: a meta-analysis. *Sustainability*, **4**(3),359-383

(2012).
246. Lee, S., Dunn, R. & Welsh, D. Impact of urbanization on coastal wetland structure and function. *Austral Ecology*, **31**,149-163 (2006).
247. Siikamaki, J., Sanchirico, J. N. & Jardine, S. L. Global economic potential for reducing carbon dioxide emissions from mangrove loss. *Proc. Natl. Acad. Sci. U. S. A.*, **109**(36),14369-74 (2012).10.1073/pnas.1200519109.
248. Yin, H., Lv, F. & Wang, R. Establishment of China Peat GIS and Its Application. *Earth Space Sci.*, **2**,21-25 (2004).(In Chinese)
249. Mao, D. et al. China's wetlands loss to urban expansion. *Land Degrad. Dev.*, **29**,2644-2657 (2018).10.1002/ldr.2939.
250. Hooijer, A. et al. Subsidence and carbon loss in drained tropical peatlands: reducing uncertainty and implications for CO2 emission reduction options. *Biogeosciences Discuss.*, **8**,9311-9356 (2011).10.5194/bgd-8-9311-2011.
251. Xiao, D., Deng, L., Kim, D. G., Huang, C. & Tian, K. Carbon budgets of wetland ecosystems in China. *Glob. Change Biol.*, **25**(6),2061-2076 (2019).10.1111/gcb.14621.
252. Wang, M., Liu, Z., Ma, X. & Wang, G. Division of Organic Carbon Reserves of Peatlands in China. *Earth Space Sci.*, **10**,156-163 (2012).10.13248/j.cnki.wetlandsci.2012.02.004. (In Chinese)
253. Niu, Z. et al. Geographical characteristics of China's wetlands derived from remotely sensed data. *Sci China Ser D Earth Sci.*, **52**(6),723-738 (2009).10.1007/s11430-009-0075-2.
254. Chu, L. & Jiang, M. Ecological Function of Peatlands and Conservation Strategies in China. *Journal of Anhui Agricultural Sciences*(5),2960-2961, 2993 (2012).
255. Ding, W. & Cai, Z. Estimation of methane emissions from mires in China. *Soils*, **34**(6),348-353 (2002).
256. Cao, Y.-M., Chen, X., Bu, Z.-J. & Zeng, L.-H. J. W. Spatial variations in the surface water chemistry of subtropical peatlands (central China) linked to anthropogenic pressures. **9**(7),505 (2017).
257. Chen, X. et al. Variations in diatom communities at genus and species levels in peatlands (central China) linked to microhabitats and environmental factors. **568**,137-146 (2016).
258. Leifeld, J., Wüst-Galley, C. & Page, S. J. N. C. C. Intact and managed peatland soils as a source and sink of GHGs from 1850 to 2100. **9**(12),945-947 (2019).
259. Rappold, A. G. et al. Peat Bog Wildfire Smoke Exposure in Rural North Carolina Is Associated with Cardiopulmonary Emergency Department Visits Assessed through Syndromic Surveillance. **119**(10),1415-1420 (2011).doi:10.1289/ehp.1003206.
260. Administration, N. F. a. G. *Special Action Plan for Mangrove Conservation and Restoration (2020-2025)*. (2020); Available from: http://www.forestry.gov.cn/main/586/20200828/143227685406582.html (In Chinese).
261. *Department of Natural Resources of Fujian Province. Special Action of Mangrove Protection and Restoration of Fujian Province*. (2020); Available from: http://zrzyt.fujian.gov.cn/xxgk/zfxxgkzl/zfxxgkml/ghjh/202012/t20201230_5504593.htm.
262. Administration, N. F. *National inventory of mangrove resources*. (2004); Available from: https://cyfd.cnki.com.cn/Article/N2006090392000285.htm (In Chinese).
263. Zheng, F., Qiu, G., Fan, H. & Zhang, W. Diversity, distribution and conservation of Chinese seagrass species. *Biodiv. Sci.*, **21**(5),517-526 (2014).10.3724/sp.J.1003.2013.10038.
264. Liu, Z., Cui, B. & He, Q. Shifting paradigms in coastal restoration: Six decades' lessons from China. *Sci. Total Environ.*, **566-567**,205-214 (2016).10.1016/j.scitotenv.2016.05.049.
265. Wang, F. et al. Global blue carbon accumulation in tidal wetlands increases with climate change. *Natl. Sci. Rev.*, **8**,nwaa296 (2021).10.1093/nsr/nwaa296/6035244.
266. McLeod, E. et al. A blueprint for blue carbon: toward an improved understanding of the role of vegetated coastal habitats in sequestering CO2. *Front. Ecol. Environ.*, **9**(10),552-560 (2011).10.1890/110004.
267. Wang, G. et al. Community structure and ecosystem carbon stock dynamics along a chronosequence of mangrove plantations in China. *Plant Soil*, **464**,605–620 (2021).10.1007/s11104-021-04973-2.
268. Ren, H., Chen, H., Li, Z. a. & Han, W. Biomass accumulation and carbon storage of four different aged Sonneratia apetala plantations in Southern China. *Plant Soil*, **327**,279–291 (2010).10.1007/s11104-009-0053-7.
269. Chen, G., Gao, M., Pang, B., Chen, S. & Ye, Y. Top-meter soil organic carbon stocks and sources in restored mangrove forests of different ages. *For. Ecol. Manage.*, **422**,87-94 (2018).10.1016/j.foreco.2018.03.044.
270. Lunstrum, A. & Chen, L. Soil carbon stocks and accumulation in young mangrove forests. *Soil Biol. Biochem.*, **75**,223-232 (2014).10.1016/j.soilbio.2014.04.008.
271. Zhao, Q. et al. A review of methodologies and success indicators for coastal wetland restoration. **60**,442-452 (2016).
272. Li, S. et al. A comparison of coastal habitat restoration projects in China and the United States. *Sci. Rep.*, **9**(1),14388 (2019).10.1038/s41598-019-50930-6.
273. Zhou, W. Effects of human activities on carbon fluxes and storage in the Zoige peatland of the Qinghai-Tibet Plateau. *Chinese Academy of Forestry*, (2015). (In Chinese)
274. Intergovernmental Panel on Climate Change. Supplement to the 2006 IPCC Guidelines for National Greenhouse Gas Inventories: Wetland. (2013). (In Chinese)
275. Rao, J. et al. The metallogenic regularity, development and utilization of peat deposits in China. *Acta Geologica Sinica*, **94**,192-203 (2020).(In Chinese)
276. Song, C., Sun, L., Huang, Y., Wang, Y. & Wan, Z. Carbon exchange in a freshwater marsh in the Sanjiang Plain, northeastern China. *Agric. For. Meteorol.*, **151**,1131-1138 (2011).10.1016/j.agrformet.2011.04.001.
277. Hirota, M. et al. Methane emissions from different vegetation zones in a Qinghai-Tibetan Plateau wetland. *Soil Biol. Biochem.*, **36**,737-748 (2004).10.1016/j.soilbio.2003.12.009.

278. Miao, Y. et al. Growing season methane emission from a boreal peatland in the continuous permafrost zone of Northeast China: effects of active layer depth and vegetation. *Biogeosciences*, **9**,4455-4464 (2012).10.5194/bg-9-4455-2012.
279. Wang, X., Zhang, H., Yao, Z., Zheng, X. & Zhang, S. A preliminary study on methane emission from a seasonal-freezing alpine peat wetland during a non-growing period. *Clim. Environ. Res.*, **21**,282−292 (2016).10.3878/j.issn.1006-9585.2016.15088.
280. Sun, L. et al. Wetland-atmosphere methane exchange in Northeast China: A comparison of permafrost peatland and freshwater wetlands. *Agric. For. Meteorol.*, **249**,239-249 (2018).10.1016/j.agrformet.2017.11.009.
281. Li, Y. et al. Stoichiometry ratio of CO2 and CH4 emissions in Dajiuhu peat wetland of Shennongjia. *Saf. Environ. Eng.*, **26**,22-26 (2019).
282. Ding, W. & Cai, Z. Methane Emission from Natural Wetlands in China: Summary of Years 1995–2004 Studies. *Pedosphere*, **17**,475-486 (2007).10.1016/S1002-0160(07)60057-5.
283. Yang, G. et al. Effects of soil warming, rainfall reduction and water table level on CH4 emissions from the Zoige peatland in China. *Soil Biol. Biochem.*, **78**,83-89 (2014).10.1016/j.soilbio.2014.07.013.
284. Zhou, W., Cui, L., Wang, Y. & Li, W. Methane emissions from natural and drained peatlands in the Zoigeˆ, eastern Qinghai-Tibet Plateau. *J. For. Res.*, **28**,539-547 (2017).10.1007/s11676-016-0343-x.
285. Chapman, S. et al. Exploitation of northern peatlands and biodiversity maintenance: a conflict between economy and ecology. **1**(10),525-532 (2003).
286. Zhang, X., Liu, H., Baker, C. & Graham, S. J. E. Restoration approaches used for degraded peatlands in Ruoergai (Zoige), Tibetan Plateau, China, for sustainable land management. **38**(1),86-92 (2012).
287. Guo, J. et al. Natural succession is a feasible approach for cultivated peatland restoration in Northeast China. **104**,39-44 (2017).
288. Yang, Y. et al. Yield and nutrient concentration in common green manure crops and assessment of potential for nitrogen replacement in different regions of China. *Acta Pratac. Sin.*, **29**(6),39-55 (2020).(In Chinese)
289. Tian, H. et al. Food benefit and climate warming potential of nitrogen fertilizer uses in China. *Environ. Res. Lett.*, **7**,044020 (2012).doi:10.1088/1748-9326/7/4/044020.
290. Fang, X., Tian, D. & Xu, C. Productivity and carbon dynamics of Masson Pine plantation. *J. Central South Univ. For. Tech.*, **23**(2),11-15 (2003).(In Chinese)
291. Hou, G., Delang, C. O., Lu, X. & Gao, L. Soil organic carbon storage varies with stand ages and soil depths following afforestation. *Ann. For. Res.*, **62**(1),3-20 (2019).10.15287/afr.2018.1294.
292. He, Y. et al. Carbon storage capacity of a Betula alnoides stand and a mixed Betula alnoides × Castanopsis hystrix stand in Southern Subtropical China: a comparison study. *Acta Ecol. Sin.*, **32**(23),7586-7594 (2012).(In Chinese)
293. Fang, X., Tian, D. & Xiang, W. Density, storage and distribution of carbon in Chinese fir plantation at fast growing stage. *Sci. Silv. Sin.*, **38**(3),14-19 (2002).(In Chinese)
294. Kang, B., Liu, S., Cai, D. & Lu, L. Characteristics of biomass, carbon accumulation and its spatialdistribution in cunninghamia lanceolata forest ecosystem in low subtropical area. *Sci. Silv. Sin.*, **45**(8),147-153 (2009).(In Chinese)
295. Cao, J. Above- and belowground carbon pools in different ages of Chinese Pine and oriental Arborvitae plantation forests in northern mountain areas in Beijing. *Doctoral dissertation, Beijing Forestry University* (2011).(In Chinese)
296. Wu, Q. et al. Carbon sequestration and its potential by forest ecosystems in China. *Acta Ecol. Sin.*, **28**(2),517-524 (2005).(In Chinese)
297. Li, P., Xiao, Y., Yang, Y. & Zhang, C. Ecosystem carbon storage in poplar plantations of different stand ages in Tianjin plain. *Chin. J. Ecol.*, **33**(3),567-574 (2014).10.13292/j.1000-4890.2014.0043. (In Chinese)
298. Zeng, X. et al. Changes in soil organic carbon, nitrogen, phosphorus, and bulk density after afforestation of the "Beijing–Tianjin Sandstorm Source Control" program in China. *Catena*, **118**,186-194 (2014).10.1016/j.catena.2014.01.005.
299. Hu, H. & Liu, G. Carbon sequestration of China' s National Natural Forest Protection Project. *Acta Ecol. Sin.*, **26**(1),291-296 (2006).(In Chinese)
300. Song, Y., Han, H. & Kang, F. Study on biomass and carbon storage with age-chronosequence in Pinus tabulaeformis forest in taiyue mountain of Shanxi province. *Res. Soil Water Conserv.*, **23**(1),29-33 (2016).10.13869/j.cnki.rswc.2016.01.005. (In Chinese)
301. Guo, Y. et al. Carbon Sink Effect of Afforested Populus simonii Plantations in the Agro-pasture Zigzag Zone in Inner Mongolia. *Ecol. Environ. Sci.*, **25**(6),920-926 (2016).10.16258/j.cnki.1674-5906.2016.06.002. (In Chinese)
302. Liao, G. et al. Distribution Characteristics of Carbon Storage in Larixolgensis Plantation Ecosystem of Different Ages in Eastern Liaoning Province. *J. Northeast For. Univ.*, **48**(11),8-14 (2020).10.13759/j.cnki.dlxb.2020.11.002. (In Chinese)
303. Zhen, W., Huang, M., Zhai, Y., Chen, K. & Gong, Y. Variation of forest vegetation carbon storage and carbon sequestration rate in Liaoning Province, Northeast China. *Chin. J. Appl. Ecol.*, **25**(5),1259-1265 (2014).10.13287/j.1001-9332.2014.0019.
304. Wang, C., Shao, B. & Wang, R. Carbon sequestration potential of ecosystem of two main trees species in Northeast China. *Acta Ecol. Sin.*, **30**(7),1764-1772 (2010).(In Chinese)
305. Yu, C. & Liu, D. Analysis on CO2 Flux during growth season of natural broadleaved mixed forest in Xiaoxinganling mountains. *Chin. J. Agrometeorol.*, **32**(04),525-529 (2011).(In Chinese)
306. Xing, W., Qi, W., Zhao, Q. & Ge, Z. Analysis on carbon storage of poplar plantation in Jiangsu Province. *J. Jiangsu For. Sci. Tech.*, **42**(2),15-18 (2015).(In Chinese)
307. Ye, J. & Jiang, Z. Some ecological aspect of the root system of Chinese Fir in the south part of Jiangsu province. *J. Nanjing For. Prod. Univ.*, **1**,43-51 (1980).(In Chinese)
308. Zhang, J. et al. Carbon storage by ecological service forests in Zhejiang Province, subtropical China. *For. Ecol. Manage.*, **245**(1-3),64-75 (2007).10.1016/j.foreco.2007.03.042.
309. Jiang, B. et al. A preliminary study on the plantation biomass and produce structure of Pinus Massonia, Pinus elliottii and Pinus taeda. *J. Zhejiang For. Sci. Tech.*, **12**,1-8 (1992).(In Chinese)
310. Zhao, M. & Zhou, G.-S. Estimation of biomass and net primary productivity of major planted forests in China based on forest inventory data. *For. Ecol. Manage.*, **207**(3),295-313 (2005).10.1016/j.foreco.2004.10.049.
311. FAEC. Forest in Anhui. *Chinese Forestry Publishers, Beijing, China* (1993).(In Chinese)
312. Shi, W. et al. Biomass model and carbon storage of Chinese Fir plantation in Dabieshan mountains in Anhui. *Resour. Environ. Yangtze Basin*, **24**(5),758-764 (2015).(In Chinese)

313. Tu, H., Sun, Y., Liu, S., Dong, Y. & Fang, J. Stand biomass and carbon storage distribution of Chinese fi r plantation in Subtropical China. *J. Central South Univ. For. Tech.*, **35**(7),94-99 (2015).10.14067/j.cnki.1673-923x.2015.07.017. (In Chinese)
314. Ye, J., Jiang, Z., Zhou, B., Han, F. & Chen, S. Annual dynamic of the biomass of Chinese Fir on Yangkou forestry farm, Fujian province. *J. Nanjing Insti. For.*, **4**,1-9 (1984).(In Chinese)
315. Ye, Z., Yu, X. & Lin, R. The primary inventory of natural Chinese fir mixed forests in Meihua mountain. *J. For. Environ.*, **S1**(26-51) (1983).(In Chinese)
316. Wang, H., Fan, X., Hua, Y., Sun, Y. & Wang, J. Variation characteristics of carbon storage in Chinese fir plantation ecosystem with different age sequences. *Jiangsu Agric. Sci.*, **21**(45),286-288 (2017).(In Chinese)
317. Chen, D. The carbon sequestration status and potential of three typical plantations in Jiangxi Province. *Jiangxi Agricultural University，Master Dissertation* (2016).(In Chinese)
318. Ma, Q. A study on biomass and primary productivity of Chinese Pine. *J. Beijing For. Univ.*,89–96 (1989).(In Chinese)
319. Hou, J. Carbon sequestration characteristics of Robinia pseudoacacia plantation in central and southern Henan Province. *Central South University of Forestry and Technology，Master Dissertation* (2018).(In Chinese)
320. Wang, Y., Liu, L., Deng, L. & Shangguan, Z. Evaluation of carbon storage and the carbon sequestration potential under cutting and no-cutting scenarios for the Grain for Green Project in Western Henan，China. *Acta Ecol. Sin.*, **36**(5),1400-1408 (2016).(In Chinese)
321. Feng, Z. et al. The biological productivity on Chinese fir stands at different zone. *Acta Phytoecol. Geob. Sin.*, **8**(2),93–100 (1984).(In Chinese)
322. Li, D. & Chen, H. The inventory study on biological produce of different stand age of plantation Chinese fir. *J. Middle China Agric. Univ.*, **1**,94-98 (1982).(In Chinese)
323. Fang, Q. Effects of strengthening soil and cover plants management on energy utilization and nutrient cycle of ecosys-tem biomass in Cunningamia lanceolata. *Sci. Silv. Sin.*, **26**(3),201-205 (1990).(In Chinese)
324. Pan, W., Li, L., Gao, Z., Zhang, X. & Tang, D. Study on biological produce and productivity of planted Chinese fir forests. *Middle-South For. Tech.*, **5**,1-12 (1978).(In Chinese)
325. Xiao, F., Fan, S. & Wang, S. Estimation of the Carbon Balance in Moso Bamboo and Chinese Fir Plantation Ecosystem. *Sci. Silv. Sin.*, **46**(11),59-65 (2010).(In Chinese)
326. Huang, X. Study on biomass and content of nutrient elements and their allocation of Chinese fir in Xijiang. *Middle South For. Investigation and Planning*, **1**,13-21 (1988).(In Chinese)
327. Huang, Y. et al. Carbon storage of young conifer and broadleaf mixed forest on a Cunninghamia lanceolata site in south subtropics. *Ecol. Sci.*, **36**(4),137-145 (2017).10.14108/j.cnki.1008-8873.2017.04.019. (In Chinese)
328. Liu, K. & Zeng, T. An investigation on the content and distribution of major nutrient elements in young mixed stands of Cunninghamia lancbolata and Michblia macclubri. *J. South China Agric. Univ.*, **11**(4),86-91 (1990).(In Chinese)
329. Kang, W., Tian, Z., He, J. & Cui, S. Carbon cycle in ten kinds of forest ecosystem in Guangzhou City. *J. Appl. Ecol.*, **20**(12),2917-2924 (2009).10.13287/j.1001. (In Chinese)
330. Ren, H., Peng, S. & Yu, Z. Comparison biomass and productivity of major planted communities in Guangdong province. *Dynam. Ecol. Res.*, **7**(3),22-25 (1996).(In Chinese)
331. Zhang, H. et al. Biomass and carbon storage in an age-sequence of Cyclobalanopsis glauca plantations in southwest China. *Ecol. Eng.*, **73**,184-191 (2014).10.1016/j.ecoleng.2014.09.008.
332. Liu, E. Carbon storage of typical plantations in South Sub-tropical area. *Chinese Academy of Forestry，Master Dissertation* (2012).(In Chinese)
333. Xie, M. et al. Carbon sequestration of different aged Taiwania Flousiana plantations in Northwestern Guangxi. *For. Res.*, **5**,106-113 (2020).10.13275/j.cnki.lykxyj.2020.05.013. (In Chinese)
334. FSEC. Forest in Sichuan. *Chinese Forestry Publishers, Beijing, China* (1992).(In Chinese)
335. Justine, M. F., Yang, W., Wu, F. & Khan, M. N. Dynamics of biomass and carbon sequestration across a chronosequence of masson pine plantations. *J. Geophys. Res.: Biogeosciences*, **122**(3),578-591 (2017).10.1002/2016jg003619.
336. Yao, P. et al. Carbon sequestration potential of the major stands under the Grain for Green Program in Southwest China in the next 50 years. *Acta Ecol. Sin.*, **34**(11),3025-3037 (2014).(In Chinese)
337. An, H., Jin, X. & Yang, C. Study of Biomass ant its variation of little region of Banqiao river. *J. Guizhou For. Tech.*, **19**(4),20-34 (1991).(In Chinese)
338. Li, M. & Ding, G. Study on carbon storage of main forest types in southeast part of Guizhou province. *J. Central South Univ. For. Tech.*, **33**(7),119-124 (2013).10.14067/j.cnki.1673-923x.2013.07.024. (In Chinese)
339. Xia, J. Carbon storage of Pinus armandii Franch Plantation at different stand ages in Guizhou Province. *Guizhou For. Sci. Tech.*, **43**(2),6-9 (2015).10.16709/j.cnki.gzlykj.2015.02.008. (In Chinese)
340. Liu, Y. et al. Ecosystems carbon storage and carbon sequestration potential of two main tree species for the Grain for Green Project on China's hilly Loess Plateau. *Acta Ecol. Sin.*, **31**(15),4277-4286 (2011).(In Chinese)
341. Xiao, Y. Comparative studies on biomass and productivity of Pinus tabulaeformis plantations in different climatic zones in Shannxi province. *Acta Phytoecol. Geob. Sin.*, **14**(3),237-246 (1990).(In Chinese)
342. Xiao, Y. et al. The primary study of biomass of Pinus tabulaeformis forests. *Shanxi For. Sci. Tech.*(2),5-14 (1983).(In Chinese)
343. Cheng, R. et al. Carbon storage and sequestration potential of five typical plantation ecosystems in Gansu Province, China. *Chin. J. Appl. Ecol.*, **28**(4),1112—1120 (2017).(In Chinese)
344. Fang, J., Liu, G., Zhu, B., Wang, X. & Liu, S. Carbon cycling in three temperate forest ecosystems in Dongling Mountain, Beijing. *Sci. China-Life Sci.*, **1**(6),533-543 (2006).(In Chinese)
345. Zhu, J. et al. A significant carbon sink in temperate forests in Beijing: based on 20-year field measurements in three stands. *Sci. China-Life Sci.*, **45**(11),1132-1139 (2015).10.1007/s11427-015-4935-z. (In Chinese)
346. Huang, X., Xin, Z., Zhao, Y. & Ma, F. Effects of stand ages and site conditions on carbon stock of Pinus tabuliformis plantations in Beijing Mountainous area. *J. Soil Water Conserv.*, **29**(6),184-190 (2015).(In Chinese)

347. Yang, J. Carbon storage of Pinus tabulaeformis plantation at different stand ages in Pingquan of Heibei province. *Beijing Forestry University, Master Dissertation* (2012).(In Chinese)
348. Liu, B., Chen, Y., Cao, Y. & Wu, X. Storage and allocation of carbon and nitrogen in Pinus tabuliformis plantations on the south slope of the East Qinling Mountains, China. *J. Appl. Ecol.*, **26**(3),643-652 (2015).10.13287/j.1001-9332.20150106.006. (In Chinese)
349. Cheng, X., Han, H. & Kang, F. Biomass，carbon accumulation and its partitioning of a Pinus tabulaeformis plantation ecosystem in Shanxi Province, China. *Chin. J. Ecol.*, **31**(10),2455-2460 (2012).10.13292/j.1000-4890.2012.0355. (In Chinese)
350. Tang, X., Zha, Y., Tang, X., Guo, H. & ZHANG, X. Carbon Sequestration Characteristics of Pinus tabulaeformis Plantations in Different Forest Ages in Eastern Inner Mongolia. *Acta Agric. Jiangxi*, **32**(1),53-58 (2020).(In Chinese)
351. Chen, D., Zhou, X., Zhao, H., Wang, Y. & Jin, Y. Structure, function and succession of four natural secondary forest types. *J. Northeastern For. Insti.*, **2**,2-10 (1982).(In Chinese)
352. Zhang, Q. Carbon density and carbon sequestration capacity of six temperate forests in Northeast China. *Northeast Forestry University, Master Dissertation* (2010).(In Chinese)
353. Ruan, H., Jiang, Z. & Gao, S. Preliminary Studies of Carbon Cycling in Three Types of Forests in the Hilly Regions of Southern Jiangsu Province. *Chin. J. Ecol.*, **16**(6),17-21 (1997).(In Chinese)
354. Ji, Y. et al. Current forest carbon stocks and carbon sequestration potential in Anhui Province, China. *Chin. J. Plant Ecol.*, **40**(4),395-404 (2016).10.17521/cjpe.2015.0147. (In Chinese)
355. Yang, Y. et al. Carbon Sequestration and Balance in Castanopsis kawakamii and Cunninghamia lanceolata Plantations in Subtropical China. *Sci. Silv. Sin.*, **43**(3),113-117 (2007).(In Chinese)
356. Wang, H. et al. Carbon fluxes and their response to environmental variables in a Dahurian larch forest ecosystem in northeast China. *J. For. Res.*, **19**(1),1-10 (2008).10.1007/s11676-008-0001-z.
357. Tong, X. et al. Characteristics of Net Carbon Exchange over a Mixed Plantation in a Hilly Area of the North China. *Sci. Silv. Sin.*, **46**(3),37-43 (2010).(In Chinese)
358. Feng, Y., Xiao, W., Zhu, J. & Li, Q. Impacts of afforestation on the carbon stocks and carbon sequestration rates of regional forest ecosystems. *J. Ecol. Rural Environ.*, **36**(3),281-290 (2020).(In Chinese)
359. Liang, M., Chen, L. & Wang, S. The allocation pattern of carbon storage and carbon sequestration potential in Chinese fir plantation ecosystems in Hunan Province. *Chin. J. Ecol.*, **35**(4),896-902 (2016).(In Chinese)
360. Deng, S., Wang, K. & Gao, H. The distribution of biological produce and nutrient content of old age Cunninghamia laecedatia planted forests. *J. Ecol.*, **7**(1),13-18 (1988).(In Chinese)
361. Guan, D. The biomass and the productivity of the four stands in the forest Area of the Liuxihe Reservior. *J. Ecol.*, **2**(Journal of Ecol.),45-52 (1986).(In Chinese)
362. Xu, H., Zheng, S. & Lu, Y. The biomass of (I-72/85) poplar plantation. *Sci. Silv. Sin.*, **28**(1),22-27 (1990).(In Chinese)
363. Peng, S. & Fang, W. Features of biomass and productivity dynamics in successional process of low subtropical forest. *Ecol. Sci.*, **2**,1-9 (1995).(In Chinese)
364. Jiang, L., Lin, N., Mo, D. & Zhuo, Y. Study on Carbon Storage and Allocation of Cryptomeria fortunei Plantation in the Low Mountain of Southeast Guangxi. *J. Anhui Agric. Sci.*, **18**,9728-9730 (2012).10.13989/j.cnki.0517-6611.2012.18.127. (In Chinese)
365. Liu, X. Studying biomass of different age of Pinus massoniana. *J. Central South For. Univ.*, **16**(4),47-51 (1996).(In Chinese)
366. Xiang, Y. Spatial and temporal pattern of biomass and carbon storage of eucalypt platation ecosystems in Hainan. *Chinese Academy of Forestry, Doctoral Dissertation* (2012).(In Chinese)
367. Zhu, M. Research of carbon and nitrogen storage of Rubber and Eucalyptus plantations in Hainan island. *Hainan University, Master Dissertation* (2016).(In Chinese)
368. Zhao, G. The carbon mitigation potential and present situation of coniferous forests and plantations in the Midwest of Yunan. *Yunnan University, Master Dissertation* (2016).(In Chinese)
369. Yue, J. Carbon sequestration dynamics, potential and influence mechanism of main forest types in Gansu Province. *University of Chinese Academy of Sciences，Dorctor Dissertation* (2018).(In Chinese)
370. Zhu, X., Xiao, Y. & Tian, L. Equations of measuring leaves, branches, and roots biomass and analyses of natural secondary Populus davidiana forests. *Qinghai Agric. For. Tech.*, **1**,35-38 (1988).(In Chinese)
371. Cheng, J. & Zou, H. Study on forest biomass of liupan Mountain and its ecohydrology. *J. Beijing For. Univ.*, **12**(1),55-63 (1990).(In Chinese)
372. State Forestry Administration. (2002) National Mangrove Resource Inventory Report. *Web Page* (2002).
373. Ministry of Natural Resources of the People's Republic of China. The special action plan for mangrove protection and restoration the current area of mangroves is 28,900 hectares in China (http://vod.mnr.gov.cn/spxw/202008/t20200828_2544856.htm). (2020).(In Chinese)
374. Ministry of Natural Resources of the People's Republic of China. A special action plan for mangrove protection and restoration in Zhejiang was finalized (http://www.mnr.gov.cn/dt/hy/202012/t20201221_2595737.html). (2020).(In Chinese)
375. National Forestry and Grassland Administration. 5,500 hectares of mangroves is planning to restore in five years in Guangdong province (http://www.forestry.gov.cn/main/416/20201204/212955575903628.html). (2020).(In Chinese)